AD-A080 384 MICHIGAN TECHNOLOGICAL UNIV HOUGHTON DEPT OF METALLU--ETC F/G 11/6
BARRIERS TO THE MIGRATION OF INTERPHASE BOUNDARIES, PARTICULARL--ETC(U)
DEC 79 H I AARONSON, T ABE, J R BRADLEY DAAG29-77-G-0019
UNCLASSIFIED ARO-14217.1-MS NL

1 OF 2
AD A080384

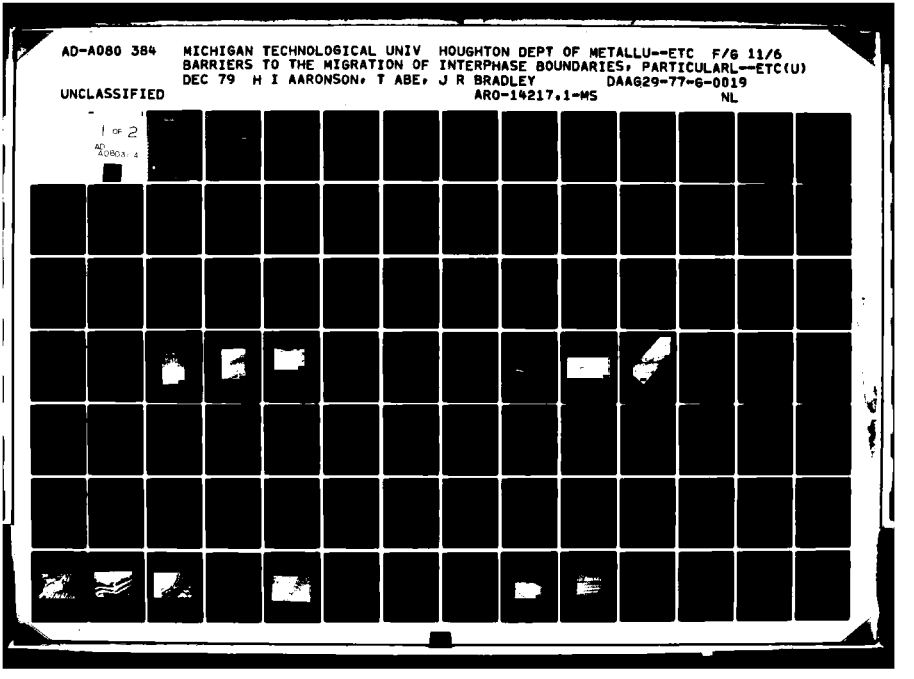

(9) [Rept. no. 17 (Final) 15 Oct 76 - 14 Sep 79]

Unclassified

SECURITY CLASSIFICATION OF THIS PAGE (When Data Entered)

REPORT DOCUMENTATION PAGE

READ INSTRUCTIONS BEFORE COMPLETING FORM

1. REPORT NUMBER: 17
2. GOVT ACCESSION NO.
3. RECIPIENT'S CATALOG NUMBER

4. TITLE (and Subtitle): (6) BARRIERS TO THE MIGRATION OF INTERPHASE BOUNDARIES, PARTICULARLY IN STEEL.

5. TYPE OF REPORT & PERIOD COVERED: Final: 15 October 1976 - 14 September 1979

6. PERFORMING ORG. REPORT NUMBER

7. AUTHOR(s): (10) H. I. Aaronson, T. Abe, J. R. Bradley, W. A. T. Clark, T. Obara and G. J. Shiflet

8. CONTRACT OR GRANT NUMBER(s): (15) DAAG29-77-G-0019

9. PERFORMING ORGANIZATION NAME AND ADDRESS: Michigan Technological University, Houghton, MI 49931

10. PROGRAM ELEMENT, PROJECT, TASK AREA & WORK UNIT NUMBERS: P-14217-MS; 2172040 76A-7307 P611102. H5700-2583. S31124

11. CONTROLLING OFFICE NAME AND ADDRESS: U. S. Army Research Office, P. O. Box 12211, Research Triangle Park, NC 27709

12. REPORT DATE: (11) 20 Dec[illegible]79

13. NUMBER OF PAGES

14. MONITORING AGENCY NAME & ADDRESS (if different from Controlling Office): (14) ARO; (19) 14217.1-MS

15. SECURITY CLASS. (of this report): Unclassified

15a. DECLASSIFICATION/DOWNGRADING SCHEDULE

16. DISTRIBUTION STATEMENT (of this Report)

Approved for public release; distribution unlimited.

17. DISTRIBUTION STATEMENT (of the abstract entered in Block 20, if different from Report)

18. SUPPLEMENTARY NOTES

The view, opinions, and/or findings contained in this report are those of the author(s) and should not be construed as an official Department of the Army position, policy, or decision, unless so designated by other documentation.

19. KEY WORDS (Continue on reverse side if necessary and identify by block number)

diffusional growth, alloying element effects, partition, kinetics, misfit dislocations, interfacial structure, carbides, alloy steels, lamellar eutectic, massive transformation, incomplete transformation, thermodynamics, shear, growth mechanism

20. ABSTRACT (Continue on reverse side if necessary and identify by block number)

The growth kinetics of proeutectoid ferrite, in the form of grain boundary allotriomorphs, were measured vs. reaction temperature in Fe-C-X alloys where X was Si, Mn, Cr and Ni. Comparison of measured growth kinetics with those calculated often shows poor agreement with the local equilibrium model; order of magnitude agreement was obtained with both the pileup and the paraequilibrium models. A limiting alloying element penetration calculation, however, showed

(continued on reverse side)

DD FORM 1 JAN 73 1473 EDITION OF 1 NOV 65 IS OBSOLETE

Unclassified

SECURITY CLASSIFICATION OF THIS PAGE (When Data Entered)

402 311

20. Abstract (continued)

that only the paraequilibrium model is basically consistent with the experimental data. TEM studies showed that measured growth kinetics somewhat slower than those predicted by the paraequilibrium model are not due to carbide precipitation at austenite:ferrite boundaries. Such slower growth kinetics appear to be best explained by a solute drag-like effect. Carbide precipitation at austenite:ferrite boundaries in Fe-C-X alloys was shown to increase growth kinetics when X is Si, Ni and V. Incomplete transformation in Fe-C-Mo alloys was demonstrated to occur only when critical proportions of C and Mo are exceeded. Thermodynamics of the proeutectoid ferrite reaction in Fe-C alloys were reassessed using recent theory and thermodynamic data. Structural ledges were observed to occur reproducibly on planar facets formed during the $(\beta) \rightarrow (\alpha_m)$ Cu-Zn massive transformation. The misfit dislocation structure of the lamellar interfaces in the Co(Al)-CoAl eutectic was observed to be significantly affected by the presence of LRO in the CoAl phase.

BETA ALPHA

Accession For	
NTIS GRA&I	☒
DDC TAB	☐
Unannounced	☐
Justification	
By	
Distribution/	
Availability Codes	
Dist	Avail and/or special
A	

Barriers to the Migration of Interphase Boundaries, Particularly in Steel

H. I. Aaronson, T. Abe, J. R. Bradley, W. A. T. Clark
T. Obara and G. J. Shiflet
Formerly of the Department of Metallurgical Engineering
Michigan Technological University
Houghton, MI. 49931

I. Foreword

This report summarizes, in some detail, research accomplished with the support of Army Research Office Grant DAAG29 77 G 0019 from 15 October 1976 through 14 September 1979. All of this work was performed at Michigan Technological University. Since then, HIA, TO and GJS have moved to Carnegie-Mellon University, where further research is presently being undertaken with the support of an extension ARO grant/contract. (JRB is now with the General Motors Research Center, WATC is presently Asst. Prof. at Ohio State Univ. and TA has returned to the National Research Institute for Metals in Japan).

Two types of barriers are considered: a structural barrier, resulting from partial coherency between precipitate and matrix phases, and a chemical barrier, probably derived from the adsorption of a slow diffusing substitutional solute, X, at austenite:ferrite boundaries in Fe-C-X alloys. Although many of the alloys on which these studies were conducted are Fe-C or Fe-C-X, some non-ferrous alloys, including Cu-38% Zn and the Co(Al)-CoAl eutectic, have been used to study structural barriers between crystal structures similar to those present during the proeutectoid ferrite reaction in steel.

II. Table of Contents

III. List of Captions

Figure 1. Typical plot of allotriomorph half-thickness, S/2, and half-length, L/2, as a function of the square root of the reaction time.

Figure 2. Typical plot of ln S/2 and ln L/2 versus ln t for the data shown in Figure 1.

Figure 3. Parabolic growth rate constants as a function of reaction temperature: (a) for thickening, α, and (b) for lengthening, β, of ferrite allotriomorphs in Fe-0.40% C-1.73% Si.

Figure 4. Parabolic growth rate constants as a function of reaction temperature: (a) for thickening, α, and (b) for lengthening, β, of ferrite allotriomorphs in Fe-0.12% C-3.28% Ni.

Figure 5 Parabolic growth rate constants as a function of reaction temperature: (a) for thickening, α, and (b) for lengthening, β, of ferrite allotriomorphs in Fe-0.43% C-7.51% Ni.

Figure 6. Parabolic growth rate constants as a function of reaction temperature: (a) for thickening, α, and (b) for lengthening, β, of ferrite allotriomorphs in Fe-0.12% C-3.08% Mn.

Figure 7. Parabolic growth rate constants as a function of reaction temperature: (a) for thickening, α, and (b) for lengthening β, of ferrite allotriomorphs in Fe-0.13% C-2.99% Cr.

Figure 8. Schematic representation of alloying element (X) distribution during ferrite growth for: (a) local equilibrium with X partition between austenite and ferrite; (b) local equilibrium with "pile-up" in austenite; and (c) paraequilibrium.

Figure 9. $\alpha_{corr}/\alpha_{equil}$ versus reaction temperature.

Figure 10. $\alpha_{corr}/\alpha_{pile\text{-}up}$ versus reaction temperature.

Figure 11. $\alpha_{corr}/\alpha_{para}$ versus reaction temperature.

Figure 12. Variation of the maximum penetration distance of alloying element, ℓ_{max}, with reaction temperature.

Figure 13. Fe-0.12% C-3.08% Mn. (a) reacted 360 secs. at 600°C, bright field; (b) same area in dark field; (c) reacted 16 secs. at 550°C, weak-beam, dark-field, X85,000.

Figure 14. Precipitation of carbides on broad faces of ledges; light area at top is martensite. Fe-0.40% C-1.73% Si, reacted 5 secs. at 700°C, dark-field, X75,000.

Figure 15. Grain boundary allotriomorphs and "snakes" in Fe-0.12% C-0.11% V, reacted 60 secs. at 826°C, X500.

Figure 16. "Row" or interphase boundary carbides formed in association with a grain boundary ferrite allotriomorph in Fe-0.12% C-0.11% V, reacted 60 secs. at 830°C, dark-field.

Figure 17. Composite micrograph of a nearly continuous film of interphase boundary carbide precipitated on one face of a "snake" in Fe-0.12% C-0.11% V, reacted 60 secs. at 846°C, dark-field. M = martensite, F = ferrite.

Figure 18. Parabolic rate constant for thickening, α, vs. temperature for grain boundary allotriomorphs (upper experimental data set) and "snakes" (lower experimental data set) vs. temperature, compared with calculated values of α for aspect ratios, K, of 0.51 and 0 (thin curves). Fe-0.12% C-0.11% V.

Figure 19. Fe-0.11% C-1.95% Mo. (D) Recrystallized as described in text and then reacted 30 min. at 810°C, X400. (U) Conventionally austenitized and immediately reacted for one min. at 810°C, X400.

Figure 20. Bay region of TTT-diagrams for initiation of transformation in Fe-C-Mo alloys. (Experimental points omitted.) Key to alloys: (1) 0.15% C, 2.55% Mo; (2) 0.17% C, 3.0% Mo; (3) 0.20% C, 3.0% Mo; (4) 0.15% C, 3.4% Mo; (5) 0.15% C, 4.0% Mo; (6) 0.25% C, 3.2% Mo; (7) 0.20% C, 4.0% Mo; (8) 0.27% C, 3.0% Mo; (9) 0.25% C, 4.3% Mo.

Figure 21. Temperature of the bay in the TTT-diagram for initiation of transformation in Fe-C-Mo alloys versus carbon content and Mo content. For key to alloy numbers see caption of Figure 20.

Figure 22. Fraction of austenite transformed to ferrite at temperatures in the bay region of Fe-0.17% C-3.0% Mo.

Figure 23. Fraction of austenite transformed to ferrite at temperatures in the bay region of Fe-0.25% C-3.2% Mo.

Figure 24. Fraction of austenite transformed to ferrite at temperatures in the bay region of Fe-0.23% C-4.3% Mo.

Figure 25. Calculated versions of Ae3 curve and its metastable equilibrium extrapolation for Fe-C alloys. Hansen--experimental curve; Eqn. (10) denotes best LFG curve from ADP; Eqn. (13), w_γ = 1925 cal./mole denotes best LFG/MD curve from present investigation.

Figure 26. Calculation versions of $\alpha'/(\alpha + \gamma)$ curve and its metastable equilibrium extrapolation for Fe-C alloys. Hansen--experimental curve; Eqn. (24) denotes best LFG curve from ADP; Eqns. (15, 16), w_γ = 1925 cal./mole denotes best LFG/MD curve from present investigation.

Figure 27. Cu-38% Zn. Bright field micrograph with g = 020_α (crystal A); scale marker is 50 nm. Note the line defects in the interface with spacing of 2.68 nm.

Figure 28. Same areas as Figure 27. Dark field micrograph with g = 200_α ; scale marker is 25 nm. Note apparent absence of defects in region B.

List of Tables

IV. Body of Report

A. Publications Resulting in Whole or in Part from Research Supported by This Grant

1. First Three Grant Years (1973 - 1976)

1. C. Atkinson, K. R. Kinsman and H. I. Aaronson, "Relative Growth Kinetics of Ledged and Disordered Interphase Boundaries," Scripta Met., 7, 1105 (1973).

2. K. C. Russell, M. G. Hall, K. R. Kinsman and H. I. Aaronson, "The Nature of the Barrier to Growth at Partially Coherent FCC:BCC Boundaries," Met. Trans., 5, 1503 (1974).

3. K. C. Russell and H. I. Aaronson, "On the Driving Force for the Growth of Grain Boundary Allotriomorphs by the 'Collector Plate' Mechanism," Scripta Met., 8, 559 (1974).

4. K. R. Kinsman, E. Eichen and H. I. Aaronson, "Thickening Kinetics of Proeutectoid Ferrite Plates in Fe-C Alloys," Met. Trans., 6A, 303 (1975).

5. H. I. Aaronson, "Observations on Interphase Boundary Structure," Jnl. of Microscopy, 102, 275 (1974).

6. M. R. Plichta and H. I. Aaronson, "Influence of Alloying Elements upon the Morphology of Austenite Formed from Martensite in Fe-C-X Alloys," Met. Trans., 5, 2611 (1974).

7. G. W. Lorimer, G. Cliff, H. I. Aaronson and K. R. Kinsman, "Analysis of the Composition of α_1 Plates Precipitated from β' Cu-Zn Using Analytical Electron Microscopy," Scripta Met., 9, 705 (1975).

8. H. I. Aaronson, M. G. Hall, D. M. Barnett and K. R. Kinsman, "The Watson-McDougall Shear: Proof That Widmanstatten Ferrite Cannot Grow Martensitically," Scripta Met., 9, 705 (1975).

9. M. G. Hall, H. I. Aaronson and G. W. Lorimer, "Considerations on a Martensitic Mechanism for the F.C.C.→B.C.C. Transformation in A Cu-0.33 W/O Cr Alloy," Scripta Met., 9, 533 (1975).

10. M. R. Plichta, H. I. Aaronson and W. F. Lange III, "Application of a Rapid Chemical Polish to Preparation of High-Carbon Steel Specimens for Optical Microscopy," Metallography, 9, 455 (1976).

11. G. W. Lorimer, G. Cliff, H. I. Aaronson and K. R. Kinsman, "Reply to 'Comments on "Analysis of the Composition of α_1 Plates Precipitated from β' Cu-Zn Using Analytical Electron Microscopy," Scripta Met., 9, 1175 (1975).

12. K. R. Kinsman and H. I. Aaronson, "A Critical Test of Two Theories of Non-IPS Geometric Surface Relief Effects Associated with Diffusional Phase Transformations," Met. Trans., 7A, 896 (1976).

13. H. I. Aaronson and K. R. Kinsman, "Growth Mechanisms of AuCu II Plates," Acta Met. 25, 367 (1977).

14. J. R. Bradley and H. I. Aaronson, "The Stereology of Grain Boundary Allotriomorphs," Met. Trans., 8A, 317 (1977).

15. J. R. Bradley, J. M. Rigsbee and H. I. Aaronson, "Growth Kinetics of Grain Boundary Ferrite Allotriomorphs," Met. Trans., 8A, 323 (1977).

2. Second Three Grant Years (1976 - 1979/80)

16. H. I. Aaronson, "The Proeutectoid Reactions in Steel," Materials Science and Engineering, 25, 145 (1976).

17. K. R. Kinsman and H. I. Aaronson, "Reply to 'Discussion of "A Critical Test of Two Theories of Non-IPS Geometric Surface Relief Effects Associated with Diffusional Phase Transformations'," Met. Trans., 8A, 209 (1977).

18. H. I. Aaronson, "Discussion of 'On the Growth Kinetics of Plate-Shaped Precipitates in Aluminum-Copper and Aluminum-Gold Alloys' by Y. H. Chen and R. D. Doherty," Scripta Met., 11, 731 (1977).

19. H. I. Aaronson, K. C. Russell and G. W. Lorimer, "Cessation of the Dislocation Splitting Mechanism for γ' Al-Ag Formation Above a Critical Temperature," Met. Trans., 8A, 1885 (1977).

20. J. R. Bradley, H. I. Aaronson, K. C. Russell and W. C. Johnson, "Effects of Austenitizing Temperature on the Kinetics of the Proeutectoid Ferrite Reaction at Constant Austenite Grain Size in an Fe-C Alloy," Met. Trans., 8A, 1955 (1977).

21. H. I. Aaronson, "Comments on 'Reply to Discussion on The Growth Kinetics of Plate-Shaped Precipitates'", Scripta Met., 11, 741 (1977).

22. H. I. Aaronson, J. K. Lee and K. C. Russell, "Diffusional Nucleation and Growth," 'Precipitation Processes in Solids', TMS-AIME, New York, p. 31 (1978).

23. G. J. Shiflet, J. R. Bradley and H. I. Aaronson, "A Re-examination of the Thermodynamics of the Proeutectoid Ferrite Transformation in Fe-C Alloys," Met. Trans., 9A, 999 (1978).

24. J. M. Rigsbee and H. I. Aaronson, "The Interfacial Structure of the Broad Faces of Ferrite Plates," Acta Met., 27, 365 (1979).

25. J. M. Rigsbee and H. I. Aaronson, "A Computer Modeling Study of Partially Coherent F.C.C.:B.C.C. Boundaries," Acta Met., 27, 365 (1979).

26. H. I. Aaronson, "Mechanisms of Diffusional Growth," 'Phase Transformations', Vol. I, p. II-1, The Institution of Metallurgists/Chameleon Press (April, 1979).

27. H. I. Aaronson, "An Emerging Viewpoint on Interphase Boundaries Developed During Diffusional Phase Transformations," Proceedings of the (1977) International Conference on Metal Sciences--The Emerging Frontiers, Banaras Hindu University, Varanasi, India, in press.

28. W. A. T. Clark, A. Guha, H. I. Aaronson and J. M. Rigsbee, "Discussion to a Series of Papers on the Structure of Interphase Boundaries in Brass," Scripta Met., in press.

29. J. R. Bradley and H. I. Aaronson, "Growth Kinetics of Grain Boundary Ferrite Allotriomorphs in Fe-C-X Alloys," Met. Trans., in press.

3. Manuscripts Presently in Preparation

(30) W. A. T. Clark and H. I. Aaronson, "The Interfacial Structure of Planar Facets on $\beta:\alpha_m$ Cu-Zn Boundaries," to be submitted to Acta Met.

(31) W. A. T. Clark and H. I. Aaronson, "An O-Lattice Approach to the Structure of Partially Coherent F.C.C.:B.C.C. Boundaries," to be submitted to Acta Met.

(32) A. Guha, H. I. Aaronson and W. A. T. Clark, "Interfacial Structure of the Lamellar Interfaces in the Co(Al)-CoAl Eutectic," to be submitted to Met. Trans.

(33) J. R. Bradley, T. Abe and H. I. Aaronson, "Maintenance of Constant Carbon Concentration During Heat Treatment of Steel," to be submitted to Rev. Sci. Instruments.

(34) G. J. Shiflet, H. I. Aaronson and J. R. Bradley, "Carbide Precipitation in Association with Proeutectoid Ferrite and Its Influence on Ferrite Growth Kinetics," to be submitted to Met. Trans.

(35) T. Abe, H. I. Aaronson and G. J. Shiflet, "Effects of Interphase Boundary Precipitation Upon the Growth Kinetics of Grain Boundary Ferrite Allotriomorphs in an Fe-C-V Alloy," to be submitted to Met. Trans.

(36) J. R. Bradley, G. J. Shiflet, Y. W. Lee, H. I. Aaronson and W. C. Johnson, "On the Binding Free Energy of Carbon to Austenite Grain Boundaries," to be submitted to Met. Trans.

(37) H. I. Aaronson and G. J. Shiflet, "Discussion to 'The Bainite Transformation in a Silicon Steel' by H. K. D. H. Bhadeshia and D. V. Edmonds, Met. Trans., 10A, 895 (1979)," to be submitted to Met. Trans.

B. Personnel and Supplemental Support Situations

During the tenure of this three years of our ARO Contract, both the personnel and the supplemental suport situations for the constituent projects can be safely termed bizarre. A well qualified postdoctoral research associate was engaged in October, 1976 to undertake the planned TEM interfacial structure studies. He originally promised to report for work at Michigan Tech in January of 1977; thesis completion problems, however, caused repeated delays until a final reporting date of June 1 was agreed upon. On May 31, this gentleman telephoned to say that an industrial firm (General Motors Research Laboratories) had "made him an offer he couldn't refuse." We subsequently learned that he had interviewed continuously after receiving our offer, evidently being more interested in securing a permanent

visa than in either interfacial structure studies or honor. Meanwhile, it became apparent, from experiences with a related study on another grant, that a TEM-qualified Ph.D. of considerable ability and background would be required to carry out any portion of the planned program. Accordingly, we waited until May, 1978 to obtain the services, for little more than a year, of Dr. William A. T. Clark, a graduate of Oxford University and a truly exceptional microscopist and metallurgist. Dr. Clark succeeded in completing about one-third of the probably overambitious program of interfacial structure studies originally proposed; he is now writing up the results of his work at Michigan Tech at Ohio State University, where he has begun work as Assistant Professor. (The first postdoctoral on this Grant, who successfully studied the interfacial structure of the broad faces of ferrite plates (87, 88), Dr. J. Michael Rigsbee, is now an Assistant Professor at the University of Illinois at Urbana-Champaign.) Because of the long delay in obtaining a postdoctoral, the expiration date of the present three-year Grant has been extended from October 14, 1979 to April 30, 1980. A suitable replacement for Dr. Clark, to work on the next phase of the originally planned program at least until the revised expiration date, has just been engaged.

During most of the present grant period we have enjoyed the benefit of a Republic Steel Corporation Fellowship. This funding has supported the classroom studies and Ph.D. thesis research of Mr. Gary J. Shiflet, who has contributed importantly to studies on proeutectoid ferrite growth kinetics and thermodynamics and carbide precipitation in Fe-C-X alloys. Only his rather small laboratory expenses have been defrayed by this grant. Unfortunately, when the P.I. and his research group moved from Michigan Technological University to Carnegie-Mellon University in August, 1979, the Fellowship had to remain at Michigan Tech, and there seems little prospect that a new one will be nucleated, at least in the near future, at Carnegie-Mellon. The balance of Mr. Shiflet's Ph.D. research is being supported theough the P.I.'s NSF grant, with the permission of Dr. R. J. Reynik, Metallurgy

Program Director of NSF. Credit will continue to accrue to ARO, however, for all of his remaining work at CMU.

Shortly before Mr. John R. Bradley completed his Ph.D. thesis research in December, 1979, which was wholly supported by this grant, Mr. Takashi Obara, of the Kawasaki Steel Company, Japan, began a two-year sabbatical with the P.I.; he is being partially supported by ARO through receipt of the graduate student's stipend and will remain with the P.I. (if the present Contract is renewed) through September, 1980, when he would be replaced by a graduate student. Mr. Obara has contributed ably and vigorously to the austenite decomposition studies in the Fe-C-X alloys portion of the program. At about the same time Mr. Obara arrived, Mr. Toshihiko Abe, of Japan's National Research Institute for Metals, joined the P.I.'s research group with the support of a one year fellowship from the Japanese Government. He also undertook a portion of the Fe-C-X program. Mr. Abe has now returned to Japan; we were sorry to lose an exceptionally vigorous colleague and contributor but greatly appreciate the contributions he made to this program.

Finally, it seems worth noting that the P.I. accepted Carnegie-Mellon University's offer of the first R. F. Mehl Professorship of Metallurgy and Materials Science because of the exceptional environment for phase transformations studies at CMU. With the generous cooperation and assistance of both Michigan Tech and CMU, and of ARO, NSF and AFOSR, the P.I. moved all of his grants, laboratory equipment, graduate students, Mr. Obara and a postdoctoral fellow to CMU on August 20, 1979. We hope that heat treatment activities, which are central to all components of our ARO program, can be resumed by the end of the year.

C. Growth Kinetics of Grain Boundary Allotriomorphs of Proeutectoid Ferrite in Fe-C-X Alloys

This investigation, which has been completed, represented the principal component of John R. Bradley's Ph.D. thesis.

This study was undertaken to obtain data on the growth kinetics of grain boundary ferrite allotriomorphs in high-purity Fe-C-X alloys for the purpose

of evaluating several different models of their growth. Allotriomorphs were chosen as the morphology to be studied becasue they are considered to have the largest proportion of essentially disordered interfacial area of any of the basic Dube' (1) morphologies. As part of Bradley's M.S. thesis, an improved method for measuring the growth kinetics of grain boundary allotriomorphs was developed and applied to ferrite allotriomorphs formed in high-purity Fe-C alloys (2, 3). This method appreciably reduces the scatter in the growth kinetics data encountered with other techniques (4, 5, 6). Data were obtained in the alloys listed in Table I over the temperature ranges indicated; these ranges extended from close to the no-partition Ae3 temperature to the lowest temperature made practicable for accurate measurements by the kinetics of nucleation and growth.

Modeling ferrite allotriomorphs as oblate ellipsoids of revolution (2-7), theory (8) predicts that both the half-length, S/2, and the half-thickness, L/2, will vary parabolically with time, i.e., as $S/2 = \alpha t^{1/2}$ and $L/2 = \beta t^{1/2}$. A typical set of plots from which α and β are determined is shown in Figure 1. To test the validity of the assumption that parabolic growth kinetics obtain, ln S/2 and ln L/2 were plotted against ln t for all data sets. Figure 2 shows the data of Figure 1 replotted in this manner. The slopes are shown, typically, to approximate adequately the theoretically expected value of 1/2.

Experimental parabolic growth rate constants for thickening and lengthening in each alloy are presented as a function of isothermal reaction temperature in Figures 3-7. In each plot, a correction has been made for faceting of the allotriomorphs. This effect was found, in Fe-C alloys (3), to be more pronounced the smaller the undercooling below the Ae3 temperature, reducing the rate constants by about an order of magnitude below those calculated at the temperature closest to the Ae3 in each alloy. An approximate correction for faceting was made to the experimentally measured α values by multipying them by the ratio α(calculated)/α(experimental) obtained from an Fe-C alloy of essentially the same carbon content reacted at the

Table I. Alloy Composition (weight per cent) and Reaction Temperature Ranges

Alloy	C	X	Mn	Si	P	S	Temperature Range
A	0.40	1.73 Si	<0.002	-	0.001	0.006	725-825°C
B	0.12	3.28 Ni	<0.002	0.001	0.001	0.004	650-715°C
C	0.43	7.51 Ni	<0.01	<0.004	0.010	0.004	530-570°C
D	0.12	3.08 Mn	-	0.080	0.001	0.007	550-650°C
E	0.13	2.99 Cr	<0.002	0.001	0.001	0.006	600-800°C

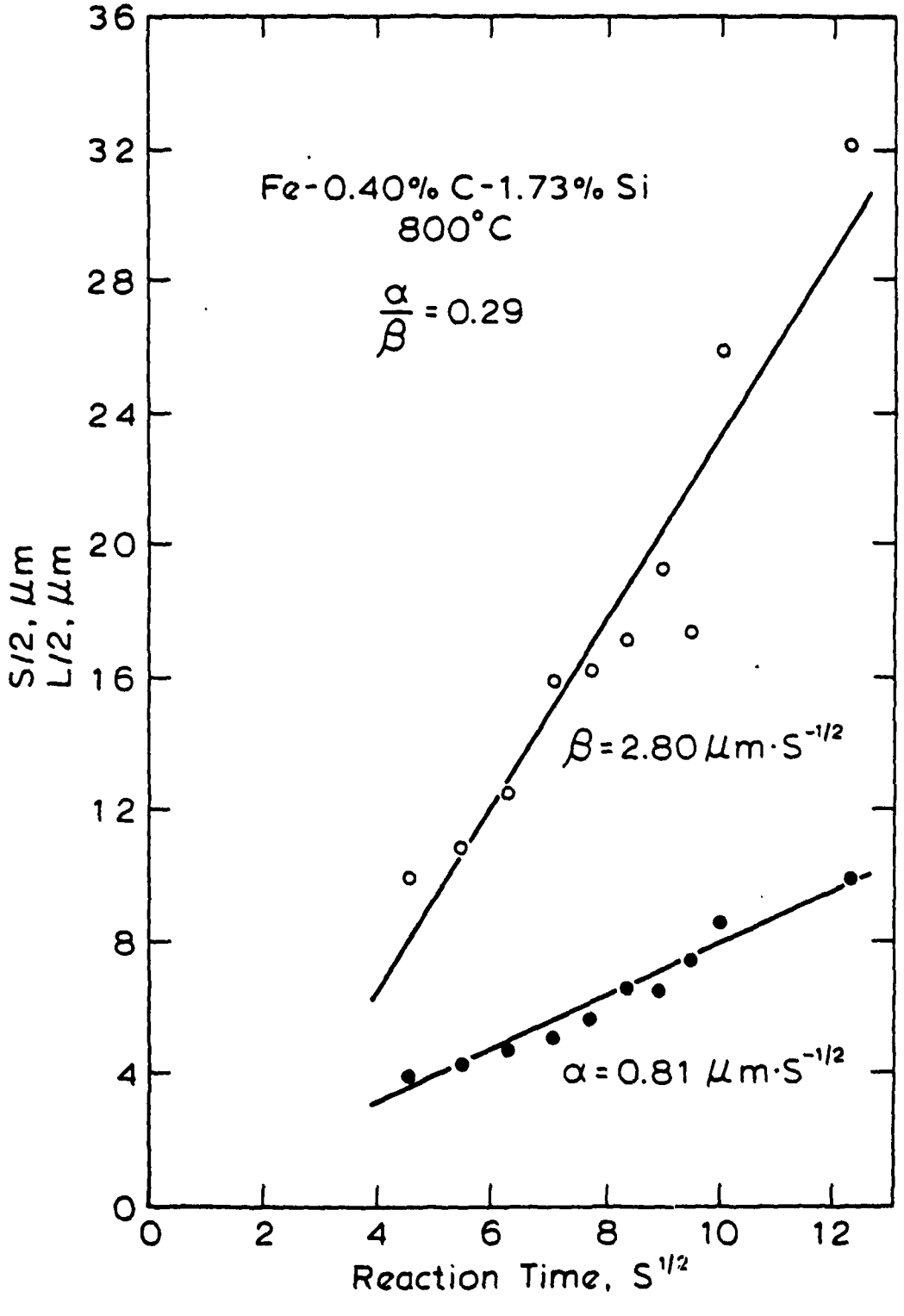
Fe-0.40% C-1.73% Si
800°C
α/β = 0.29
β = 2.80 μm·S^-1/2
α = 0.81 μm·S^-1/2
S/2, μm
L/2, μm
Reaction Time, S^1/2
0
4
8
12
16
20
24
28
32
36
0
2
4
6
8
10
12

Figure 1

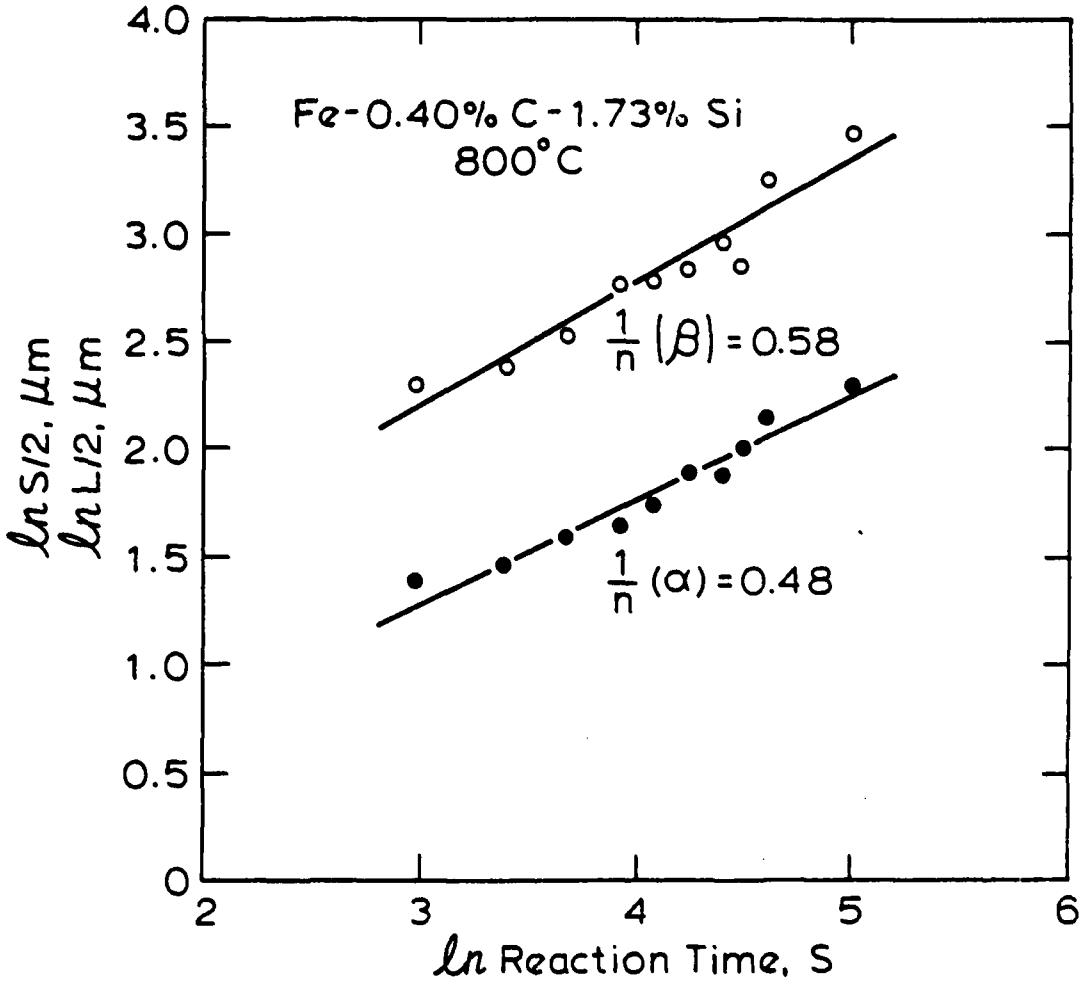
Fe-0.40% C-1.73% Si
800°C
$\frac{1}{n}(\beta) = 0.58$
$\frac{1}{n}(\alpha) = 0.48$
ln S/2, μm
ln L/2, μm
ln Reaction Time, S
4.0
3.5
3.0
2.5
2.0
1.5
1.0
0.5
0
2
3
4
5
6

Figure 2

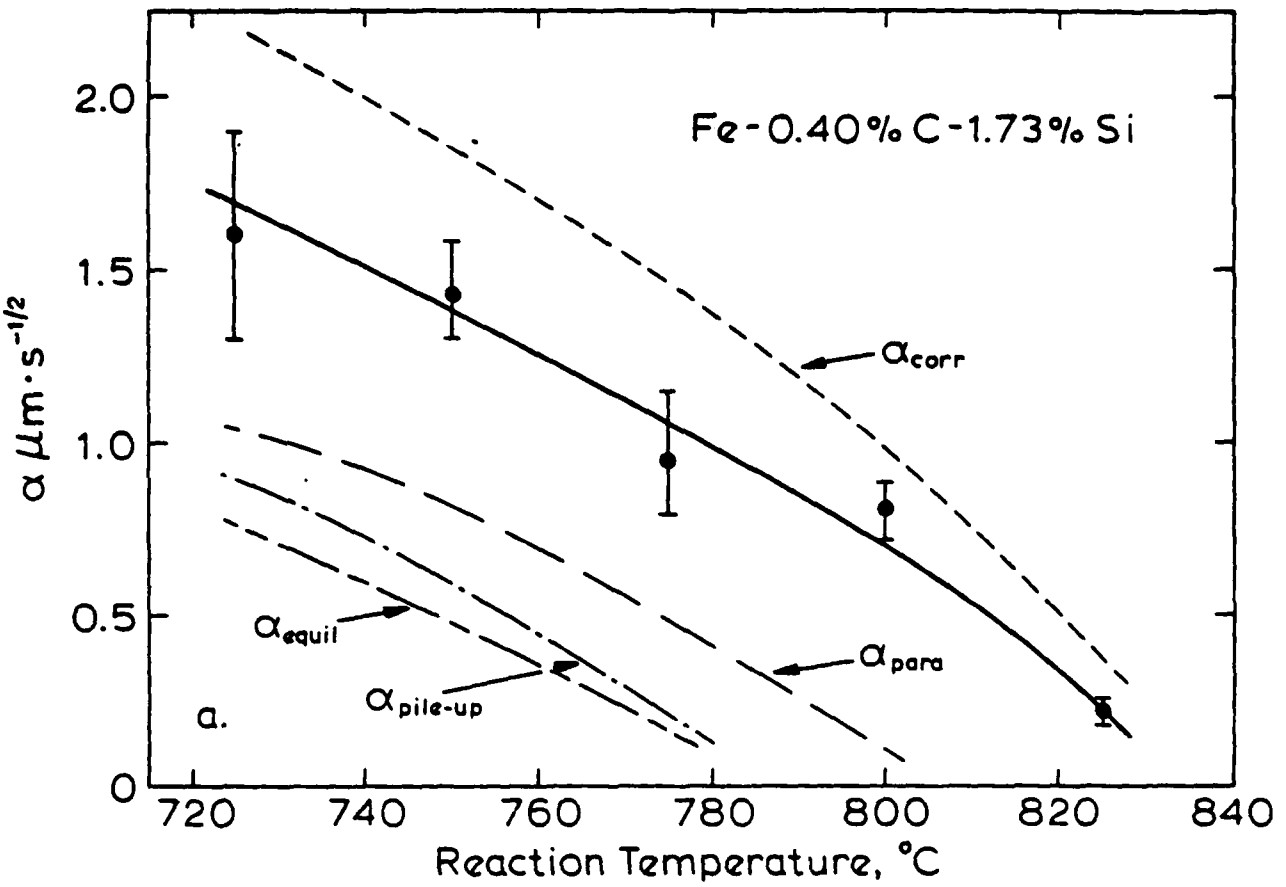
Fe-0.40% C-1.73% Si
α_{corr}
α_{equil}
α_{para}
$\alpha_{pile-up}$
a.
$\alpha\ \mu m \cdot s^{-1/2}$
2.0
1.5
1.0
0.5
0
720
740
760
780
800
820
840
Reaction Temperature, °C

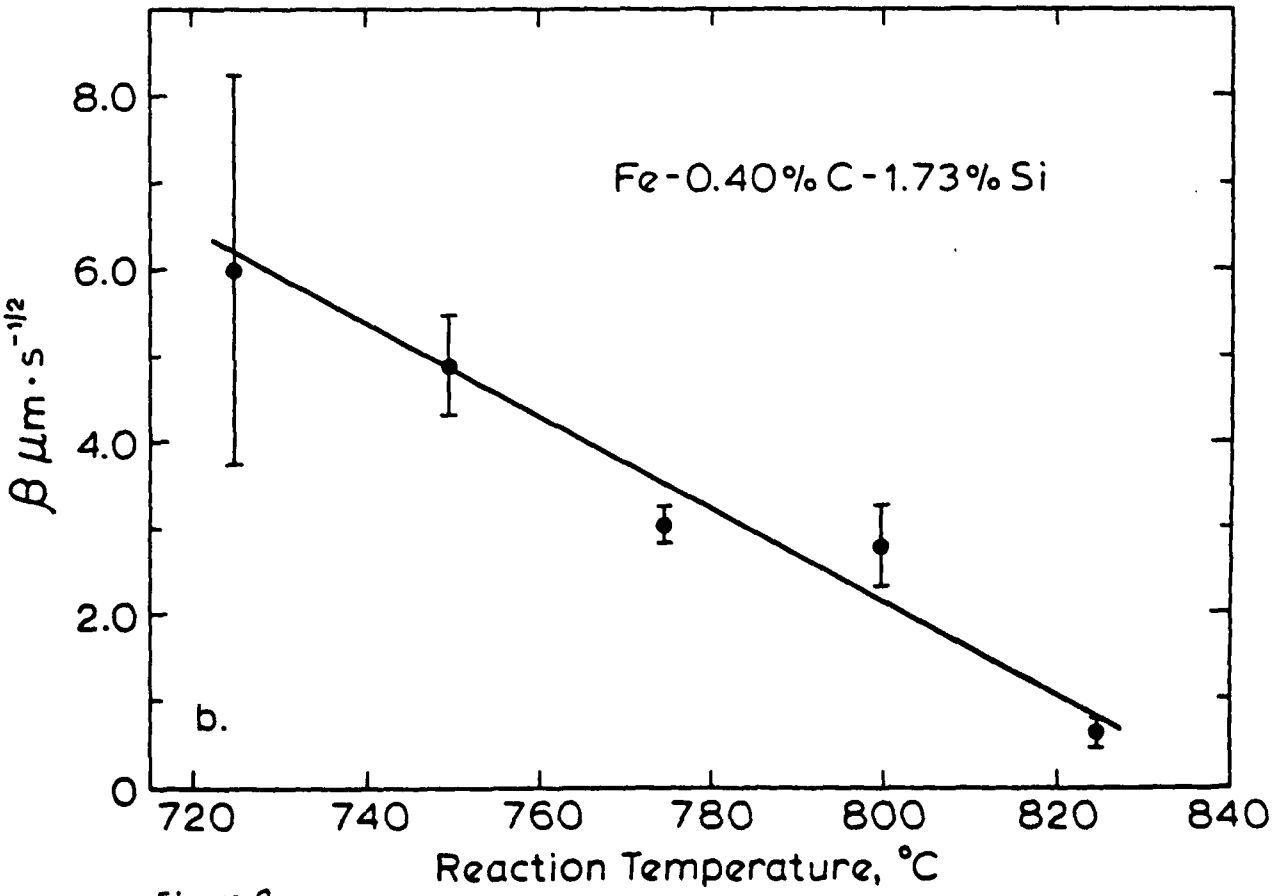
Fe-0.40% C-1.73% Si
b.
$\beta\ \mu m \cdot s^{-1/2}$
8.0
6.0
4.0
2.0
0
720
740
760
780
800
820
840
Reaction Temperature, °C

Figure 3

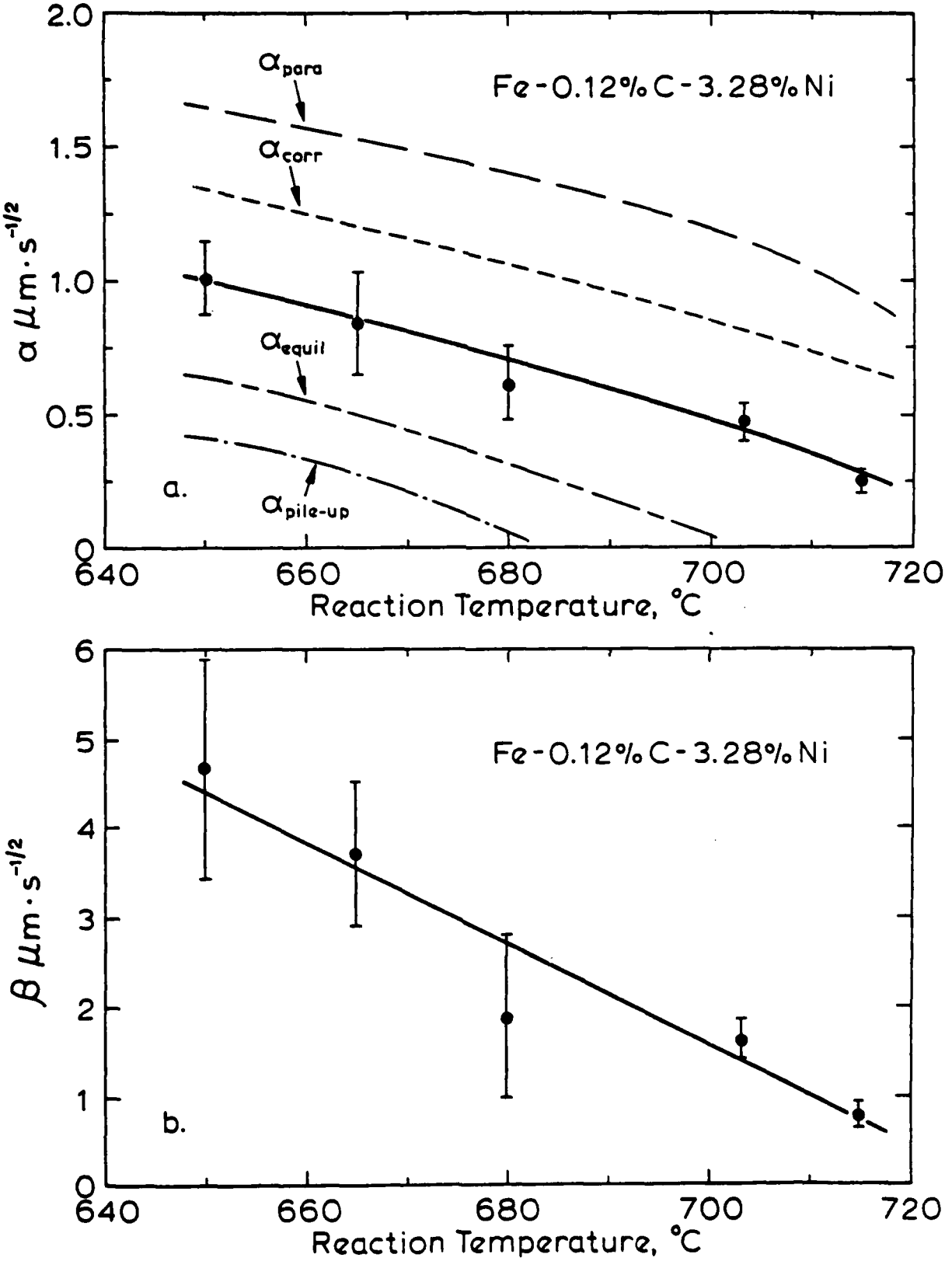
Fe-0.12% C-3.28% Ni
α_{para}
α_{corr}
α_{equil}
$\alpha_{pile-up}$
a.
$\alpha\ \mu m \cdot s^{-1/2}$
2.0
1.5
1.0
0.5
0
640
660
680
700
720
Reaction Temperature, °C
Fe-0.12% C-3.28% Ni
b.
$\beta\ \mu m \cdot s^{-1/2}$
6
5
4
3
2
1
0
640
660
680
700
720
Reaction Temperature, °C

Figure 4

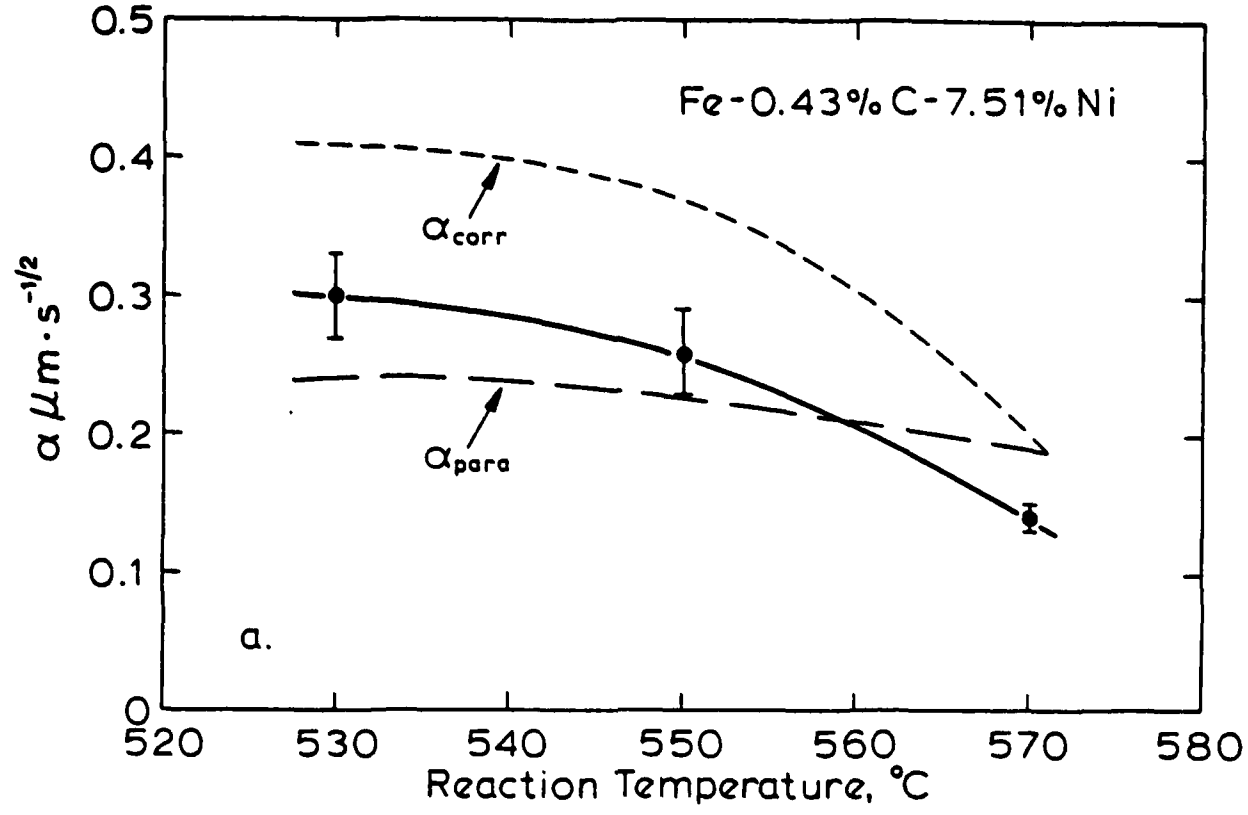
Fe-0.43% C-7.51% Ni
α_{corr}
α_{para}
a.
$\alpha\ \mu m \cdot s^{-1/2}$
0.5
0.4
0.3
0.2
0.1
0
520
530
540
550
560
570
580
Reaction Temperature, °C

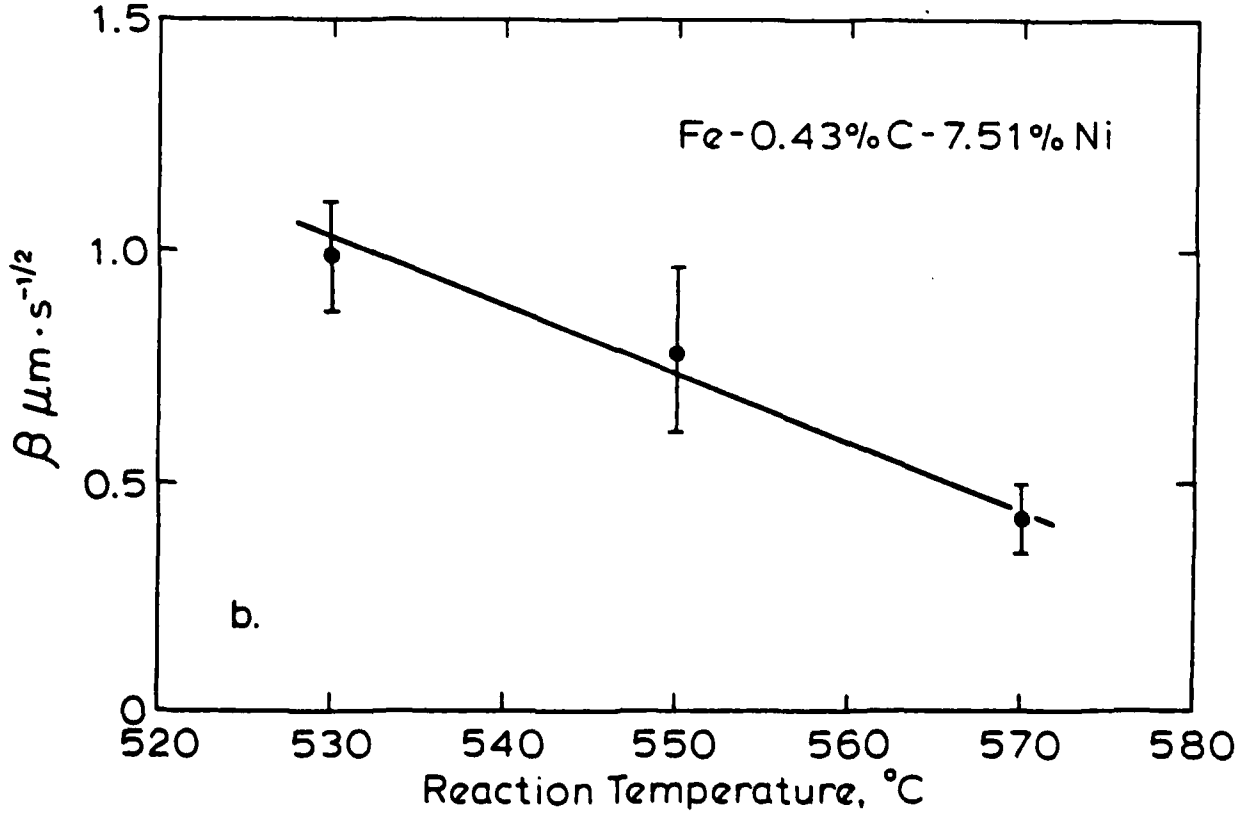
Fe-0.43% C-7.51% Ni
b.
$\beta\ \mu m \cdot s^{-1/2}$
1.5
1.0
0.5
0
520
530
540
550
560
570
580
Reaction Temperature, °C

Figure 5

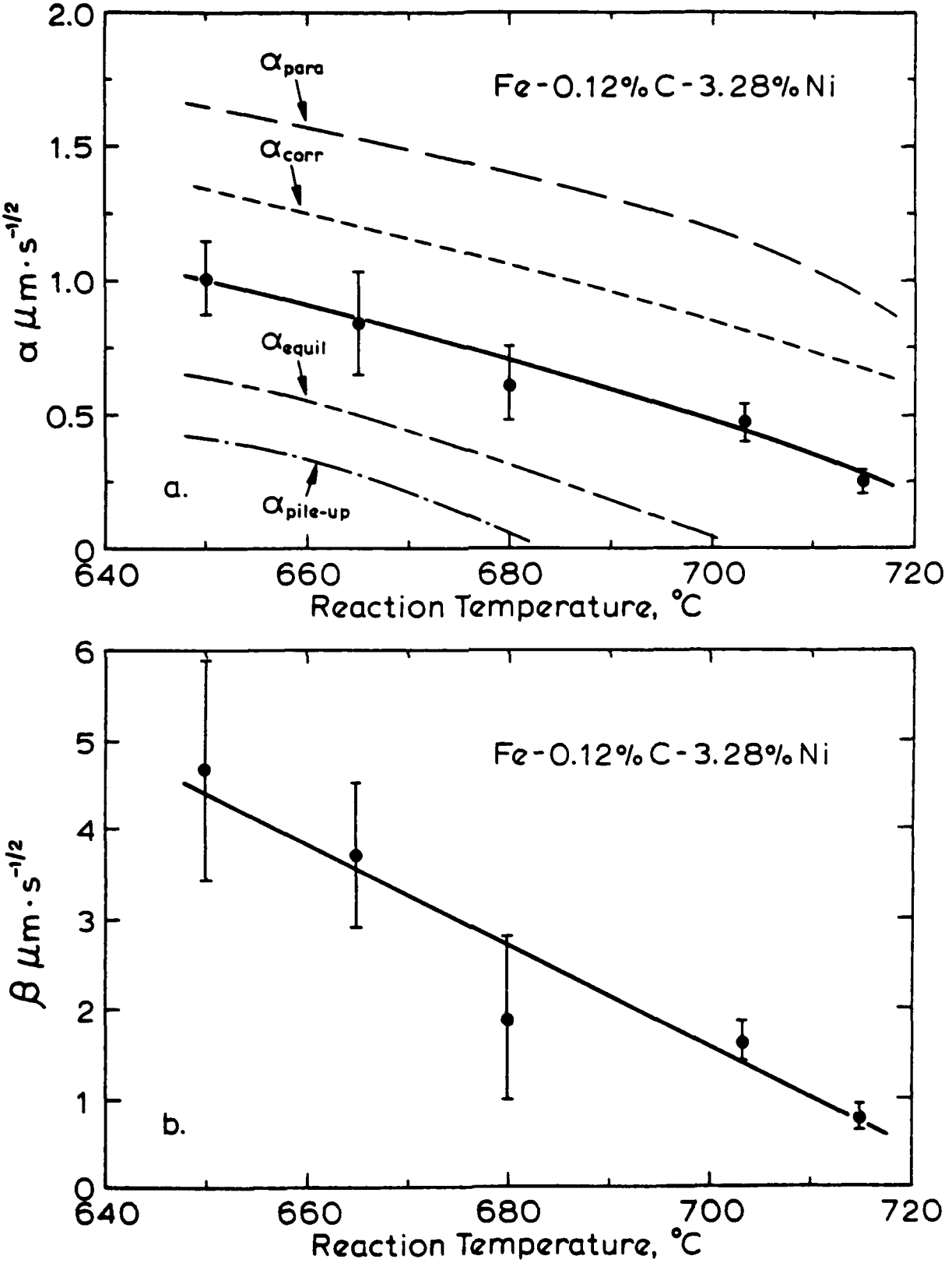
Fe-0.12% C-3.28% Ni
α_{para}
α_{corr}
α_{equil}
$\alpha_{pile-up}$
a.
$\alpha\ \mu m \cdot s^{-1/2}$
2.0
1.5
1.0
0.5
0
640
660
680
700
720
Reaction Temperature, °C
Fe-0.12% C-3.28% Ni
b.
$\beta\ \mu m \cdot s^{-1/2}$
6
5
4
3
2
1
0
640
660
680
700
720
Reaction Temperature, °C

Figure 4

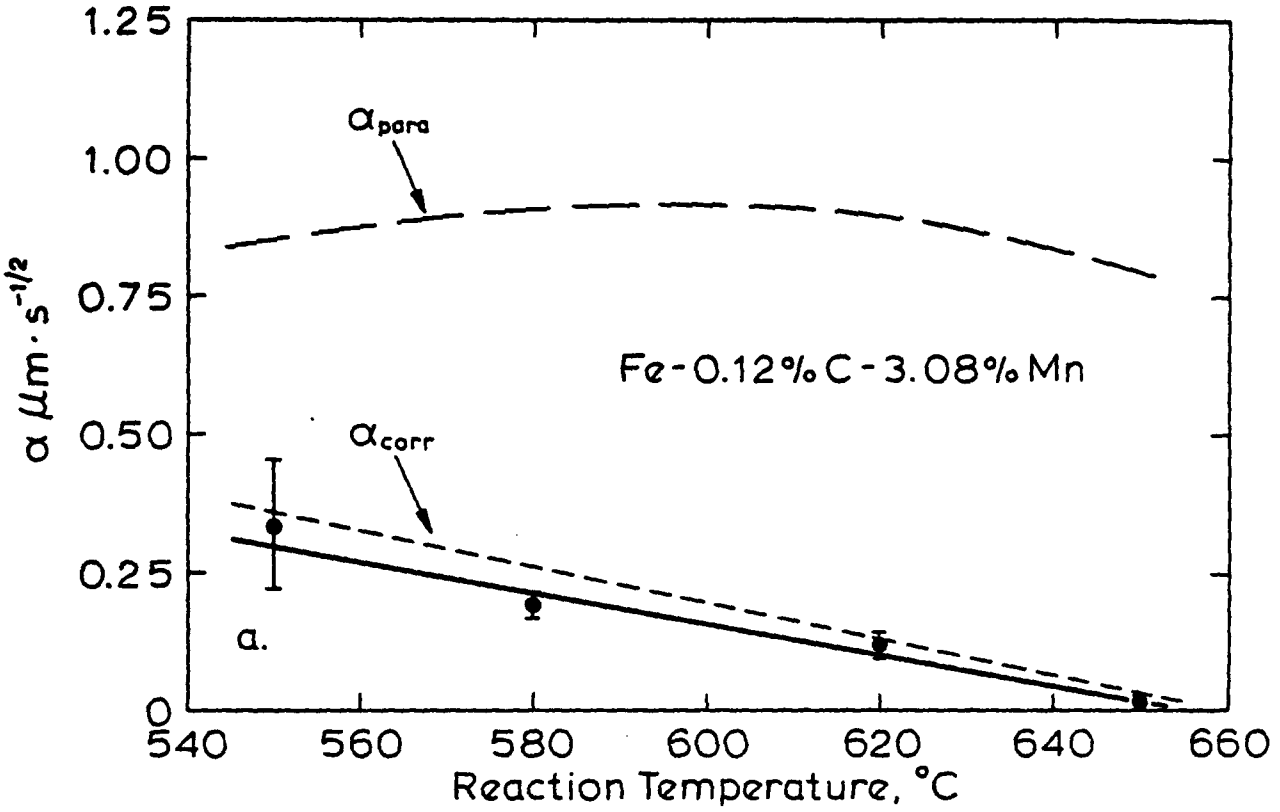
1.25
1.00
0.75
0.50
0.25
0
α μm · s^-1/2
α para
α corr
Fe - 0.12% C - 3.08% Mn
a.
540
560
580
600
620
640
660
Reaction Temperature, °C

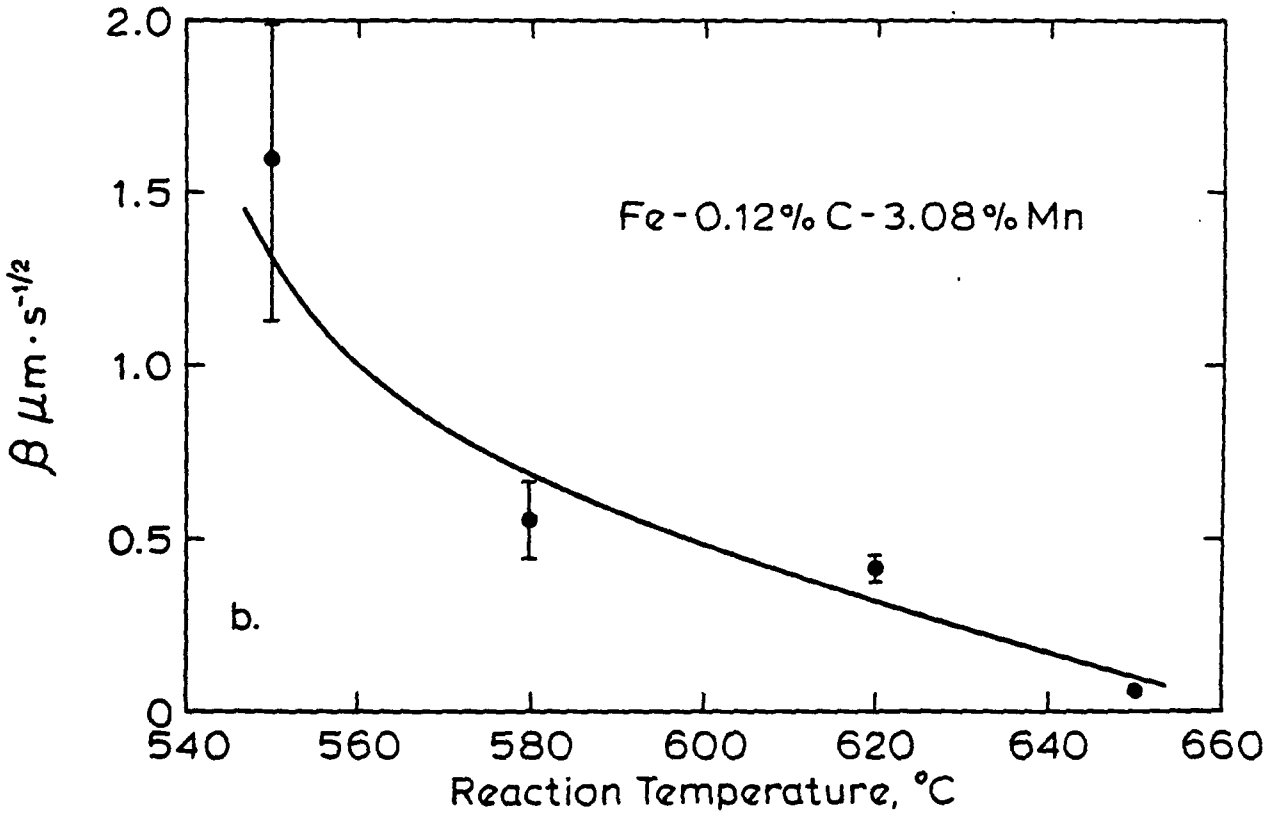
2.0
1.5
1.0
0.5
0
β μm · s^-1/2
Fe - 0.12% C - 3.08% Mn
b.
540
560
580
600
620
640
660
Reaction Temperature, °C

Figure 6

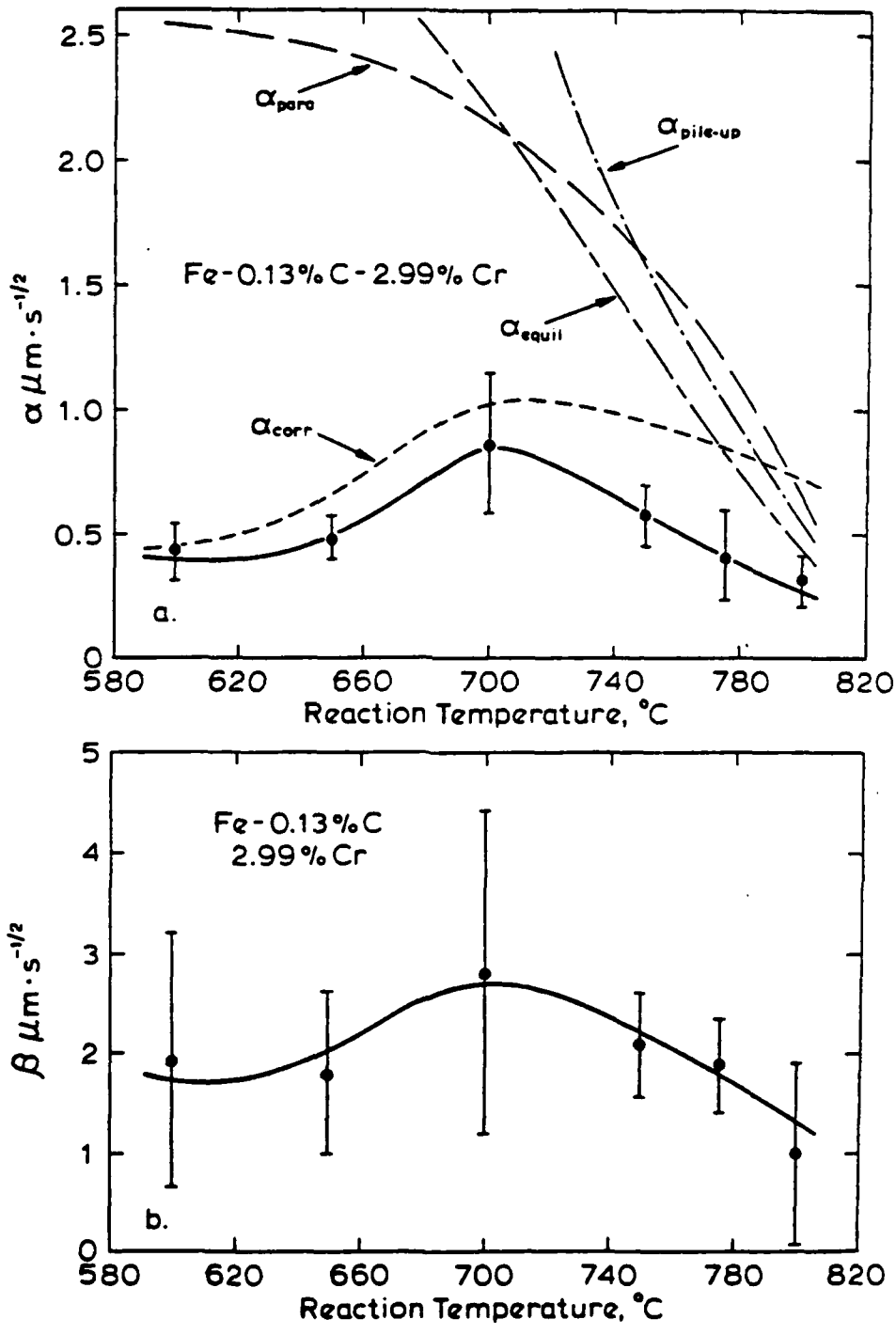
2.5
2.0
1.5
1.0
0.5
0
α μm·s^-1/2
α para
α pile-up
Fe-0.13% C - 2.99% Cr
α equil
α corr
a.
580
620
660
700
740
780
820
Reaction Temperature, °C
5
4
3
2
1
0
β μm·s^-1/2
Fe-0.13% C
2.99% Cr
b.
580
620
660
700
740
780
820
Reaction Temperature, °C

Figure 7

same undercooling. In Figures 3-7 the data points for the x_{corr} values are omitted in order to minimize crowding of the plots. As discussed below, no corection was made to the data on β because comparisons with theory were restricted to thickening kinetics.

Figure 8 shows schematic concentration-penetration curves for alloying element, X, through an austenite:ferrite boundary for the three different mathematically described models of ferrite growth kinetics applied to the experimental data. Part A of this Figure represents the equilibrium model; this is based on the assumption that the equilibrium concentrations of X are present in both austenite and in ferrite at the austenite:ferrite boundaries. This model has been analyzed in detail by members of the Kirkaldy-Purdy school (9-13). The diffusivity of carbon in austenite is usually 4-5 orders of magnitude higher than that of X at a given temperature. On the equilibrium model, however, the tie line across the $\alpha + \gamma$ phase field operative during growth connects interface compositions in the two phases with nearly identical X/Fe ratios at large undercoolings, thereby allowing growth to be controlled by the diffusion of carbon in austenite. Only at small undercoolings is the X/Fe ratio appreciably different across the α:γ boundary, and hence is ferrite growth controlled by X diffusion in austenite. Part B of Figure 8 is the "pile-up" model, wherein there is no bulk partition of X between the two phases (as obtains on the equilibrium model at low undercoolings); instead a "pile-up" of X develops immediately in front of the advancing boundaries, much like the prow wave of a ship (10, 14-17). In this situation, growth kinetics are controlled by the diffusion of carbon in austenite, but the carbon concentration in austenite in contact with the α:γ boundaries is modified, as described quantitatively by Hillert (16). Part C of Figure 8 illustrates the paraequilibrium model in which the X/Fe ratio is the same in both phases right up to the atomic planes forming the α:γ boundary (17-22). Again, growth is carbon diffusion-controlled, but yet another set of carbon concentrations in austenite and in ferrite at the α:γ boundaries is

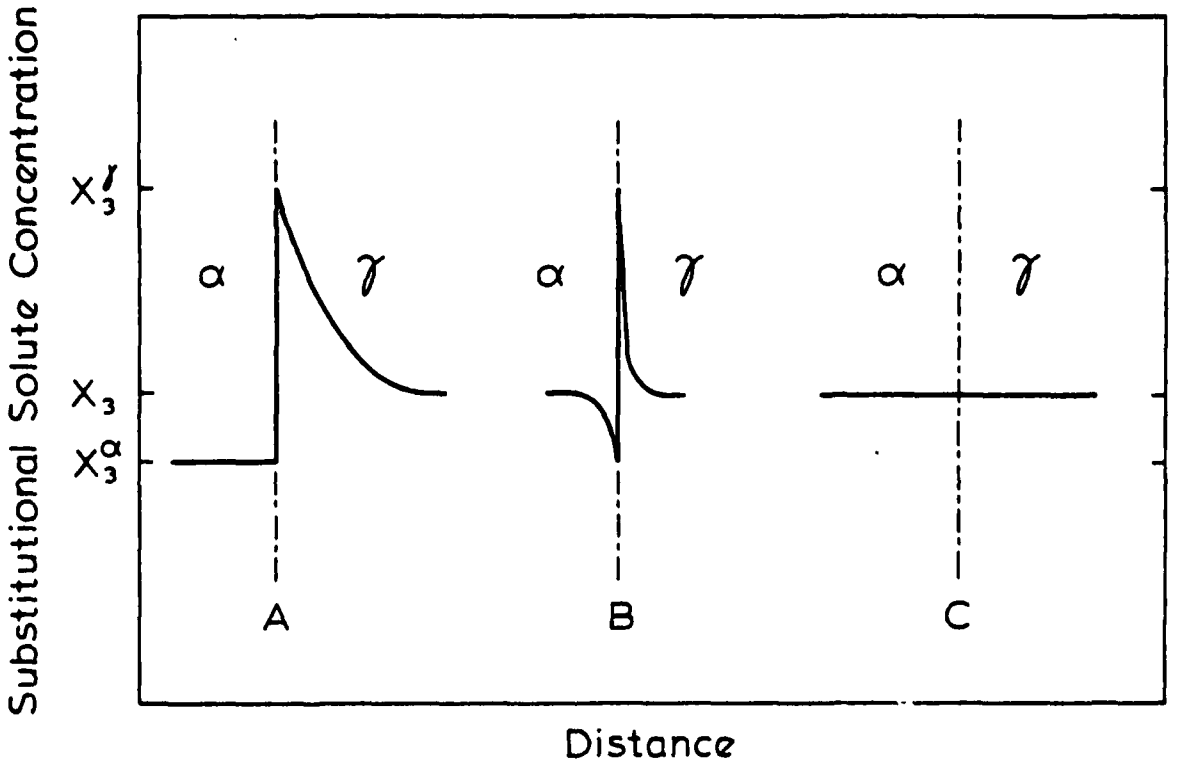
Substitutional Solute Concentration
X_3^γ
X_3
X_3^α
α
γ
α
γ
α
γ
A
B
C
Distance

Figure 8

appropriate at a given alloy composition and reaction temperature.

In order to apply these three models, it is necessary to evaluate accurately the temperature-composition paths of both the equilibrium and the paraequilibrium phase boundaries of the $\alpha + \gamma$ region. Our efforts to do this through application of the best available statistical thermodynamic treatments of the activity of carbon in Fe-C-X austenites having not yet achieved success, as discussed in a later section, we resorted to the more empirical, but carefully worked through and frequently applied ternary regular solution model of Hillert and Staffanson (23). The HS model yields the partial molar free energy of each species, Fe, C and X, in both phases. Equating the partial molar free energies of a given species in both phases permits the equilibrium concentrations at both phase boundaries to be calculated. In order to obtain the paraequilibrium concentrations, the precise thermodynamic definitions of Gilmour, Purdy and Kirkaldy (21) were applied to the HS partial molar free energies.

In order to avoid unnecessary mathematical complexity, the grain boundary allotriomorphs were treated as planes of infinite extent, rather than as oblate ellipsoids with an experimentally determined aspect ratio of 1/3 (the same as previously found for ferrite allotriomorphs in Fe-C alloys (3)). Calculation showed that this simplifying assumption did not introduce significant errors in the present context.

Application of the paraequilibrium model is straightforward. At each temperature of interest the calculated paraequilibrium phase boundary compositions (and of course the bulk carbon concentration of the alloy) are substituted into the Atkinson analysis (6, 24) for the migration kinetics of a planar interphase boundary. This analysis takes into account the influence of the variation of the diffusivity in the matrix phase with composition upon the parabolic rate constant, α. To use the pile-up model, a relationship developed by Hillert (17) is employed to compute the pile-up modified activity of carbon in austenite at the α:γ boundary.

This activity is then converted into an effective carbon concentration at the boundary through a relationship due to McLellan and Dunn (25). This concentration then replaces the paraequilibrium one in the Atkinson planar boundary analysis. In the case of the equilibrium model, it is necessary to make the further approximation that an average diffusivity of carbon in austenite can replace the concentration-dependent one: the available evidence indicates that this also did not introduce significant errors. The standard Dubé (26)-Zener (27) relationship for a planar boundary is used to express the connection between the alloying element diffusivity, the concentrations of alloying element at the boundary and in the bulk austenite, and α. The analogous expression for carbon was used in the modified form developed by Coates (12) in which the influence of the distribution of X about the boundary upon the flux of carbon is taken into account. This expression includes the off-diagonal diffusion coefficient of carbon as modified by the presence of X, which was evaluated through an expression due to Kirkaldy and co-workers (28, 29); the Wagner interaction parameters needed to apply this expression have recently been tabulated by Kirkaldy, Thomson and Baganis (30). The two equations thus written contain five unknowns: α and four phase boundary compositions. Fortunately, only one of these compositions is independent, the others being determined by the equilibrium tie-line. The equilibrium $\gamma/(\alpha + \gamma)$ and $\alpha/(\alpha + \gamma)$ phase boundaries calculated at each temperature on the HS model were expressed as fourth order least squares polynomials. These were substituted into the two equations for α and the resulting relationships were solved numerically by a Newton-Raphson technique for each alloy at each reaction temperature.

Some of the values of α calculated on the three foregoing models are plotted as a function of temperature in Figures 3-7. However, the results of these calculations may be most conveniently evaluated by means of Figures 9-11, where the ratio of α_{corr} to the various calculated α's is plotted as a function of temperature for all alloys.

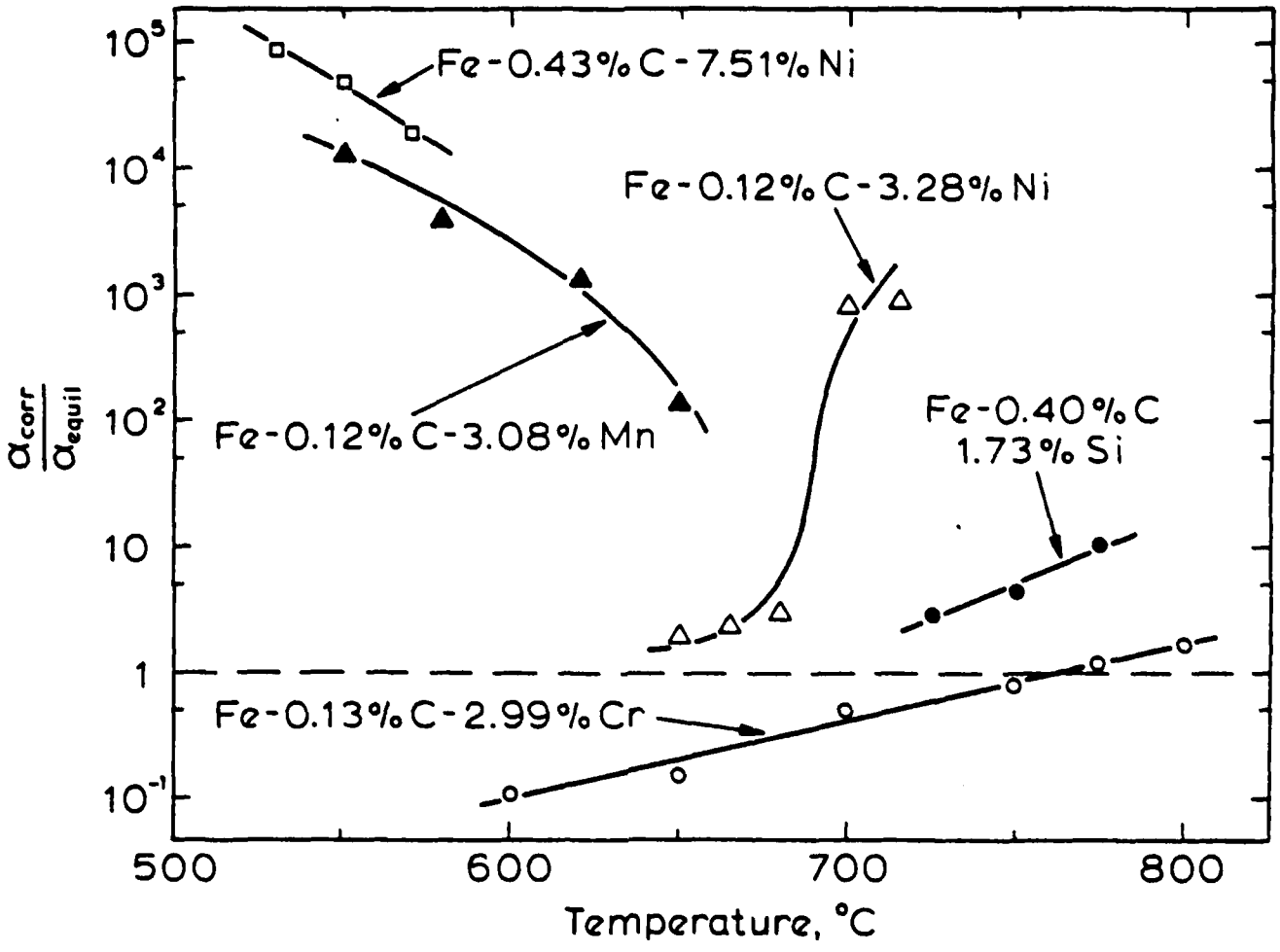
Fe-0.43% C-7.51% Ni
Fe-0.12% C-3.28% Ni
Fe-0.12% C-3.08% Mn
Fe-0.40% C
1.73% Si
Fe-0.13% C-2.99% Cr
$\frac{\alpha_{corr}}{\alpha_{equil}}$
10^5
10^4
10^3
10^2
10
1
10^{-1}
500
600
700
800
Temperature, °C

Figure 9

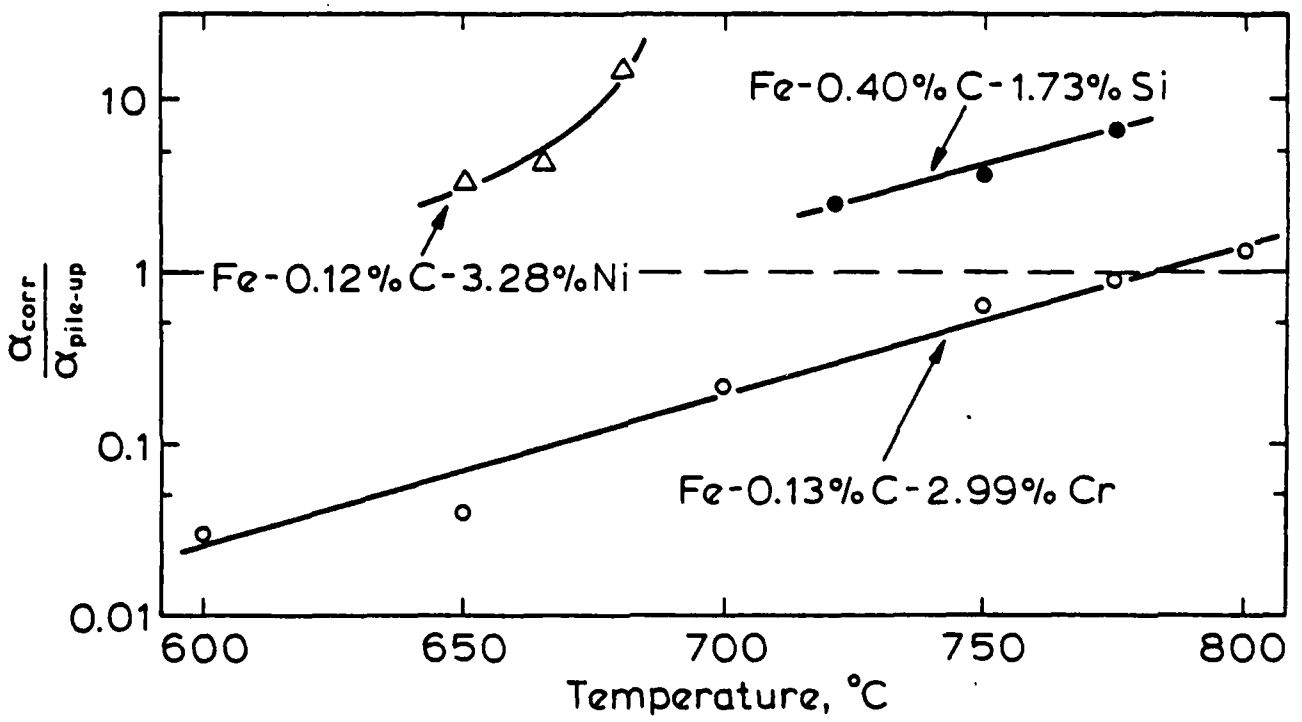
10
1
0.1
0.01
$\frac{\alpha_{corr}}{\alpha_{pile-up}}$
Fe-0.40% C-1.73% Si
Fe-0.12% C-3.28% Ni
Fe-0.13% C-2.99% Cr
600
650
700
750
800
Temperature, °C

Figure 10

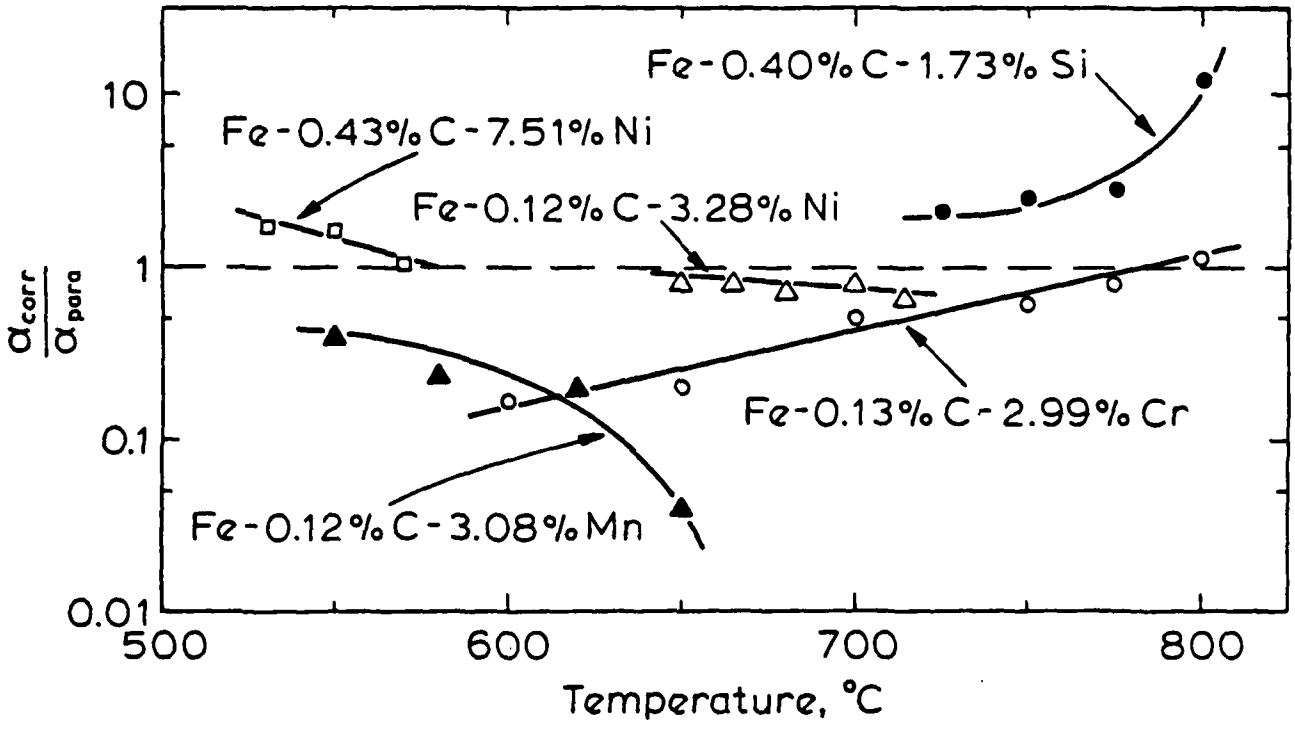
Fe-0.40% C-1.73% Si
Fe-0.43% C-7.51% Ni
Fe-0.12% C-3.28% Ni
Fe-0.13% C-2.99% Cr
Fe-0.12% C-3.08% Mn
10
1
0.1
0.01
500
600
700
800
Temperature, °C
$\frac{\alpha_{corr}}{\alpha_{para}}$

Figure 11

Figure 9, presenting $\alpha_{corr}/\alpha_{equil}$ vs. temperature for the five steels studied, shows that this ratio is in the range 10^2-10^5 at all temperatures employed for the Fe-C-Mn and for the high-Ni Fe-C-Ni alloys, and at smaller undercoolings for the low-Ni Fe-C-Ni alloy. These ratios lie well outside any plausible errors of measurements and calculation and demonstrate that the equilibrium model cannot apply to these alloys and reaction temperatures. On the other hand, at larger undercoolings in the low-Ni Fe-C-Ni alloy and at all temperatures studies in the Fe-C-Si and the Fe-C-Cr alloys, $\alpha_{corr}/\alpha_{equil}$ lies within $\pm$ one order of magnitude of unity and thus the equilibrium model may be applicable under these circumstances. Figure 10 is a comparable plot for $\alpha_{corr}/\alpha_{pile\ up}$; ratios are not shown for the high-Ni Fe-C-Ni and the Fe-C-Mn alloys because Hillert's procedure for obtaining the effective carbon concentration in austenite at the austenite:ferrite boundary yields concentrations less than those in the bulk alloy. For the other three alloys $\alpha_{corr}/\alpha_{pile\ up}$ is within an order of magnitude of unity except at the two lower reaction temperatures in the Fe-C-Cr alloy. Figure 11 demonstrates that, except at the highest temperature in the Fe-C-Mn alloy $\alpha_{corr}/\alpha_{para}$ is also within an order of magnitude of unity. Hence complete discrimination among the three different models cannot be achieved by comparing the values of α which they predict with α_{corr}.

Resort was accordingly made to an older method, proposed by Kinsman and Aaronson (5), in which the maximum penetration distance of X into austenite was calculated as a function of composition and reaction temperature by means of a linearized concentration gradient approximation. Figure 12 shows that, except at the highest reaction temperatures in the Fe-C-Si and the Fe-C-Cr alloys, this distance, ℓ_{max}, is less than a single lattice parameter. The results of Figure 12 are thus consistent only with the paraequilibrium model.

However, closer inspection of Figure 11 shows that, despite the accuracy of both the experimental measurements and the probably nearly as accurate theoretical

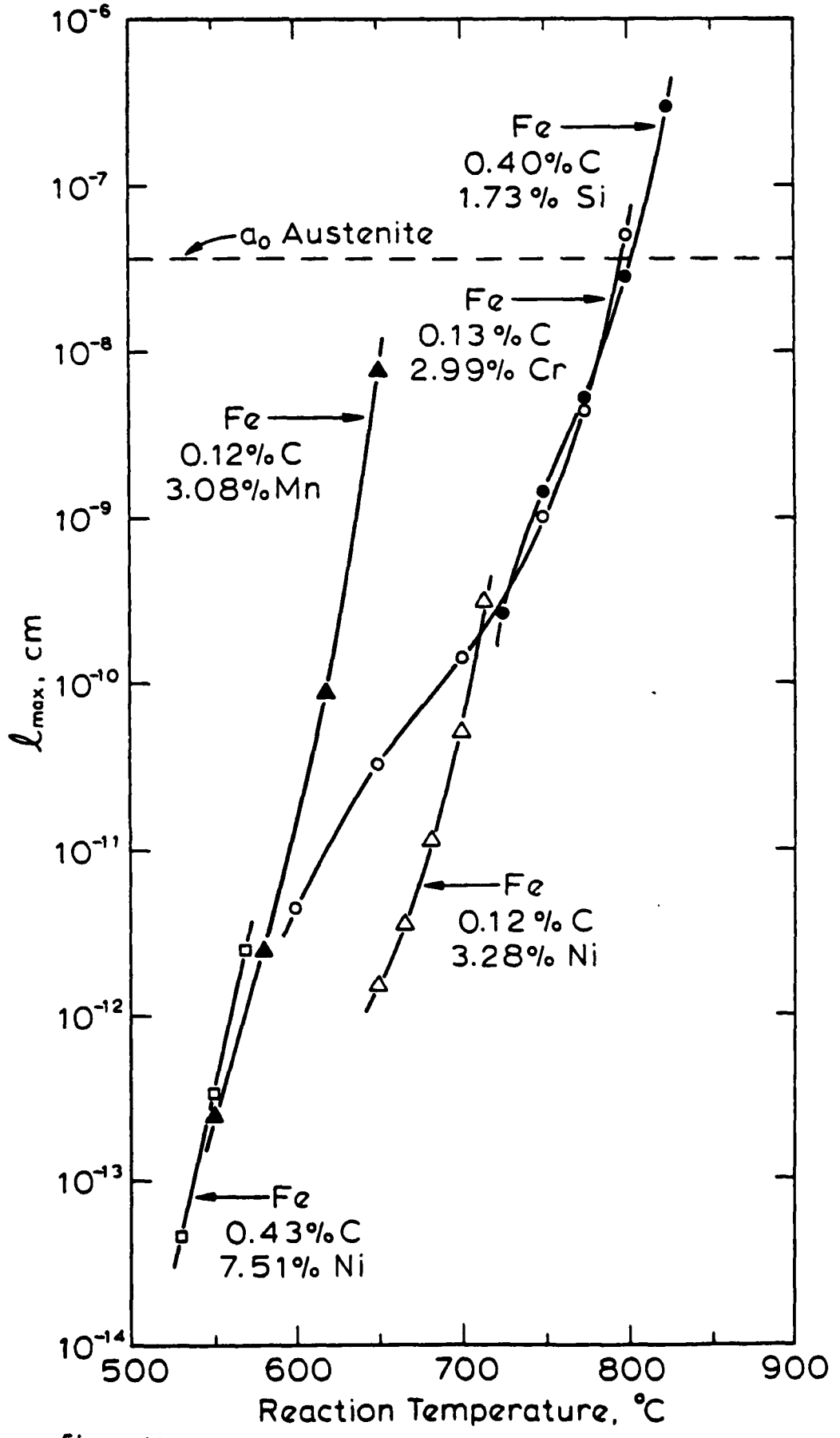
10^{-6}
10^{-7}
10^{-8}
10^{-9}
10^{-10}
10^{-11}
10^{-12}
10^{-13}
10^{-14}
ℓ_{max}, cm
a_o Austenite
Fe
0.40% C
1.73% Si
Fe
0.13% C
2.99% Cr
Fe
0.12% C
3.08% Mn
Fe
0.12% C
3.28% Ni
Fe
0.43% C
7.51% Ni
500
600
700
800
900
Reaction Temperature, °C

Figure 12

calculations, agreement between α_{corr} and α_{para} is satisfying only in the low-Ni Fe-C-Ni alloy. In both the Fe-C-Mn and the Fe-C-Cr alloys, α_{para} falls well below α_{corr} over most or all of the temperature ranges investigated. Results of this type have been previously ascribed to a solute drag-like effect (4), and are so explained here. On this view, an alloying element which markedly decreases the activity of carbon in austenite and also exhibits an appreciable size misfit with respect to iron in the austenite and/or the ferrite lattices will tend to segregate to disordered areas of austenite:ferrite boundaries. A "spike" of X which is contained wholly within these boundaries results. By reducing the activity of the carbon in austenite in contact with these boundaries the carbon concentration gradient driving the growth of ferrite is reduced, and hence so is α. The finding that $\alpha_{para} \gtrsim \alpha_{corr}$ when X is Mn or Cr but not when X is Ni or Si is consistent with this prediction.

A quantitative analysis of this concept, such as already exists for the somewhat similar phenomena of solute drag during grain growth (31-33) and the massive transformation (33) is not yet available. However, a preliminary treatment can be attempted through the use of existing theory for segregation to stationary grain boundaries. Guttmann (34) has analyzed the simultaneous segregation of interstitial and substitutional solutes to grain boundaries. However, this analysis requires information on the segregation of both X and C to grain boundaries; as will next be shown only the concentration of X at austenite:ferrite boundaries can be estimated from the growth kinetics data. Hence it is necessary to use simpler McLean adsorption isotherm (35) originally derived for binary alloys:

$$x_3^{\alpha\gamma} = \frac{x_3 e^{\Delta G_3/RT}}{1 - x_3 + x_3 e^{\Delta G_3/RT}} \qquad [1]$$

where $x_3^{\alpha\gamma}$ is the concentration of X in austenite:ferrite boundaries, x_3 is the bulk concentration of X (the same in both phases) and ΔG_3 is the adsorption free energy of X to austenite:ferrite boundaries. Estimation of $x_3^{\alpha\gamma}$ is accomplished

through the following procedure. Using the paraequilibrium approach and the planar Atkinson analysis, the value of x_2^{γ}, the atom fraction of carbon in γ at α:γ boundaries, required to bring the calculated α_{para} into agreement with α_{corr}, $x_2^{\gamma'}$ (the effective Ae3), is first computed. $x_3^{\alpha\gamma}$ is computed by varying x_3 in the paraequilibrium Ae_3 calculations until $x_2^{\gamma} = x_2^{\gamma'}$. Calculated values of ΔG_3, as well as $x_2^{\gamma'}$ and $x_3^{\alpha\gamma}$, for each reaction temperature are given in Table II.

One of the components of ΔG_3 should be the elastic strain energy of misfitting X atoms, W. This can be calculated from the relationship (35):

$$W = \frac{24\pi KGr^3\varepsilon^2}{3K + 4G} \qquad [2]$$

where K is the bulk modulus of X, G is the shear modulus of the Fe matrix, r is the atomic radius of X atoms in solid solution and $\varepsilon = (r_3 - r_1)/r_3$ where r_1 and r_3 are the radii of pure iron and pure X, respectively. Table II gives the W's associated with austenite and with ferrite. The strain energies are considered independent of temperature since the component parameters do not vary appreciably over the temperature ranges used. Only in the case of the Mn alloy are unreasonably large values of W obtained; these probably follow from unsuitable values of parameters used in Eq. [2], resulting from the complex crystal structures of Mn. The complete mutual solid solubility of Fe and Mn in the f.c.c. structure (37) supports the conclusion that these data should be ignored. Also included in Table II are values of the Wagner interaction parameter ε_{23} for α at 800°K (36) and for γ at 1000°K (30), where $\varepsilon_{23} = \partial \ln a_2/\partial X_3$ and a_2 = activity of carbon.

In the case of Si, the high strain energies apparently offset an appreciable C-Si repulsion; Si becomes concentrated at disordered austenite:ferrite boundaries, the activity of carbon in austenite in contact with these boundaries is increased and hence so is α. Although a similar opposition of W and $\varepsilon_{23}^{\gamma}$ obtains for Ni (no data on $\varepsilon_{23}^{\alpha}$ appear to be available), neither is particularly large and it is thus not surprising that they balance each other well enough so that $\alpha_{corr} \simeq \alpha_{para}$

TABLE II. Solute Drag Effect Treatment of Growth Kinetics Data

Alloy	T°C	$x_2^{\gamma'}$	$x_3^{\alpha\gamma}$	x_3	ΔG_3 kJ/mole	W_α kJ/mole	W_γ kJ/mole	$\varepsilon_{23}^{\gamma}$ at 727°C (30)	$\varepsilon_{23}^{\alpha}$ at 527°C (36)
.40%C-1.73%Si	800	0.0228	0.0686		6.79				
	775	0.0258	0.0536		4.34				
	750	0.0342	0.0812	0.0333	8.02	25.9	94.3	+12.2	+11.8
	725	0.0404	0.0776		7.41				
0.12%C-3.28%Ni	715	0.0068	0.0353		0.58				
	700	0.0096	0.0358		1.18				
	680	0.0130	0.0404	0.0311	2.15	0.18	17.3	+ 5.4	N.A.
	665	0.0182	0.0417		2.38				
	650	0.0234	0.0437		2.70				
0.43%C-7.51%Ni	570	0.0284	0.0804		0.98				
	550	0.0409	0.0798	0.0706	0.91	0.18	17.3	+ 5.4	N.A.
	530	0.0488	0.0835		1.21				
0.12%C-3.08%Mn	650	0.0054	0.0460		3.09				
	620	0.0074	0.0515		3.87				
	580	0.0126	0.0547	0.0312	4.16	109.3	252.1	- 5.1	-96.7
	550	0.0252	0.0525		3.71				
.13%C-2.99%Cr	800	0.0065	0.0350		0.85				
	775	0.0072	0.0493		3.96				
	750	0.0089	0.0591	0.0319	5.49	0.5	14.6	-14.0	-65.6
	700	0.0151	0.0666		6.25				
	650	0.0142	0.1082		10.01				
	600	0.0195	-		-				

for the two Fe-C-Ni alloys. The absence of good values of W for Mn complicates assessment of the influence of this element; however, the very large negative value of $\varepsilon_{23}^{\alpha}$ forecasts significant adsorption of Mn to austenite:ferrite boundaries. Since $\varepsilon_{23}^{\gamma} < 0$, a significant diminution of the activity of carbon in the austenite in contact with austenite:ferrite boundaries in Fe-C-Mn, and thus of growth kinetics is expected and is experimentally observed. Although $\alpha_{corr}/\alpha_{para}$ for the Cr alloy becomes less than that for Mn at low temperatures (Fig. 11), and a bay in the TTT-curve for initiation of the proeutectoid ferrite reaction appears in the Cr but not in the Mn alloy, the average ε_{23} for Mn is more negative. Although the W's for Mn have not been satisfactorily estimated, they seem unlikely to differ much from those for Cr. A possible explanation for the greater solute drag-like effect evidently exerted by Cr is that $\varepsilon_{23}^{\gamma}$ may be more influential than $\varepsilon_{23}^{\alpha}$ because the carbon concentration in austenite in contact with the boundary is the one which actually controls growth kinetics at a given temperature and composition.

Comparison of the foregoing considerations with ΔG_3 cannot be effected quantitatively because free energies have not yet been obtained for C-X interactions. Since this investigation was completed, however, it has been recognized that such a calculation may be possible upon the basis of the analyses of the thermodynamics of Fe-C-X alloys developed by Alex and McLellan (37); this matter is now being further pursued. Qualitatively, though, it seems worthwhile to note that the opposed effects of W and ε_{23} for Si and Ni yield values of ΔG_3 smaller than the average of W_{α} and W_{γ}. In the case of Cr, on the other hand, the average W exceeds ΔG_3 except at the higher temperatures, suggesting that ε_{23} may be the more important factor in determining the solute drag-like effect.

Although placing this effect on a firmer analytic basis now appears to be of considerable importance and will be emphasized during the proposed three year extension of this Grant, the foregoing considerations at least suggest that this mechanism may be a useful approach to explaining the discrepancies found between

α_{corr} and α_{para}. As described in a later section, this effect may also be able to explain the occurrence of incomplete ferrite transformation in the presence of sufficient concentrations of C and of X.

Alternate explanations for $\alpha_{corr} < \alpha_{para}$ must now be briefly considered. The Hultgren (38) explanation for the bay in the TTT-curve for the initiation of transformation in alloy steels containing an appreciable proportion of an alloying element which markedly decreases the activity of carbon in austenite is also relevant to the present situation. Hultgren proposed that equilibrium partition of X takes place betweeen austenite and ferrite above but not below the bay. This explanation has been disproved by electron probe analysis studies (39, 40) and also by the results of the present investigation. Sharma and Purdy (41) have proposed that clustering of X and C atoms, GP zone formation or carbide precipitation, all taking place wholly within austenite, might interfere with motion of austenite:ferrite boundaries. The clustering phenomenon, however, would be accounted for in the Hillert-Staffanson expressions for the partial molar free energies of carbon and X, and would be introduced into the growth rate equations by the equilibrium and paraequilibrium phase boundaries for the austenite + ferrite region thus calculated. GP zone formation has yet to be detected in low alloy austenite, though this would admittedly be quite difficult to do experimentally because the austenite is destroyed by the martensite transformation during quenching. Carbide formation wholly within austenite should increase rather than reduce the driving force for ferrite growth.

A more attractive alternate mechanism for interference with ferrite growth kinetics has recently been offered by Purdy (42, 43). On the basis of at-temperature observations made with a high-voltage transmission electron microscope, he suggested that carbide precipitation at interphase boundaries may be responsible for slower than expected ferrite growth kinetics. An investigation of the present alloys conducted specifically for the purpose of checking this suggestion is

reported in the next sub-section. At least for the alloys used in this study, this idea will be shown to be inappropriate. In fact, it will be noted in Fig. 11 that in the high-Ni Fe-C-Ni and in the Fe-C-Si alloys, α_{corr} significantly exceeds α_{para}. In the next section the probably origin of these results is shown to be the precipitation of carbides at austenite:ferrite boundaries.

D. Carbide Precipitation in Association With Proeutectoid Ferrite

1. Introduction

This subject has been the subject of intensive study at many laboratories within the past decade and has been greatly facilitated by the high resolution visual, crystallographic and chemical analysis capabilities of modern transmission electron microscopy. The work on this subject in Fe-C-X alloys by the Honeycombe group at Cambridge University has been particularly important. As summarized in a review lecture (44), Honeycombe notes that this type of carbide precipitation takes three principal forms: wholly within ferrite (usually but not always on dislocations); at austenite:ferrite boundaries in sheet-like arrays of discrete carbides, virtually all of which have identical spatial orientations along an austenite:ferrite boundary with a constant orientation; and at austenite:ferrite boundaries in the form of "fibrous carbides," with the fibers being parallel, very thin and very closely spaced. This morphological classification scheme contains important information on the origins of the carbides and thus on the role which they play in the decomposition of austenite. It will accordingly be seen to have comprised a significant proportion of the knowledge base underlying all three investigations in this area recounted in the following sub-sections.

2. Carbide Precipitation in Association with Proeutectoid Ferrite in the "Bradley Alloys"

Following publication of Purdy's (42, 43) papers on observations of carbide precipitation in association with ferrite in a molybdenum steel, and the preliminary TEM studies performed by Mr. Gary J. Shiflet (Republic Steel Corp. Fellow) on the

incomplete transformation phenomenon in Fe-C-Mo alloys (discussed in section II-D), in which he found unexpectedly high densities of very fine carbides within ferrite even when only 1-2% ferrite was present, the possibility was recognized that the results of Bradley's investigation of ferrite growth kinetics just described might have been significantly influenced by carbide precipitation in association with the ferrite allotriomorphs. The decision was therefore made to investigate carbide precipitation in each of Bradley's alloys within the temperature-time envelopes in which the growth kinetics measurements were made. The TEM portion of this study was performed by Mr. Shiflet, with Mr. Bradley supplying specially heat treated specimens of a size appropriate for thin foil preparation. This investigation was originally envisaged as a brief one. However, two factors considerably prolonged it. One was the small amounts of ferrite present when the growth kinetics studies were made; in order to study carbides in an adequate number of allotriomorphs extensive ion milling had to be undertaken in order to displace the electron transparent areas to the allotriomorphs. The second was the wide range of carbide morphologies often found in a given specimen; that this would occur was not wholly evident from the literature. Hence extensive studies had to be made of each specimen before conclusions could be safely drawn as to the nature of carbide precipitation within it.

These studies, which have now been completed and are being written up for publication, yielded the following results. In all but the Si alloy, it proved possible, though not easy, to determine the crystal structure of the carbides by means of selected area diffraction. Invariably the carbides had the orthorhombic lattice of cementite and should thus be considered $(Fe, X)_3C$. In the case of the Si steel, the carbide was almost certainly cementite, but containing a negligible proportion of Si. In the Fe-C-Cr alloy, no carbides were found within the time-temperature region investigated. In the Mn alloy, carbides were found at only one temperature, 600°C, and only at dislocations within the ferrite.

Figure 13 is a bright field TEM micrograph of such precipitation; the same area is shown in dark field in Figure 13b; the observation that many (if not all) of the carbides are illuminated by the same reflection, added to the finding that they are formed in rows, supports the conclusion that the carbides formed on dislocations. Such precipitation may possibly alter slightly the carbon concentration in ferrite at the austenite:ferrite boundaries, and thus in austenite at these boundaries, but the effect on the latter, and hence on the parabolic rate constants, is necessarily small--and will not occur at all unless such carbide precipitation occurs promptly and repeatedly on dislocations located quite close to the moving austenite:ferrite boundaries. Figure 13c, a weak-beam, dark-field micrograph taken of a specimen reacted for 16 secs. at 550°C, shows quite clearly that no carbides are present on the dislocations at this temperature.

Recalling that $\alpha_{corr}/\alpha_{para}$ is significantly less than unity in the Fe-C-Cr and the Fe-C-Mn alloys over appreciable ranges of temperature, and that α_{corr} actually passes through a minimum at the bay in the Cr alloy, these results show decisively that the slower than predicted parabolic rate constants in these alloys cannot be attributed to interference with ferrite growth by carbide precipitation.

In the low-Ni alloy, $\alpha_{corr}/\alpha_{para} \simeq 1$; carbide precipitation in this alloy was observed to occur only on dislocations. This result is consistent with the foregoing reasoning about the lack of or minimal effect of such precipitation upon ferrite growth rates.

In the high-Ni and the Si alloys, α_{corr} tended to be greater than α_{para}. In both of these alloys the TEM study disclosed that precipitation had occurred on the broad faces of ledges on austenite:ferrite boundaries, as illustrated in the characteristic "row" configuration of Figure 14. Extensive precipitation of carbides also occurred on dislocations in the Si alloy but not in the high-Ni alloy; as previously indicated, however, this difference in behavior is not likely

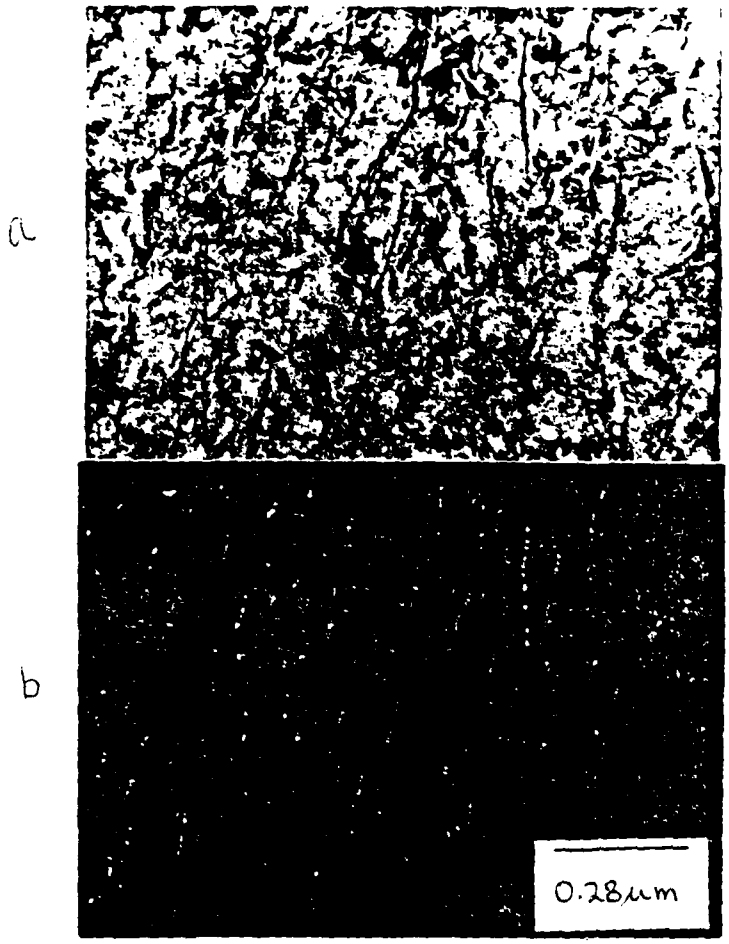

Figure 13

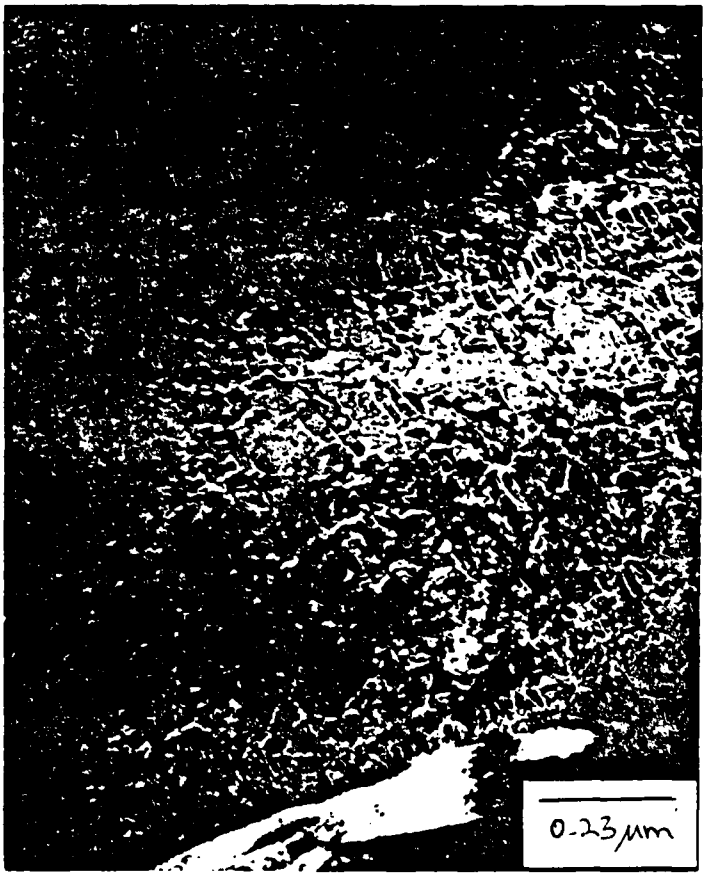

Figure 13c

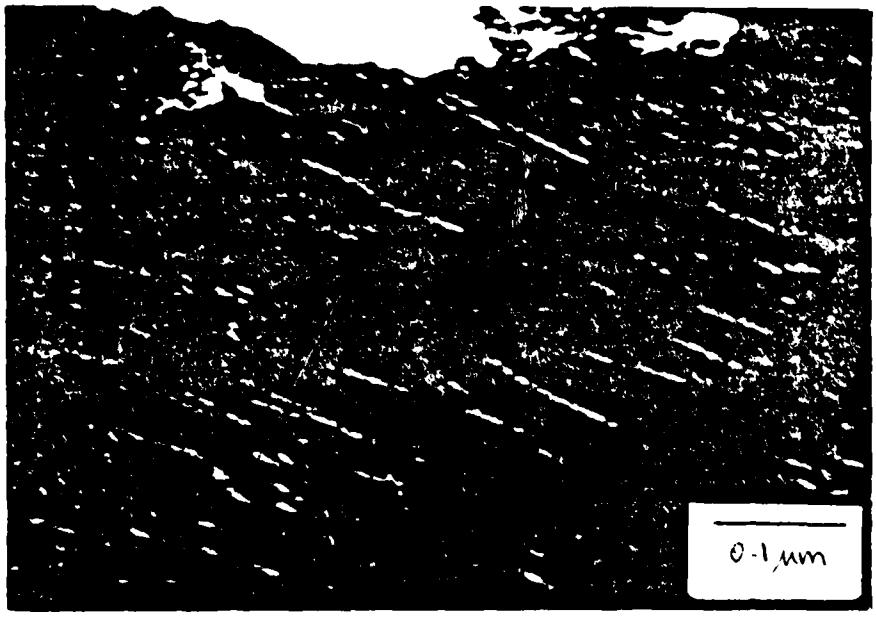

Figure 14

to be reflected to a significant extent in ferrite growth kinetics. Precipitation of carbides on the broad faces of ledges is likely to have been facilitated by the immobility of these interfaces (45, 46). However, such precipitation will increase the carbon concentration difference driving the growth of the ledge risers, on which carbide precipitation rarely occurs (44), from that between the extrapolated Ae3 curve and the bulk carbon concentration in the alloy to the difference between the extrapolated Ae3 and the extrapolated Acm curves (as during edgewise growth of pearlite). Although interphase boundary carbide precipitation occurs less frequently than that on dislocations in the Si alloy and still less often in the high-Ni alloy, since the technique used to measure ferrite growth kinetics is based upon measurement of the length of the longest and the thickness of the thickest grain boundary allotriomorph in each specimen, the allotriomorphs whose growth kinetics are most likely to be measured are accordingly those at which interphase boundary carbide precipitation has occurred.

The Si and high-Ni alloy results and interpretations are just the inverse of those suggested by Purdy (42, 43). These considerations will be further supported by the results presented in the next sub-section. It should be noted, however, that at least in the case of these two alloys another possibility is available for explaining the accelerated growth kinetics experimentally measured. Kinsman and Aaronson (5) have suggested the possibility of an "inverse solute drag" effect produced by alloying elements which raise the activity of carbon in austenite, such as Ni and Si. If such elements are attracted to austenite:ferrite boundaries, because of their size difference with respect to iron in austenite and/or ferrite despite the fact that they repel carbon atoms they would increase the concentration of carbon in austenite in contact with these boundaries. The resulting increase in the carbon concentration gradient driving growth would raise the parabolic rate constants. Since α_{corr} is significantly greater than α_{para} in the Si alloy

at 800°C even though no interphase boundary carbides are present, at least a portion of the accelerated growth kinetics in this alloy may be ascribed to the inverse solute drag effect.

3. Influence of Interphase Boundary Carbide Precipitation Upon Growth Kinetics of Ferrite Allotriomorphs in an Fe-C-V Alloy

The growth kinetics portion of this investigation was conducted by Mr. Toshihiko Abe of Japan's National Research Institute for Metals; TEM studies were carried out by Mr. Gary Shiflet, Republic Steel Corp. Fellow.

Batte and Honeycombe (47) have demonstrated that the tendency for interphase boundary carbide precipitation is very strong in Fe-C-V alloys. An alloy from this system was accordingly used to test more directly the influence of interphase boundary carbide precipitation upon ferrite growth kinetics. By selecting an alloy in which the austenite + ferrite region lies directly above the austenite + ferrite + carbide region, it becomes possible to form grain boundary ferrite allotriomorphs with and without interphase boundary carbides in immediately adjacent temperature regions. By extrapolating the parabolic rate constant plots from one region into the other the role, if any, played by interphase boundary carbides in the growth kinetics of ferrite allotriomorphs can be evaluated.

The alloy finally selected for this program contained 0.12% C and 0.11% V; higher V alloys of similar carbon content did not fulfill the prescribed sequence of phase fields, containing carbides at all reaction temperatures. Optical microscopy measurements were made of the growth kinetics of grain boundary ferrite allotriomorphs in the temperature range 800° - 870°C; this range was selected after TEM studies had shown that the highest temperature at which carbides appeared in assocation with the allotriomorphs within the time envelope in which growth kinetics measurements were feasible was ca. 845°C. The same experimental technique was used to measure allotriomorph growth kinetics as was employed in the study of Bradley (section II-C).

At the outset of the optical microscopy studies, an important difference was

noticed between the allotriomorph morphologies observed in the Fe-C-V alloy and those found in the Fe-C and Fe-C-X alloys studied in many previous investigations. In the latter alloys, all grain boundary allotriomorphs appeared to come from a single species, whose average aspect ratio in both Fe-C (3) and Fe-C-X (48) alloys is ca. 1/3 irrespective of composition, temperature or time. In Fe-C-V, on the other hand, two species of allotriomorphs are clearly present. As illustrated in Fig. 15, one is the usual species, here with an aspect ratio of ca.1/2, and the other is new species (at least in steel) with a nearly zero aspect ratio. The very low aspect ratio allotriomorphs have been previously observed in Al-Cu and Al-Ag alloys (49) and have been informally termed "snakes." TEM studies showed that below ca. 845°C there was a marked difference in the carbide morphologies associated with the two different ferrite morphologies. The cnventional allotriomorphs exhibited the expected "row" or interphase boundary carbides, here thin hexagonal discs, 10 - 30 nm. in diameter, of VC (Fig. 16). The "snakes," on the other hand, exhibited a nearly continuous film of predominantly allotriomorphic carbides (Fig. 17). Focusing attention again upon α, the parabolic rate constant for thickening (and here not attempting a correction for faceting), Fig. 18 shows that: (a) α for allotriomorphs is ca. 15-fold greater than that for "snakes" at a given temperature, and (b) the α vs. temperature plot for both species of allotriomorph exhibits a break at the same temperature, ca. 850°C. This is essentially the temperature above which carbides are no longer present.

Figure 18 shows calculated α vs. temperature curves computed from the paraequilibrium model (with the paraequilibrium phase boundaries having been calculated again from the Hillert-Staffanson (23) formulation) for aspect ratios (K) of 0.51 (the average experimental ratio for conventional allotriomorphs) and of 0 (representing "snakes"). Extrapolating the low temperature portions of the α vs. temperature plots into the high temperature regimes--to make use of the certainty that α must become zero at the no-partion or paraequilibrium Ae3--we

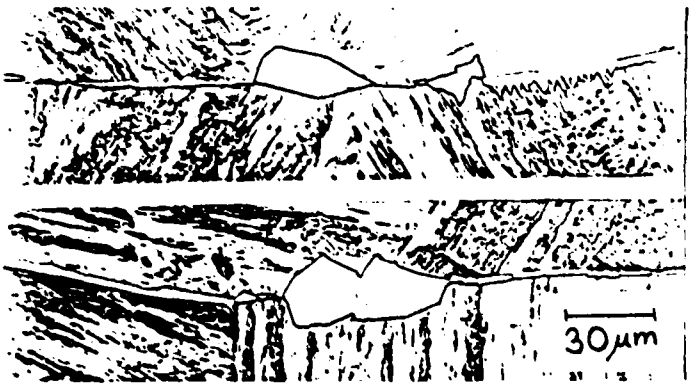

Figure 15

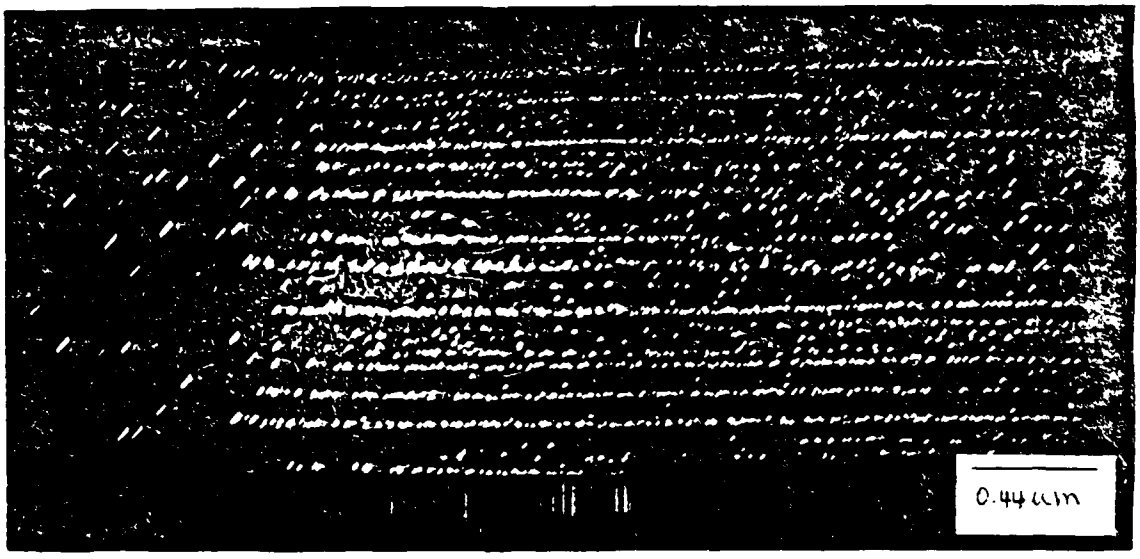

Figure 16

Figure 17

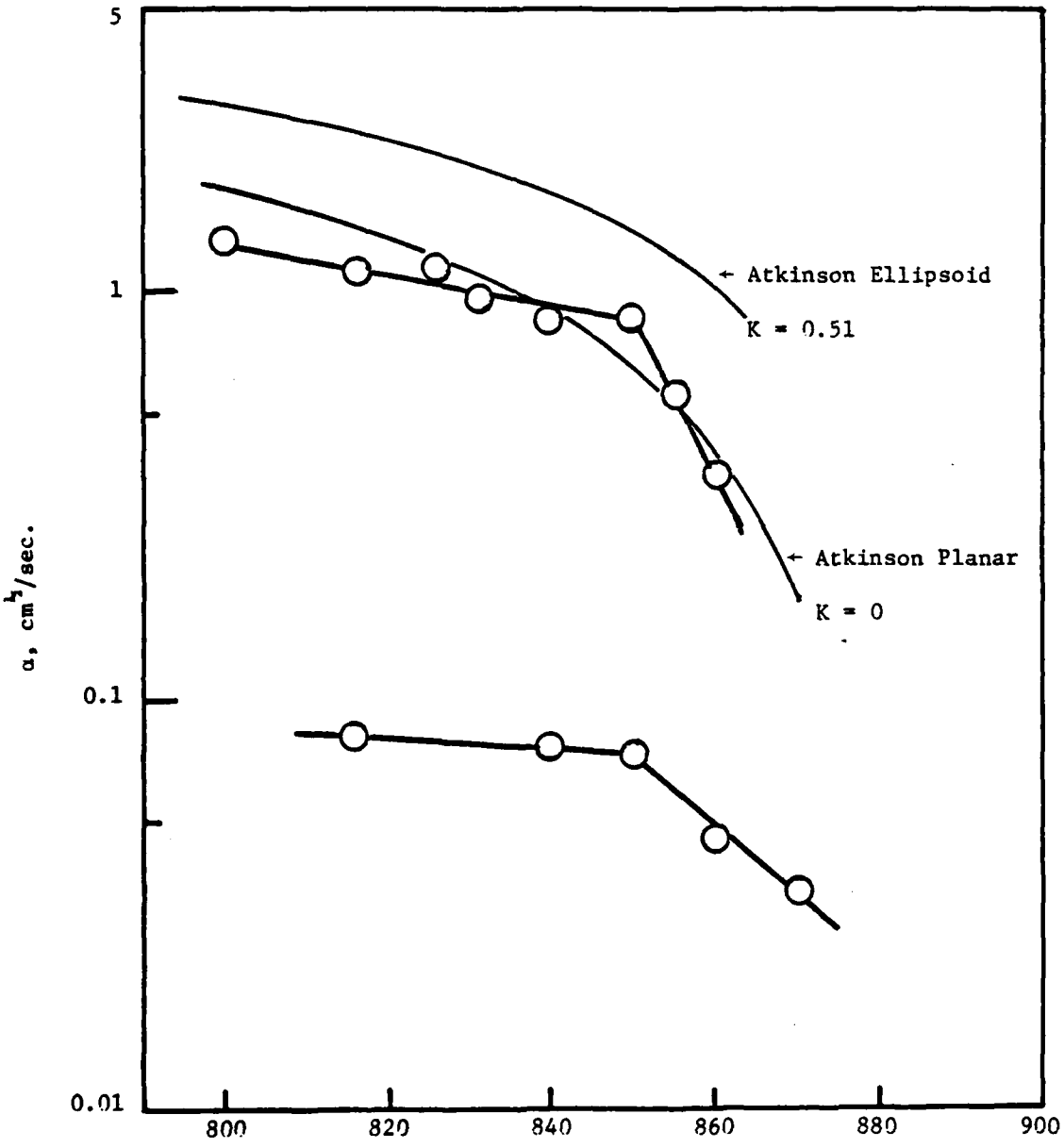
5
1
0.1
0.01
α, cm²/sec.
← Atkinson Ellipsoid
K = 0.51
← Atkinson Planar
K = 0
800
820
840
860
880
900
Reaction Temp. (°C)

Figure 18

conclude that the presence of interphase boundary carbides increases α. This is consistent with the conclusion drawn with respect to thickening kinetics in the Fe-C-Si and the high-Ni Fe-C-Ni alloys in the preceeding section. The finding the experimental α lies below the paraequilibrium one may be ascribed in part to the lack of a faceting correction in Fig. 18, but more importantly to a very potent solute drag effect (primarily because V is so effective in reducing the activity of carbon in austenite) offsetting the acceleration produced by the larger pre-drag driving force for growth provided by the presence of carbides near mobile areas of austenite:ferrite boundary.

In respect of the "snake" phenomenon, a possible explanation may be developed from a current theory of the wetting of interphase boundaries by crystals of a third phase proposed by John Cahn (50). Because of the strong attraction between V and carbon, it seems plausible that V will be more strongly attracted to austenite:ferrite than to austenite grain boundaries in Fe-C-V alloys, and thereby effect a larger reduction in the energy of the former boundaries. (In Fe-C alloys, disordered austenite:ferrite boundaries have a somewhat lower energy than disordered austenite grain boundaries (51). Hence one would expect that X should usually be more attracted to the grain than to the interphase boundaries.) It may thus be possible for ferrite to wet completely a number of austenite grain boundaries, thereby leading to the "snake" morphology. Since more V will thus be absorbed at the broad faces of "snakes" than of allotriomorphs, however, the solute drag effect will be stronger at these boundaries, leading to slower thickening kinetics, readier faceting and hence to more extensive carbide precipitation. The nearly complete coverage of the interphase boundaries of "snakes" by carbides strongly suggests that the partially coherent boundary orientation of this morphology is nearly parallel to the grain boundary plane, thereby facilitating both wetting of the austenite grain boundaries and the local cessation of thickening which is a prerequisite to interphase boundary

precipitation (45, 46).

Ti reduces the activity of carbon in austenite even more markedly than V (52). One would therefore expect that "snakes" would also be present in Fe-C-Ti alloys. Mr. T. Obara will shortly test this prediction.

4. Influence of the Interphase Boundary Structure of Ferrite Allotriomorphs Upon the Precipitation Mechanism and Kinetics of Interphase Boundary Carbides

This investigation is being undertaken by Mr. Takashi Obara of Kawasaki Steel Co., with further contributions again being made by Mr. Gary Shiflet, Republic Steel Corp. Fellow.

Both experimental (46) and theoretical (45) studies of this problem indicate that, contrary to simple expectation, interphase boundary carbides appear to precipitate on low energy, immobile, partially coherent facets on austenite:ferrite boundaries rather than on high energy, mobile, disordered areas of these boundaries. This should occur because the disordered areas of these boundaries are usually moving too rapidly to permit carbide embryos to develop to critical nucleus size without being "crippled" by movement of the boundary upon which they are attempting to develop (45). The present investigation was undertaken in order to test these considerations in more critical fashion. An Fe-0.11% C-1.95% Mo alloy was austenitized at 1300°C, transformed to the equilibrium proportion of proeutectoid ferrite in the austenite + ferrite region, quenched to room temperature, lightly tempered (to permit deformation), cold rolled 50%, re-heated in the austenite + ferrite region at a somewhat higher temperature to reform the austenite, recrystallize the ferrite and reduce the proportion of ferrite present, and then transformed just below the eutectoid temperature to permit further growth of the ferrite and precipitation of carbides. As a result of the destruction of the orientation relationships developed during nucleation, the austenite:proeutectoid ferrite boundaries should have a much larger proportion of disordered structure after recrystallization that the as-transformed grain boundary allotriomorphs.

Studies to date have been conducted at a sub-eutectoid temperature of 810°C.

Optical and TEM microstructures developed as a function of reaction time at this temperature were compared with those produced in unrecrystallized specimens, i.e., simply austenitized at 1300°C and then isothermally reacted at 810°C. The basic result obtained is shown in Fig. 19. In the upper part of this Fig. (D), recrystallization is seen to have produced a microstructure in which the carbides are more or less randomly distributed and are only occasionally observed at the austenite:ferrite boundaries. The lower part of this Fig. shows an undeformed (U) specimen heat treated at the same temperature. In several areas, particularly the one indicated by an arrowhead, there is clear evidence of "row" or interphase boundary carbide precipitation. Hence recrystallization has drastically altered the pattern of carbide precipitation in just the manner expected: the austenite:ferrite boundaries, having become mostly mobile after recrystallization, are now poor sites for interphase boundary carbide precipitation.

In the course of these studies, it has been found, in the undeformed specimens, that appreciable growth time is required before interphase boundary carbide precipitation develops. Growth kinetics should be markedly decreased by this stage of the transformation, hence allowing a given partially coherent facet more time to exist prior to being eliminated by the passage of a ledge, and thereby allowing more time for carbides to nucleate and grow. This result is also in accord with theoretical expectation (45).

As soon as our heat treatment equipment has been restored to operation at Carnegie-Mellon University, this investigation will be completed by extension of these studies to one higher and one lower temperature, probably 825° and 795°C respectively upon the basis of preliminary studies. Interphase boundary carbide precipitation is not found at higher temperatures in undeformed specimens of this alloy and excessive sympathetic nucleation of ferrite occurs in deformed specimens at lower temperatures.

E. Incomplete Transformation (Stasis) in Fe-C-Mo Alloys

This study represents the main portion of the Ph.D. thesis of Mr. Gary Shiflet,

Figure 19

Republic Steel Corp. Fellow.

The initial objective of this study was to recharacterize experimetally the basic characteristics of incomplete transformation, using Fe-C-Mo as a particularly convenient example alloy system.

Work by Boswell, Kinsman and Aaronson performed at the Ford Scientific Laboratories in 1968 (7) led to a new definition of the incomplete transformation phenomenon as it occurs in the proeutectoid ferrite reaction in alloy steel and to experimental results and interpretations much at variance with previous views. Incomplete transformation was defined as the formation of significantly less ferrite than is predicted by application of the Lever Rule to the austenite + ferrite region extrapolated to the transformation temperature. Working with Fe-C-2% Mo alloys containing from 0.05 to 0.26% C, they first showed that the TTT-curve for the initiation of transformation in each alloy exhibits a definite bay. On the generally accepted view of incomplete transformation, as particularly well summarized by Hehemann and Troiano (53) and more recently by Hehemann (54), this phenomenon should be most pronounced just below the bay of the TTT-diagram. Ideally, if the upper (pearlite) and lower (bainite) C-curves originally suggested by Zener (55) to be the elementary components of the complete TTT-curve for the initiation of transformation, are completely separated--as they sometimes are in highly alloyed steels--at the upper limit of the bainite C-curve no transformation at all should take place.

What Boswell et al found in their alloys, however, was that precisely the proportion of ferrite predicted by application of the Lever Rule to the austenite + ferrite region (as calculated from the thermodynamic treatment of Aaronson, Domian and Pound (22) was formed. Only then did plots of total fraction of the austenite transformed, f, vs. time achieve a zero slope. Hence, on the definition of incomplete transformation to ferrite which they used, this phenomenon does not obtain in their alloys. Following a private suggestion by A. T. Davenport, at the end of their study they briefly re-investigated the problem

in an Fe-0.23% C-4.3% Mo alloy--and did succeed in finding incomplete transformation over a temperature range less than 20°C wide immediately below the bay in the TTT-diagram.

This study differed from predecessor investigations in two central ways: plots of f vs. time were determined by point counting optical micrographs using procedures specified by Cahn and Hilliard (56), and the alloys used contained negligible proportions of alloying elements other than Mo. Most previous investigators have placed primary reliance upon physical property measurements, especially that of specimen dilatation, to monitor the transformation, and used commercial-type steels containing appreciable amounts of more than one substitutional alloying element. Recently, Bhadeshia and Edmonds (57) observed incomplete transformation in an Fe-0.43% C-3.00% Mn-2.12% Si alloy; however, Aaronson and Domian (40) did not observe this phenomenon in either Fe-0.40% C-1.83% Si or Fe-0.37% C-3.08% Mn; clearly Si and Mn interact synergistically to encourage the development of incomplete transformation. Bhadeshia and Edmonds also used dilatometry to monitor incomplete transformation, and on the evidence which they unwittingly provided it is clear that the correspondence between f as determined metallographically and that calculated from dilatometry can be poor; precisely the same lack of correspondence could have been deduced much earlier, e.g., from the thorough study of Lyman and Troiano (58) on Fe-C-Cr alloys, where all quantitative work was again done by dilatometry and metallography was used only for illustrative and morphological purposes.

From the work of Boswell et al it is clear that when a single substitutional alloying element is present, even though that element be as potent a bay-former as Mo, an appreciable concentration of that element is required to induce incomplete transformation. Hence the core aspect of Mr. Shiflet's Ph.D. thesis is the determination of the reaction temperature-carbon concentration-molybdenum concentration "surface" which must be exceeded in order that incomplete transformation may occur. Determination of the relevant portions of the TTT-curves for

the initiation of transformation is necessarily a part of this study. Once the incomplete transformation "surface" has been defined with adequate accuracy, measurements of the thickening, and perhaps also the lengthening kinetics of grain boundary ferrite allotriomorphs are to be made in order to provide a better insight into the mechanism of incomplete transformation.

It was more recently recognized that the results of Boswell contain another discovery, i.e., that in addition to incomplete transformation with respect to ferrite, which we shall now term "ferrite stasis," there also exists incomplete transformation with respect to carbide precipitation from austenite (presumably largely at austenite:ferrite boundaries), termed "carbide stasis." It has therefore been decided to extend this program to include the temperature-carbon content-molybdenum content "surface" for the onset of carbide stasis, and also to map the "surfaces" for the initial appearance of the bay in the TTT-curve for initiation of transformation and the initial appearance of a minimum in plots of α vs. temperature, Boswell et al having shown that a pronounced minimum in α occurs in all of their alloys at nearly the bay temperature.

For the ferrite stasis portion of the program, 24 Fe-C-Mo alloys, containing from 0.15 to 0.27% C and from 2.3 to 4.3% Mo have been obtained from the Climax Molybdenum Co. of Michigan through the courtesy of Dr. M. Semchyshen. The limited range of carbon contents being used derives directly from the rapid contraction of the austenite region with increasing Mo content (59). All of these alloys have been homogenized and studies are underway on nearly all of them. For the carbide stasis and other "surfaces" to be defined, another 20 Fe-C-Mo alloys, with Mo contents ranging from 1 down to 0.05%, and with a considerably wider range of carbon contents has been requested from the Climax Molybdenum Co.

Figure 20 shows the bay-region TTT-curves so far completed; these have been determined at temperature intervals of only 10°C. If undergraduate research assistant help can be obtained, it is planned to extend these curves (at much wider temperature intervals, of course) down to the M_s temperature and up quite

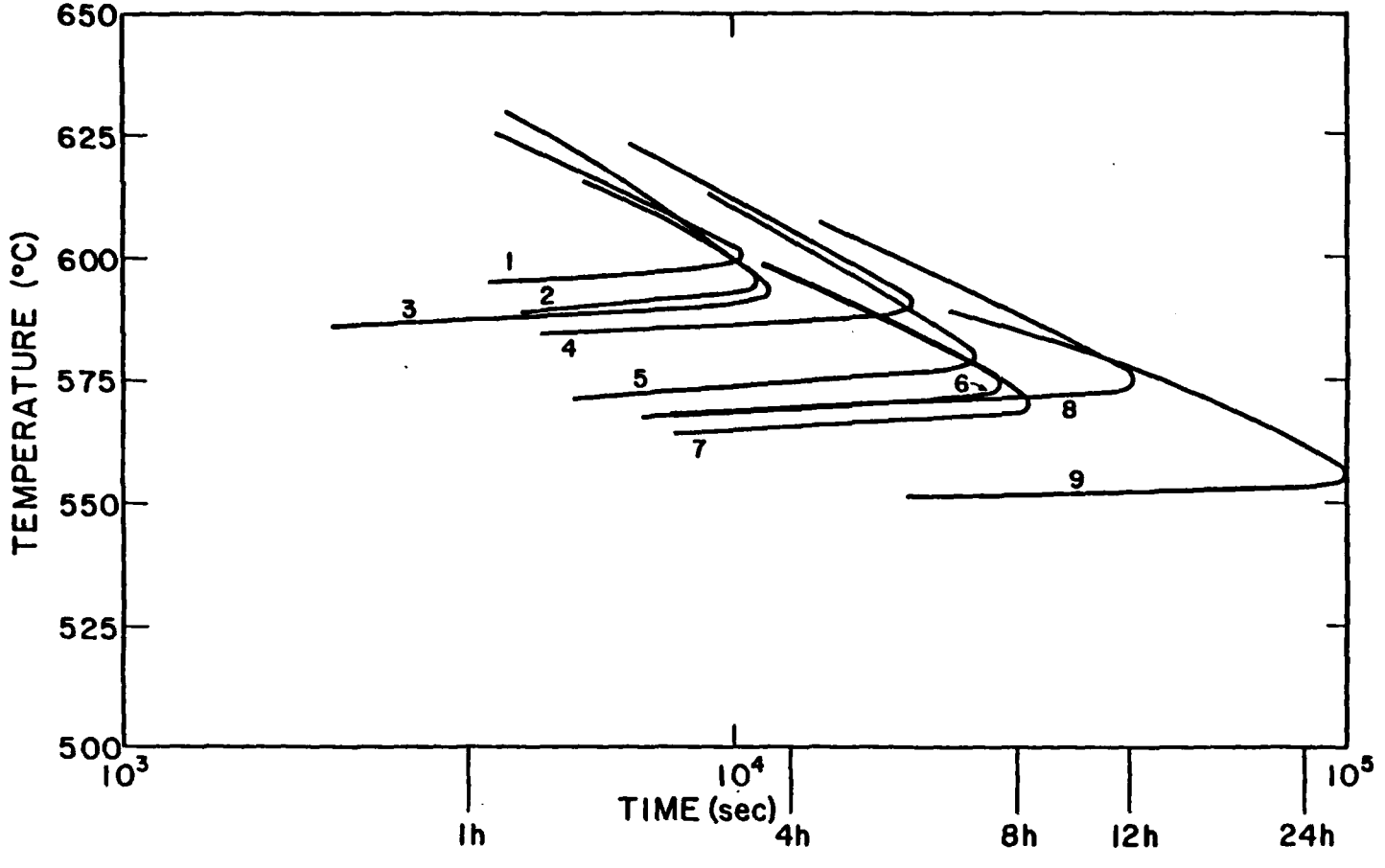
650
625
600
575
550
525
500
TEMPERATURE (°C)
1
2
3
4
5
6
7
8
9
10^3
10^4
10^5
TIME (sec)
1h
4h
8h
12h
24h

Figure 20

close to the no-partition Ae3 temperature. Figure 21 is a three-dimensional plot of the temperature of the minimum in the bay as a function of carbon and molybdenum contents. Note that with increasing carbon content the bay moves to lower temperatures and longer times. Increasing the Mo content has the same effect, though of course Mo is far less effective in making these displacements than is carbon.

Figures 22-24 are sample plots of f vs. time data for three representative alloys. All data were secured by point counting of optical micrographs. Each of these curves demonstrates incomplete transformation to ferrite. These plots contain an important discovery and also an important problem. The discovery is that, earlier impressions to the contrary (53), the proeutectoid ferrite reaction does not come to a halt in the temperature range of ferrite stasis prior to reaching the Lever Rule proportion of ferrite. This proportion was not even closely approached in Figs. 22-24. The practical consideration of specimen carburization or decarburization in the lead baths, to which Fe-C-Mo alloys are particularly prone, would make very difficult the following of this very slow transformation long enough to ascertain whether or not the f vs. time plots do level off at this percentage of ferrite. Evidently the Boswell et al definition of ferrite stasis needs modification, though in a practical rather than in a fundamental sense, perhaps to: failure to form the metastable equilibrium proportion of ferrite in times which are long relative to those required to do so in an Fe-C alloy of the same carbon content. Of course, "how long is long" remains an open question; but the experience being gained in this program seems likely to provide us with either a reasonably clear-cut answer, or better yet, a still more accurate definite of ferrite stasis.

Only preliminary TEM studies have so far been carried out on the Fe-C-Mo alloys. As noted earlier, they demonstrated dense populations of carbides in the Fe-0.23% C-4.3% Mo alloy when f was about 0.01. Since the dark-field technique demonstrated that these carbides, in addition to not appearing in rows, also are present in several different variants of the same orientation

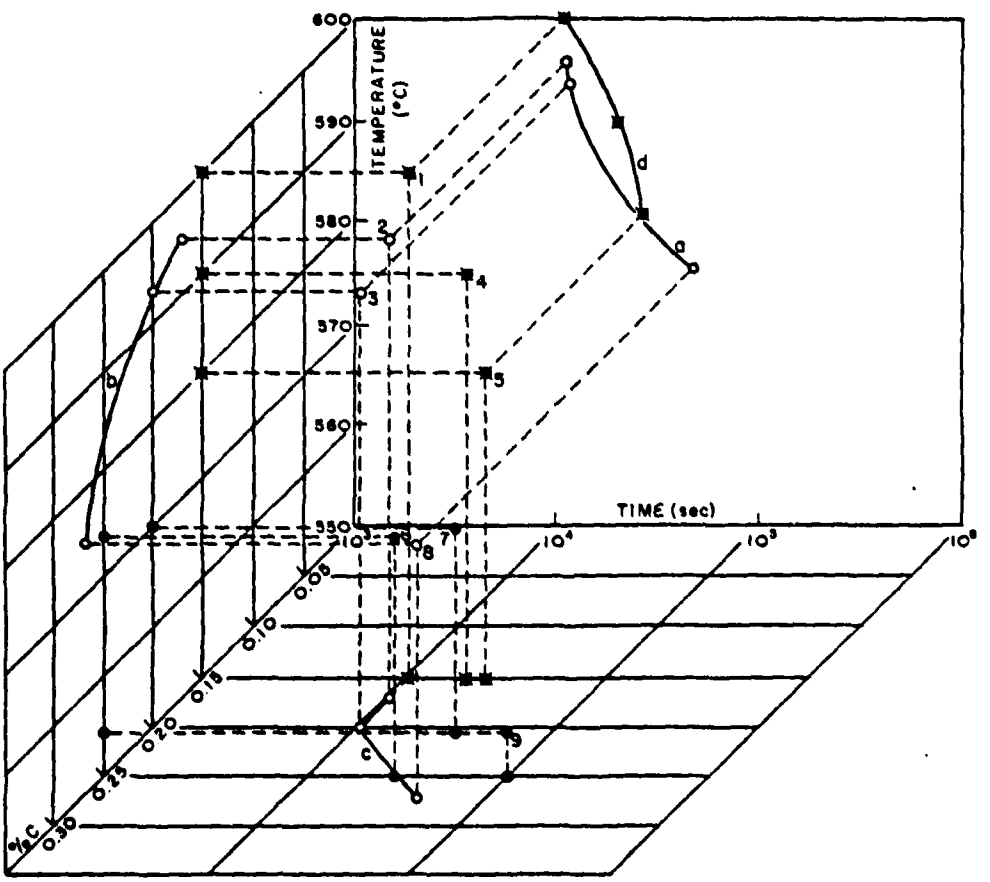
600
590
580
570
560
550
TEMPERATURE (°C)
TIME (sec)
10^3
10^4
10^5
10^6
1
2
3
4
5
6
7
8
9
a
b
c
d
0.05
0.10
0.15
0.20
0.25
0.30
%C

Figure 21

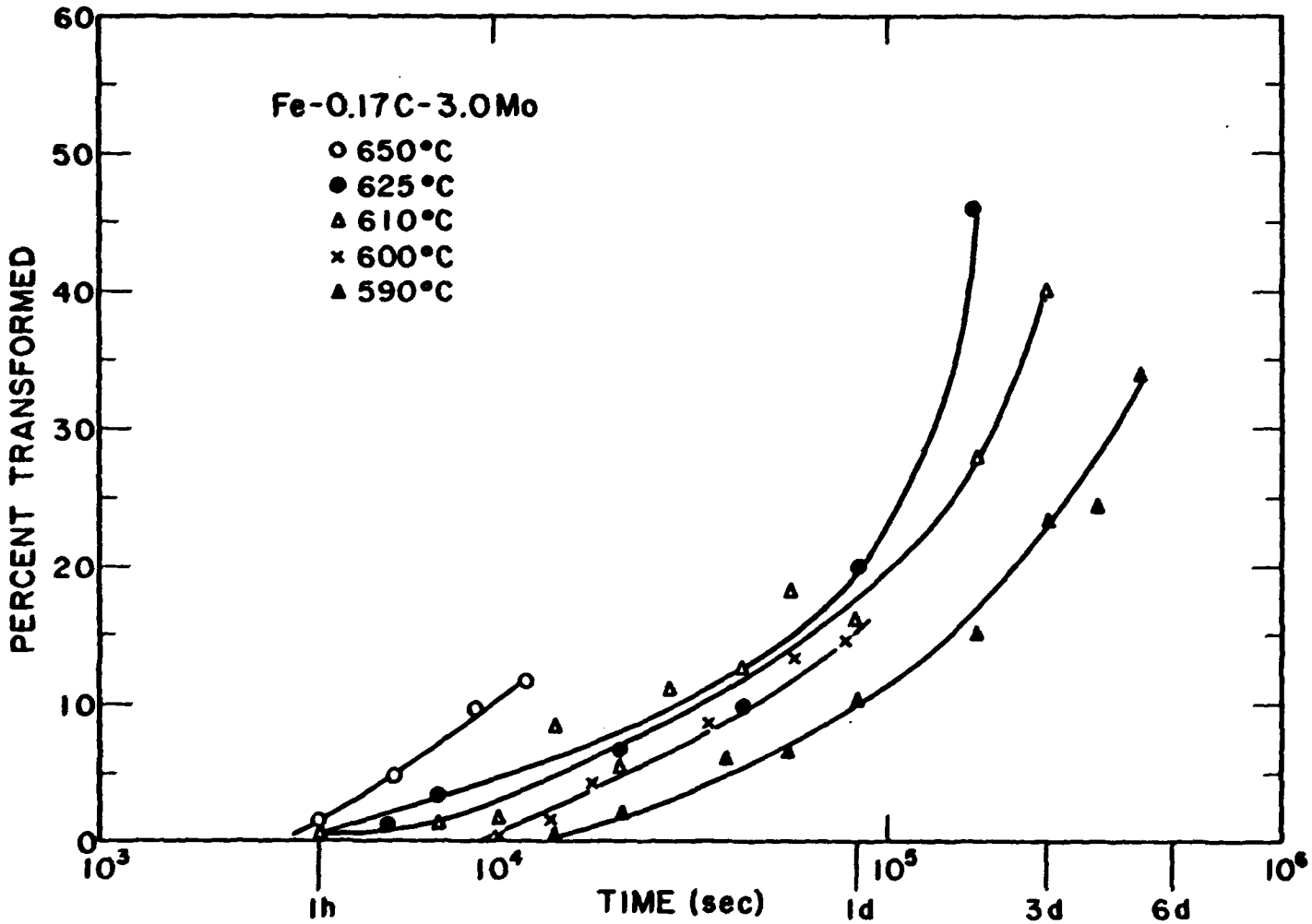
Fe-0.17C-3.0Mo
o 650°C
● 625°C
▲ 610°C
× 600°C
▲ 590°C
PERCENT TRANSFORMED
0
10
20
30
40
50
60
10^3
10^4
10^5
10^6
1h
TIME (sec)
1d
3d
6d

Figure 22

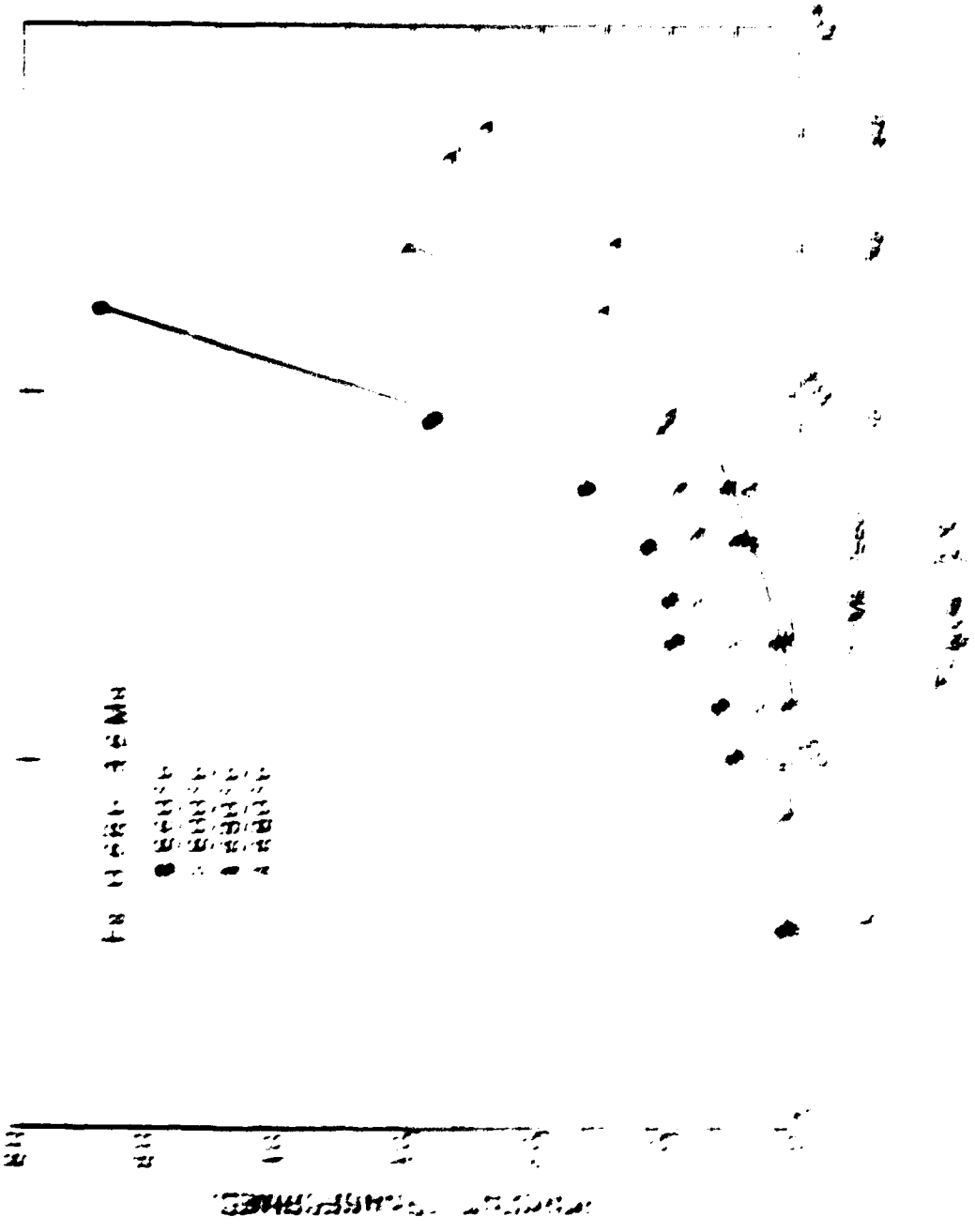

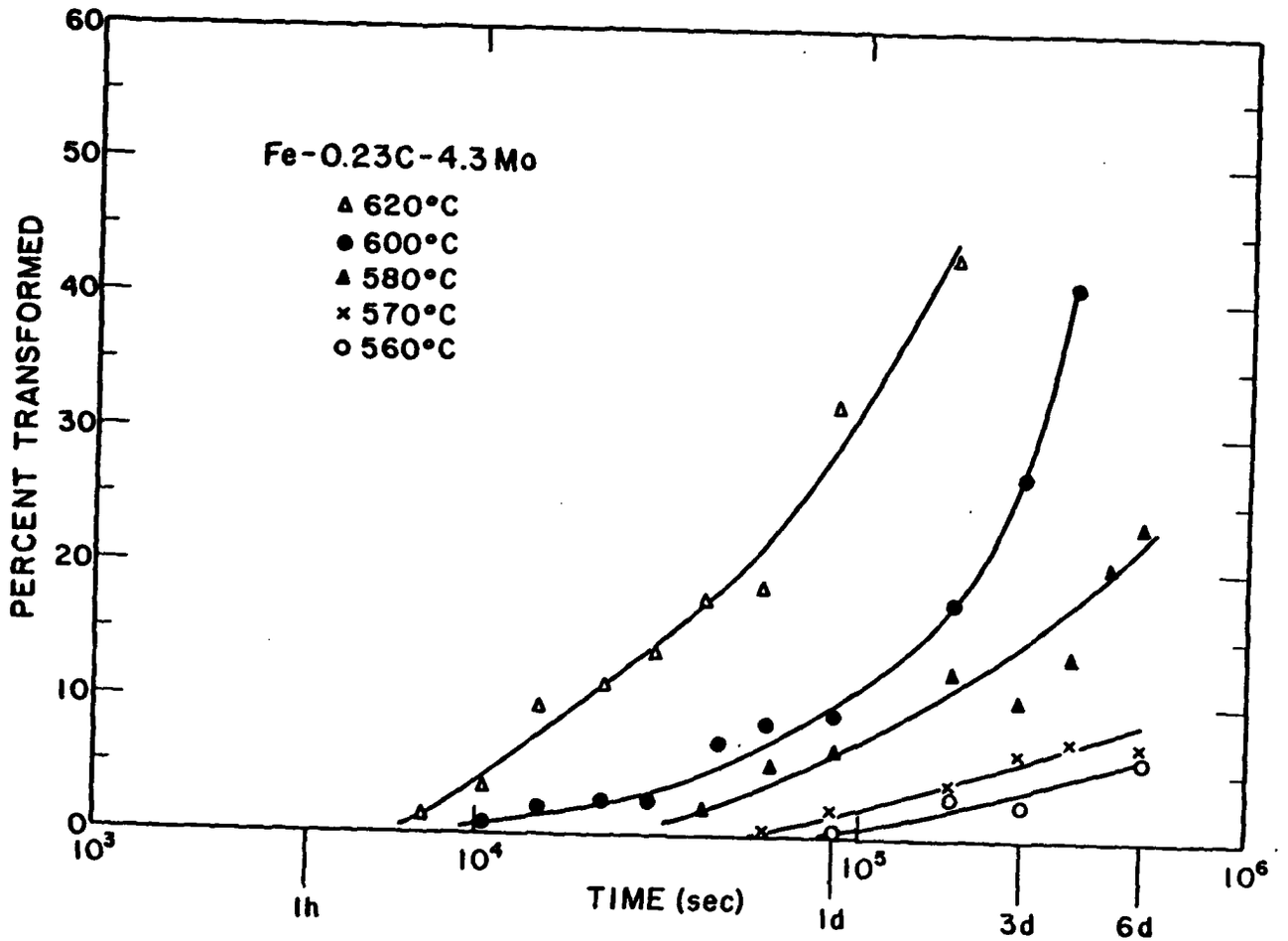
Fe-0.23C-4.3Mo
▲ 620°C
● 600°C
▲ 580°C
× 570°C
o 560°C
PERCENT TRANSFORMED
0
10
20
30
40
50
60
10^3
10^4
10^5
10^6
1h
1d
3d
6d
TIME (sec)

Figure 24

relationship, it is likely that they precipitated within the ferrite rather than at austenite:ferrite boundaries, and thus exerted minimal effects upon ferrite growth kinetics. A comprehensive TEM study of carbide morphologies and distributions is planned on both sides of both the ferrite and the carbide stasis "surfaces" after the growth kinetics measurements have been completed.

Boswell et al proposed that ferrite stasis occurs when the solute drag effect is so severe that volume diffusion of X between austenite and ferrite can begin to occur during growth. A driving force for such diffusion will almost always exist, since it is quite unlikely that the X/Fe ratio in these phases will be the same at equilibrium. Once such diffusion begins, since the diffusivity of X in austenite is usually 4-5 orders of magnitude less than that of carbon, further growth of ferrite will be controlled by X diffusion in austenite even if the penetration distance of X into austenite is initially no more than a single lattice parameter. The finding of the present investigation that transformation in the ferrite stasis region is very slow, but does not stop completely, is consistent with this concept. The discovery by Boswell et al of a break in a plot of half-thickness of allotriomorphs vs. $(\text{growth time})^{1/2}$ in the Fe-0.23% C-4.3% Mo alloy, beyond which α is markedly smaller, and their calculation that the maximum diffusion distance is less than one austenite lattice parameter prior to the break, but appreciably greater than that at times beyond the break, further supports this theory.

F. Effects of Austenitizing Temperature Per Se Upon the Nucleation and Growth Kinetics of Ferrite Allotriomorphs in an Fe-C Alloy

This investigation was performed by Mr. John Bradley as a supplementary part of his Ph.D. thesis and was undertaken in collaboration with Dr. William C. Johnson, then with the Scientific Laboratory of Ford Motor Co. and now with Physical Electronics, Eden Prairie, MN.

That austenite grain size affects the transformation kinetics of grain boundary-nucleated products of the decomposition of austenite has been well

local cessation of thickening which is a prerequisite to interphase boundary

known for about half a century. It is much less appreciated that, independently of austenite grain size, austenitizing temperature per se affects these transformation kinetics. In a commercial-type 0.4% C steel, Mazanec and Cadek (60) have shown that the rate of nucleation of proeutectoid ferrite per unit unreacted grain boundary area at a given reaction temperature increases with decreasing austenitizing temperature. Krahe et al (61) observed qualitatively that austenitizing a high-purity Fe-0.11% C alloy at 1300°C to set the austenite grain size and then further austenitizing at a lower temperature prior to isothermal reaction markedly increases the overall kinetics of the proeutectoid ferrite reaction. Effects of this type have also been identified in connection with the pearlite (62, 63) reactions.

The initial explanation of this effect, based upon the quenching in of ferrite embryos, has been decisively disproved by Russell (64) who has shown that the diffusivity of carbon in austenite is too rapid to make such a process feasible under usual quenching conditions. Grange (65) has suggested a more promising explanation, in terms of increasing adsorption of an impurity to austenite grain boundaries with decreasing temperature of a type which will accelerate the kinetics of transformation. This investigation was undertaken to test Grange's idea, using measurements of nucleation and growth rates to characterize the austenitizing temperature effect and a scanning Auger microprobe (SAM) to determine the grain boundary chemistry as a function of austenitizing treatment.

A high-purity Fe-0.23% C alloy (containing 0.001% P, 0.001% O, 0.001% N and 0.005% S) was employed. Control specimens were austenitized for 30 min. at 1300°C and isothermally reacted for various times at 725° or 775°C if intended for transformation kinetics studies or quenched directly into iced brine if designed for the SAM component of the investigation. Test specimens for the kinetics studies were given a lower temperature austenitizing treatment of 15 min. at 900°C directly after the 1300°C austenitizing anneal and prior to isothermal

reaction. SAM test specimens were given a lower temperature austenitizing anneal for 15 min. at 1000°, 950°, 900° or 850°C and then quenched directly into iced brine.

The SAM studies disclosed enrichment of the grain boundaries in only two elements: carbon and sulphur. Adsorption of both elements is essentially Gibbsian, and is confined to a region only a few atoms wide about the grain boundaries. Carbon enrichment will clearly not affect the driving force for nucleation as long as it occurs to the equilibrium extent. This effect, it may be noted, has been found to be relatively small, corresponding to a binding free energy of ca. 1.2-1.4 kcal./mole, as compared with 13-16 kcal./mole for carbon to ferrite grain boundaries (66); interpretation of the carbon adsorption results is being separately pursued (67) using the thermodynamic information described in the next sub-section. The results of the sulphur enrichment determinations are summarized in Table III. Note that substantial (two orders of magnitude) enrichment occurs and that a binding free energy of ca. 13 kcal./mole was computed from these results and Eq. (1). This binding free energy is 4-5 kcal./mole lower than that for sulphur to ferrite grain boundaries (68, 69), perhaps because of the larger distance of closest approach of Fe atoms in γ than in α Fe (0.2585 vs. 0.2481 nm. (70)).

Table IV summarizes the kinetics results. The parabolic rate constants for thickening (α) and lengthening (β) were obtained by the method employed in Bradley's original Fe-C studies (3). The average nucleation rates (J^*_{av}) were evaluated indirectly, from the growth kinetics data, measurements of fraction of the austenite transformed to grain boundary ferrite allotriomorphs and Dube's (26) modification of the Johnson-Mehl equation. The introduction of a lower austenitizing temperature is seen to decrease somewhat the nucleation rate but to increase the growth kinetics. Since on the Dube version of the J-M equation, the fraction

Table III. Average Grain Boundary Sulfur Ratios, Coverages and Binding Energies

Heat Treatment, °C	Average Ratio	Pct Coverage	Enrichment	$\Delta G_{\gamma\gamma}$, kcal/mole
1300	0.027	0.8	91	14
1100	0.034	1.0	115	13
1000*	0.020	0.9	103	12
950*	0.038	1.1	126	12
900*	0.066	1.9	218	13
850*	0.081	2.4	276	13

*These spceimens were quenched to the indicated temperatures after an initial 1300°C austenitizing treatment to fix the grain size.

Table IV. Summary of Kinetics Results

Lower Austenitizing Temperature, °C	Transformation Temperature, °C	$\alpha \times 10^4$ cm/s$^{\frac{1}{2}}$	$\beta \times 10^4$ cm/s$^{\frac{1}{2}}$	J^*_{ss}, Number/cm^3,s
None	775	0.80 ± 0.18	2.48 ± 0.42	1.1×10^7
900	775	1.15 ± 0.22	4.06 ± 0.99	7.9×10^6
None	725	1.17 ± 0.25	3.60 ± 0.96	7.2×10^8
900	725	1.56 ± 0.36	4.72 ± 1.20	5.4×10^7

transformed, f, varies as:

$$f = 1 - e^{-\frac{8}{15}\pi\alpha^3 J^*_{av} t^{5/2}} \qquad [3]$$

where t is the isothermal reaction time, the overriding influence of the growth kinetics effect upon the overall transformation rate is readily understood. The diminution of the nucleation rate by sulphur adsorption follows from the reduction in austenite grain boundary energy which necessarily accompanies it. Since the austenite:ferrite boundaries enclosing the ferrite critical nuclei are largely or entirely coherent (71), much less sulphur adsorption is expected on these boundaries. Hence there is a net diminution in the cataltyic potency of austenite grain boundaries for ferrite nucleation. On the other hand, some areas of disordered austenite:ferrite boundary are necessarily present during the growth stage (72); sulphur adsorption at these boundaries should markedly increase the carbon concentration in austenite in contact with such boundaries because sulphur so greatly increases the activity of carbon in austenite (52). Hence, an "inverse solute drag-like effect" is held responsible for the increased growth kinetics.

The swift increases in the kinetics of nucleation and growth with decreasing temperature in Fe-C alloys prevented carrying the isothermal reaction studies to lower temperatures. Provided that the substantial concentrations of Mn present in commercial steels do not sequester effectively all of the sulphur present, however, it may be worth pursuing this effect, in an industrial context, as a possible means of increasing the hardenability of steel merely by raising the austenitizing temperature prior to transformation. As long as the austenite grain size is not significantly increased by such a treatment, as will be the case when most austenite grain growth occurs within a relatively narrow "coarsening" range, and the cost of the additional energy required for the higher final austenitizing treatment is not excessive, this concept may be of industrial value.

G. Thermodynamics of the Proeutectoid Ferrite Transformation in Fe-C Alloys

This investigation formed part of the Ph.D. thesis of J. R. Bradley and will also be included in G. J. Shiflet's Ph.D. thesis.

In 1966, Aaronson, Domian and Pound (72) published the results of a comparative study of several statistical thermodynamic models of the austenite and ferrite solid solutions. They determined interaction energies between adjacent carbon atoms in both solutions, calculated both boundaries of the austenite + ferrite region, the T_o-composition curve, the driving forces for the formation of ferrite of both equilibrium composition and the same composition as the parent austenite and proved that, on these models, austenite decomposition cannot take place by a spinodal mechanism. In the subsequent decade much new experimental data has been obtained on the activities of carbon in both austenite and ferrite and substantial additional advances were made in the statistical thermodynamic modeling of interstitial solid solutions. Accordingly, the present study was initiated to update the ADP study and, more importantly, to provide the best available basis for an investigation of the thermodynamics of the proeutectoid ferrite reaction in Fe-C-X alloys. As described in section II-C, such data are essential for interpretation of measurements of the growth kinetics (and, of course, also for the nucleation kinetics) of proeutectoid ferrite in the presence of an alloying element.

Three statistical thermodynamic models were employed. The first two, the Kaufman, Radcliffe and Cohen (73) or KRC, and the Lacher (74), Fowler and Guggenheim (75) or LFG, were previously used by ADP. The third model, developed subsequent to the work of ADP, was that of McLellan and Dunn (25) or MD. The latter was chosen in view of the thorough and searching analyses of the statistical thermodynamics of interstitial solid solutions (particularly in Fe) reported in a long series of papers by the McLellan group, and in particular appeared to be the most sophisticated model which was later extended, by Alex and McLellan (37),

to Fe-C-X solid solutions. In the KRC model, excluded nearest neighboring interstitial sites about a particular carbon atom are considered, but no account is taken of overlapping exclusion shells. The LFG model remedies this deficiency but fails to yield the correct expression for the activity of the interstitial species in the limit of an infinite pairwise interaction energy. The MD model, in turn, eliminated this defect.

In applying the thermodynamics of interstitial solid solutions to the thermodynamics of the proeutectoid ferrite reaction, the central mathematical step required is the Gibbs-Duhem integration of the expression reported for the activity of the interstitial to secure a counterpart equation for the activity of the substitutional or solvent species. After about 50 pages of derivation, the Gibbs-Duhem integration of the MD expression for the activity of the interstitial species was accomplished. ADP had previously performed this integration, much more readily, on the considerably handier LFG relationship for the interstitial activity. We were much surprised to find that, despite the substantial differences between the MD and the LFG equations for interstitial activity, the counterpart relationships for the activity of the substitutional solvent were identical! The MD and the LFG equations for interstitial activity, made specific to the activity of carbon in austenite, were then numerically compared. In the range of carbon-carbon interaction energy appropriate to austenite, the differences in the carbon activities obtained from the two relationships were found to be negligible. Not until the interaction energy was made an order of magnitude larger did these differences become appreciable.

Thus the main thrust of this effort was redirected toward examining the numerical changes resulting from the availability of the considerably more comprehensive data on the activity of carbon in austenite vs. temperature vs. carbon content reported by Ban-ya, Elliott and Chipman (76) and on the activity of carbon in ferrite as a function of temperature and composition presented by

Dunn and McLellan (77) and by Lobo and Geiger (78).

Using the best available data, the repulsion energy between adjacent carbon atoms in austenite was computed to be 1925 cal./mole = 8055 J/mole from the work of Ban-ya et al, as compared with the 1500 cal./mole = 6275 J/mole obtained by ADP from the much more limited experimental data of R. P. Smith (79). Although far more experimental data on the activity of carbon in ferrite are now available, and the carbon-carbon interaction energy was again determined to be attractive, the value of this energy was once again found to vary markedly and erratically with temperature, now suggesting that the available statistical thermodynamic models are not satisfactory for attractive interactions between adjacent interstitial atoms. The extrapolated Ae3 curve obtained during this investigation differs appreciably from the best such curve computed by ADP at low temperatures. At 200°C, for example, the new Ae3 curve lies at a carbon content 4.5 A/O C below that of the best ADP curve (Fig. 25). The calculated $\alpha/(\alpha + \gamma)$ curve is now in appreciably poorer agreement with the experimental curve above the eutectoid temperature (Fig. 26); one must presume that the extrapolation of the newly calculated $\alpha/(\alpha + \gamma)$ curve below the eutectoid temperature is also less satisfactory than that of ADP. This result further illuminates the inadequacy of the thermodynamic treatments available for carbon in ferrite. The total free energy change associated with the proeutectoid ferrite reaction is significantly less negative on the current treatment; little effect was produced, however, on the T_o-composition curve.

H. Thermodynamics of the Proeutectoid Ferrite Reaction in Fe-C-X Alloys

This effort was initiated by J. R. Bradley as part of his Ph.D. thesis research and is being continued by G. J. Shiflet.

As indicated in section II-C, a serious and quite substantial effort was made to Gibbs-Duhem integrate the Alex-McLellan (37) equation for the activity of an interstitial, say C, in an Fe-C-X alloy; this effort was, however, unsuccessful; thanks to logarithmic terms, infinities appear during the integration, and cannot

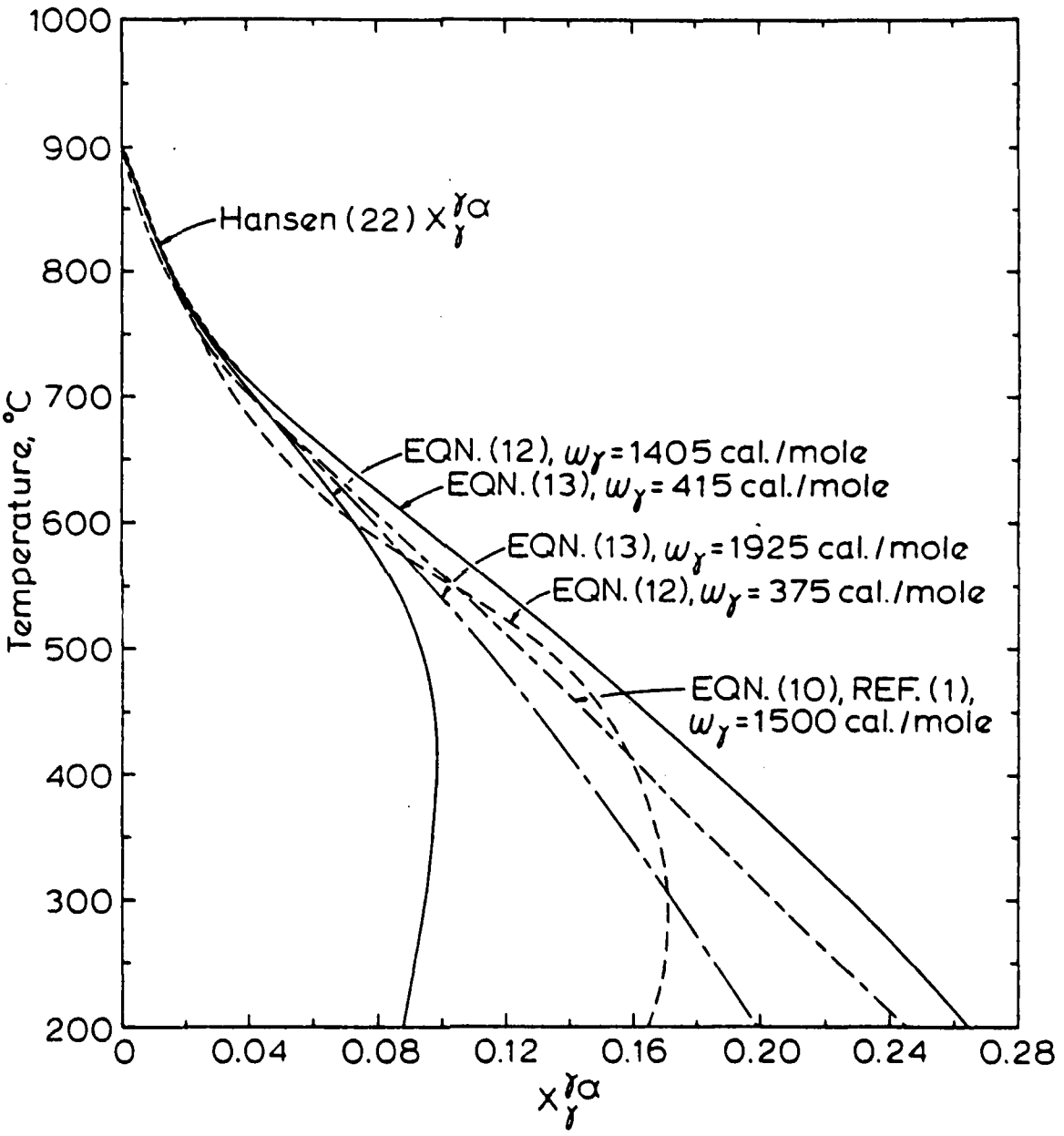
1000
900
800
700
600
500
400
300
200
Temperature, °C
0
0.04
0.08
0.12
0.16
0.20
0.24
0.28
$X_\gamma^{\gamma\alpha}$
Hansen (22) $X_\gamma^{\gamma\alpha}$
EQN. (12), w_γ = 1405 cal./mole
EQN. (13), w_γ = 415 cal./mole
EQN. (13), w_γ = 1925 cal./mole
EQN. (12), w_γ = 375 cal./mole
EQN. (10), REF. (1),
w_γ = 1500 cal./mole

Figure 25

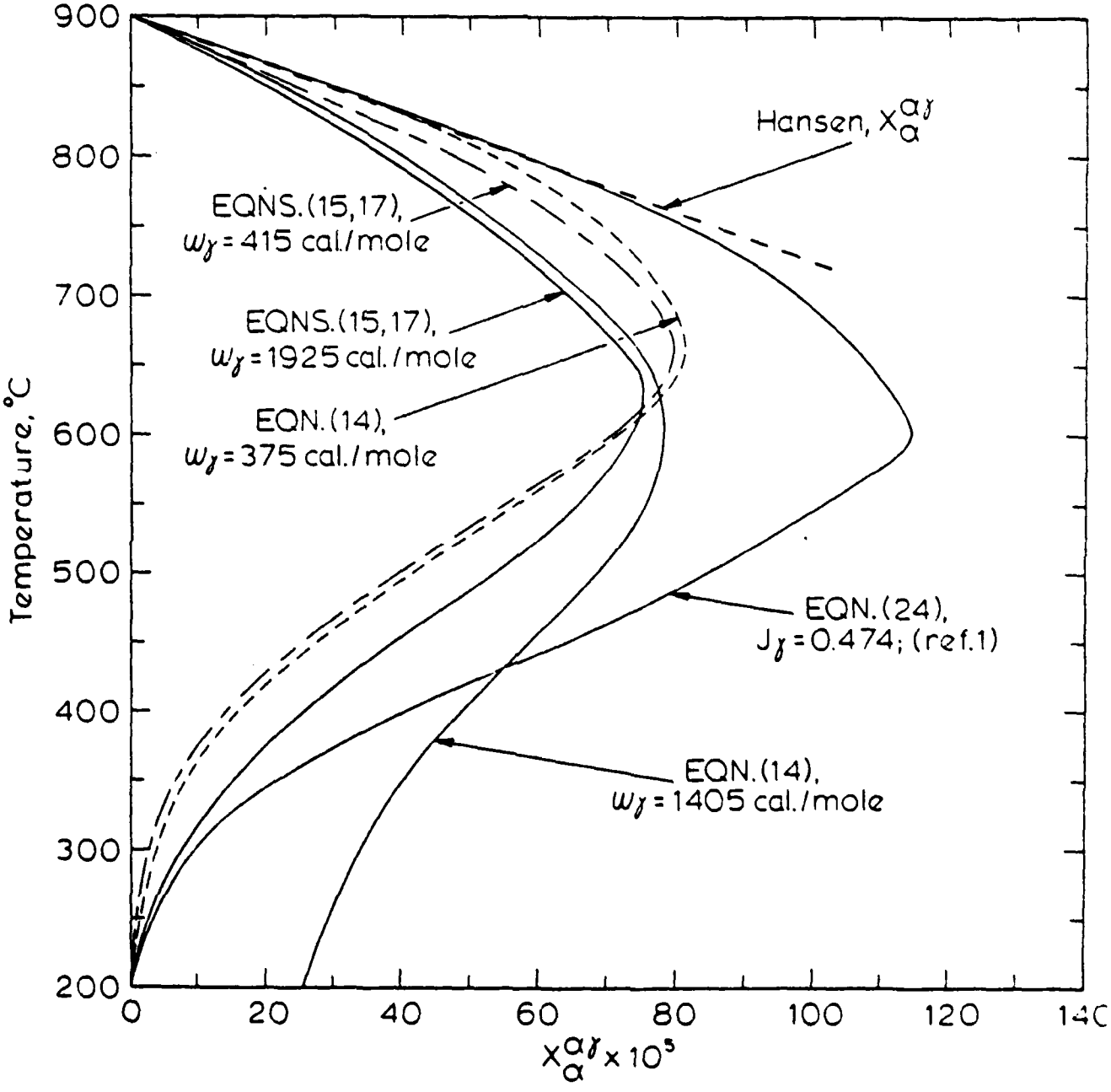
900
800
700
600
500
400
300
200
Temperature, °C
0
20
40
60
80
100
120
140
$X_\alpha^{\alpha\gamma} \times 10^5$
Hansen, $X_\alpha^{\alpha\gamma}$
EQNS.(15,17), w_γ = 415 cal./mole
EQNS.(15,17), w_γ = 1925 cal./mole
EQN.(14), w_γ = 375 cal./mole
EQN.(24), J_γ = 0.474; (ref.1)
EQN.(14), w_γ = 1405 cal./mole

Figure 26

be avoided even by numerical methods. The move from Michigan Tech to Carnegie-Mellon has prompted a closer examination of the papers by CMU Professor C. H. P. Lupis and his students in which the "central atoms" model has been used to treat the activity of carbon in austenite in Fe-C and Fe-C-X alloys (and related problems). Although this model is less "physical" than those of KRC, LFG and MD, using a Taylor's Series expansion of activity coefficients instead of carbon-carbon, and in Fe-C-X alloys, the difference between carbon-X and carbon-Fe interaction energies, it nonetheless gives a promising accounting of experimental data on carbon activities. Application of the Lupis treatment for Fe-C alloys to calculation of the extrapolated Ae3 curve yielded good agreement with the LFG/MD treatments. Foo and Lupis (80) have written equations in generalized form for the activities of both Fe and X in Fe-C-X alloys. Professor Lupis has agreed to complete these derivations. Recalculation of all of the quantities of interest for Fe-C-X alloys should then be straightforward, particularly since the thermodynamic data on carbon activities in Fe-C-X alloys are now available in well digested form (30). Particular emphasis will be placed upon calculation of both equilibrium and paraequilibrium phase boundaries of the $\alpha + \gamma$ region in the Fe-C-X systems in which Bradley measured growth kinetics and also in the Fe-C-Mo system which Shiflet is using as a prototype for his investigation of incomplete transformation.

J. A Summary of Our Current View on the Effects of Alloying Elements on the Growth Kinetics of Ferrite Allotriomorphs in Fe-C-X Alloys

Both ADP and Kirkaldy and co-workers have proposed that alloying elements which raise the no-partition or paraequilibrium Ae3 relative to that of an Fe-C alloy with the same bulk carbon content increase the driving force for growth (and also for nucleation), and vice versa. Kinsman and Aaronson (4) have suggested that alloying elements which markedly decrease the activity of carbon in austenite and/or ferrite and exhibit an appreciable size difference with respect to Fe in either or both lattices will tend to segregate to disordered austenite:

ferrite boundaries. By decreasing the activity of the carbon in the bulk austenite which is in contact with the boundaries the boundary segregate decreases the carbon concentration gradient in austenite driving growth and thus the parabolic rate constants. They termed this a solute drag-like effect. When the size difference, i.e., the elastic strain energy driving force for segregation is sufficiently large, even though X increases the activity coefficient of carbon in austenite it will still segregate to disordered austenite:ferrite boundaries. In this circumstance, however, the activity of carbon in the austenite in contact with these boundaries will be increased and thus so will the parabolic rate constants for growth. Hence this is termed an "inverse solute drag-like effect." On the basis of the current research described in section II-D, we now conclude that when X encourages carbide precipitation at partially coherent austenite:ferrite boundaries, the increased concentration gradient austenite which thus becomes available to drive the growth of adjacent disordered areas of these boundaries will act to increase overall ferrite growth kinetics. Although Si is obviously an exception, it appears that alloying elements which very strongly reduce the activity of carbon in austenite, such as V and probably also Ti, also encourage interphase boundary carbide precipitation, thereby at least partially nullifying the solute drag-like effect. Hence an alloying element which displaces the parabolic rate constant vs. temperature curves to longer reaction times the furthest per atomic percent X is one which maximizes the solute drag-like effect while producing minimal nucleation rates of carbides at austenite:ferrite boundaries. Preliminary TEM observations by Mr. Shiflet indicate that Mo does not produce a significant amount of interphase boundary carbide precipitation even at the bay of the TTT-diagram for initiation of transformation. Perhaps the remarkably potent effects of Mo upon the hardenability of steel arise because this element is one which comes close to achieving the optimum balance between these two effects. The study which Mr. T. Obara plans to undertake on the growth kinetics of ferrite allotriomorphs and carbide precipitation in association with the

allotriomorphs in Fe-C-V and Fe-C-Ti alloys during the balance of this Contract should provide a good test of this concept because V and Ti are both very strong carbide-formers and depressants of the activity of carbon in austenite.

K. Structure of Partially Coherent FCC:BCC Boundaries

The work reported in the following three sub-sections was accomplished by postdoctoral research associate Dr. William A. T. Clark in less than 15 months.

1. Structure of Planar Facets on β:α_m Cu-Zn Boundaries

These boundaries are formed during the massive transformation bcc $\beta \rightarrow$ fcc α_m in Cu-Zn alloys containing ca. 38 A/O An (81). The generally accepted view of massive transformations, for which $\beta \rightarrow_m \alpha$ Cu-Zn is often taken to be a prototype, is that there is no specific, rational and reproducible lattice orientation relationship between the matrix and product phases, and that as a result the interphase boundaries created during these transformations are of the disordered type (11). The earliest quantitative evidence on the crystallography of the $\beta \rightarrow \alpha_m$ Cu-Zn transformation is that of Hull and Garwood (82), published in 1955, who found that planar facets on α_m crystals correspond to a limited number of habit planes in the β matrix. However, these results were obtained from single surface analysis, a procedure of limited accuracy and reliability, and they have accordingly often been ignored in the literature subsequently developed. Hawbolt and Massalski (81), seeking to test a proposal by Aaronson, Laird and Kinsman (83), sought a dislocation structure on planar α_m facets but observed nothing reproducible and showed no micrographs of their TEM study. They also sought orientation relationships between β and α_m and found only random scatter. Ayres and Joy (84) used selected area electron channeling patterns (SACP) and reported essentially the same result. Aaronson, Laird and Kinsman (83) used nucleation theory to predict that specific orientation relationships and low energy habit planes ought to obtain during massive transformations just as they

do during precipitation. Plichta et al (85) made a more detailed theoretical analysis of the nucleation kinetics of the $\beta \rightarrow \alpha_m$ transformation in Cu-38 A/O Zn, a composition chosen in order to utilize the thermodynamics of the transformation in this alloy evaluated experimentally by Karlyn, Cahn and Cohen (86). They concluded that even when critical nuclei are formed at high energy grain boundaries they must have at least one low energy facet, and must thus have an orientation relationship permitting formation of closely matching habit planes in the matrix and massive phases. The present investigation was undertaken to test by high-resolution TEM the prediction of Aaronson et al and Plichta et al that planar facets on α_m crystals are low energy, partially coherent interfaces. Of equal importance, this study was performed as a means of ascertaining whether or not the partially coherent fcc:bcc interfacial structures observed by Rigsbee and Aaronson (87) on the broad faces of ferrite sideplates in an Fe-C-Si alloy would also appear when both phases are substitutional rather than interstitial solid solutions.

Repeated attempts to procure a Cu-38 A/O Zn alloy from external sources were unsuccessful. The following procedure was finally adopted for preparing this alloy ourselves. High-purity Cu and Zn were melted together under 0.5 atmosphere of purified He in silica tubes. Vigorous shaking of the molten alloy was followed by brief air cooling and then by accelerated cooling achieved through immersion of the capsules in iced water. Direct quenching of the molten alloy led to cracking of the capsules; some solidification appeared to be required prior to quenching. The ingots were then re-encapsulated in silica and homogenized for 48 hrs. at 885°C, i.e., within the β region. Then ingots were then cold rolled ca. 75%, recrystallized in a salt bath for one min. at 500°C, cold rolled a further 50% and again recrystallized. They were then given a final cold roll to a thickness of ca. 5×10^{-4} m. At this stage the composition of the alloys was checked using a Philips X-ray fluorescence spectrometer, calibrated against several standard Cu-Zn alloys. Those alloys with the appropriate composition were

solution annealed for 30 secs. at 885°C in molten salt and then quenched directly into 16% NaOH at 0°C to produce an adequate volume fraction of α_m.

Specimens were prepared for TEM by electropolishing 3×10^{-3} m. discs in a Fischione unit using Struers' D2 electrolyte at ca. 4.5 volts and at room temperature. Because of the high growth rates and consequent large sizes of both matrix grains and α_m product crystals, the initial perforations produced by electropolishing did not occur close to a β:α_m interface. Argon ion milling, at 100uA and ca. 5kV, was used to displace an electron transparent area to such a boundary. Observations on the interphase boundaries were made with a JEOL 120CX microscope.

Considerable twinning within α_m and dislocation substructure in both β and α_m phases (81) complicated and restricted but did not prevent detailed study of the interphase boundary structures observed. Application of the $g.b = 0$ criterion for determination of Burgers vectors was confined to the α_m phase in order to circumvent both the marked elastic anisotropy (88) and the deviations from the simple b.c.c. structure (89) of the β phase. Half a dozen planar α_m interfaces were studied in detail; qualitative observations on other such interfaces indicate that these observations are general.

The most important background observation is that the orientation relationships between β and α_m were not in the usual Kurdjumow-Sachs to Nishiyama-Wasserman range, nor were any other relationships based upon $\{111\}\ \alpha_m \,||\, \{110\}\beta$ discerned. Instead, a number of low index poles in the two lattices are nearly parallel, e.g.:

α_m-Direction	β-Direction	Angular Separation
$[1\ 3\ \bar{1}]$	$[0\ 1\ 0]$	5.8°
$[1\ \bar{1}\ 1]$	$[1\ \bar{1}\ 1]$	9.5°
$[3\ 1\ \bar{1}]$	$[1\ 1\ 0]$	2.2°

One possible explanation for this result is that a K-S or a N-W orientation

relationship did obtain between the α_m crystal and the "other" β grain. In the $\beta \rightarrow \xi_m$ transformation in Ag-26 A/O Al, for example, an exactly or nearly Burgers orientation relationship normally obtains with respect to only one of the two β grains forming a grain face (90). Because of the small size of the electron transparent areas relative to that of the α_m crystals, this possibility could not be tested experimentally. However, the SACP studies on α_m crystals formed at β grain boundaries reported by Ayres and Joy (84) indicate that the usual orientation relationships are normally not present with respect to either β grain. Another is that a compromise orientation relathionship between the α_m nucleus and the two nucleating β grains produces the critical nucleus with the smallest volume, hence the lowest free energy of activation and (normally) the highest nucleation rate. Hillert (91) has previously made such a suggestion for grain boundary nucleated ferrite in steel; King and Bell (92) studied such precipitates by means of a Kossel X-ray microdiffraction technique and found direct evidence for deviant orientation relationships. However, the observed deviations were small enough to be described as rotations apart of $\{111\}_\gamma$ and $\{110\}_\alpha$. In directionally solidified samples of Cu-Cr eutectic, Clarke and Stobbs (93) discovered that two quite different orientation relationships prodominated, one a rotational modification of the K-S and the other an inverted N-W. Hence the present results may be regarded as a further evolution of an already developed theme.

The absence of the usual orientation relationships thus makes direct observation of the structure of planar $\beta:\alpha_m$ facets even more important. A typical result of such studies is shown in Figs. 27-29, portraying essentially the same area of a $\beta:\alpha_m$ boundary in three different reflections. As previously shown by Hawbolt and Massalski (81) and repeatedly confirmed during this investigation, the interface is markedly faceted. In this area, the two larger facets lie within ±4° of $(11\bar{1})_\alpha$ (itself only 10.5° from $(1\bar{1}1)_\beta$) and $(\bar{1}\bar{1}1)_{\alpha_m}$ for the short facet between them. The new observation made in the present investigation is that a

Figure 27

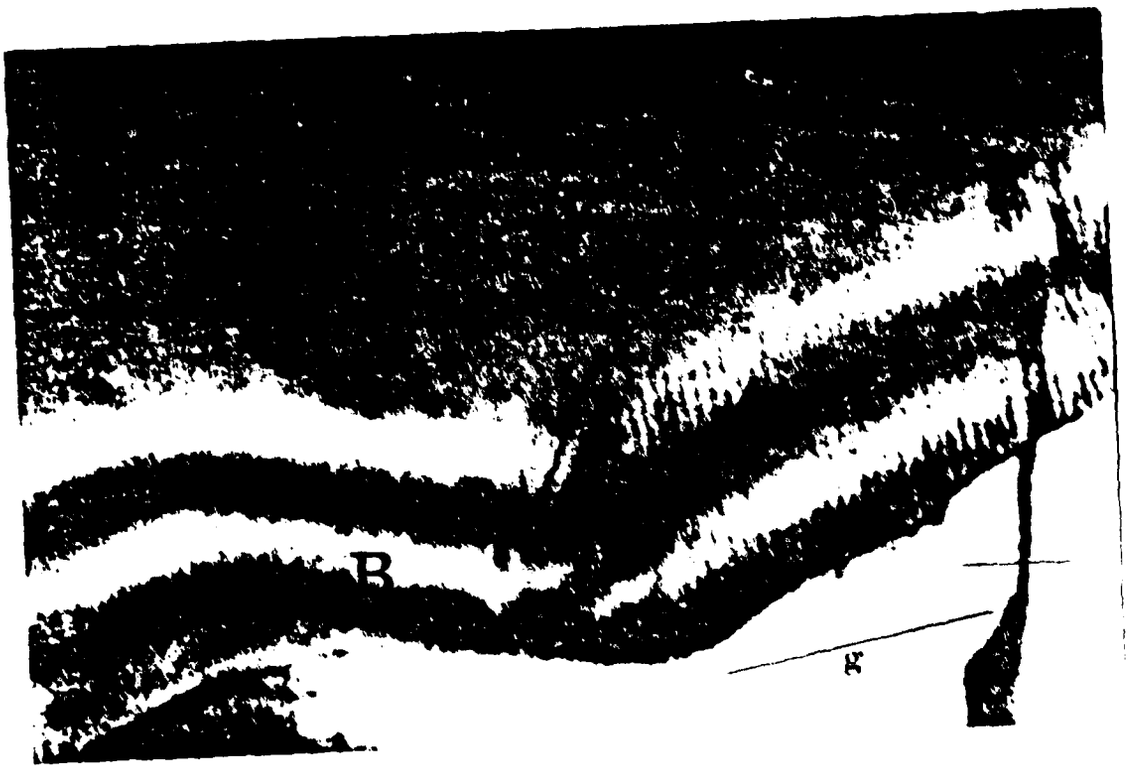

Figure 28

Figure 29

set of parallel linear defects is present. In this set of micrographs they are visible only on the larger facets and are spaced 2.68 nm apart. Figure 30, taken with $g = 2\bar{2}0_{\alpha}$ under near weak-beam conditions indicates that linear defects may also be present at the short facet; however, the contrast which they produce is insufficient to permit their identification. These defects change in contrast as the diffracting vector is changed (Figs. 27-29), indicating that a displacement field is associated with them. Additionally, the spacing between the defects varies with the orientation of the boundary plane, thereby demonstrating that the defects are an intrinsic part of the interfacial structure rather than being merely dislocations randomly adsorbed from one or both bounding grains.

Amongst the diffraction vectors used in Figs. 27-29, only when $g = 2\bar{2}0_{\alpha_m}$ (Fig. 29) are the defects placed out of contrast. Hence the displacement field is in the $[110]_{\alpha_m}$ direction. This is normal to the short facet in the interface and steeply inclined with respect to the two longer facets. The linear defects accordingly appear to be structural ledges. Because of their close spacing and the displacement field associated with them, their height cannot be measured by means of thickness fringe offsets. However, for the apparent habit plane observed, a ledge spacing of 2.68 nm. and an assumed $[\bar{1}\bar{1}1]_{\alpha_m}$ habit plane on the flats between risers indicate a ledge height of ca. 3 nm. This is about an order of magnitude higher than the structural ledge heights observed on the broad faces of ferrite plates (87); evidently considerable consolidation of ledges occurred. This is not possible, however, for misfit dislocations. Even for optimal orientation relationships between fcc and bcc with the present lattice parameter ratio, 1.252, the maximum spacing between the misfit dislocations expected between structural ledges (87, 88, 94) is only ca. 2 nm (88). For the orientation relationships found during the present investigation rather smaller inter-dislocation spacings are to be expected; such spacings cannot be resolved even by the weak-beam, dark-

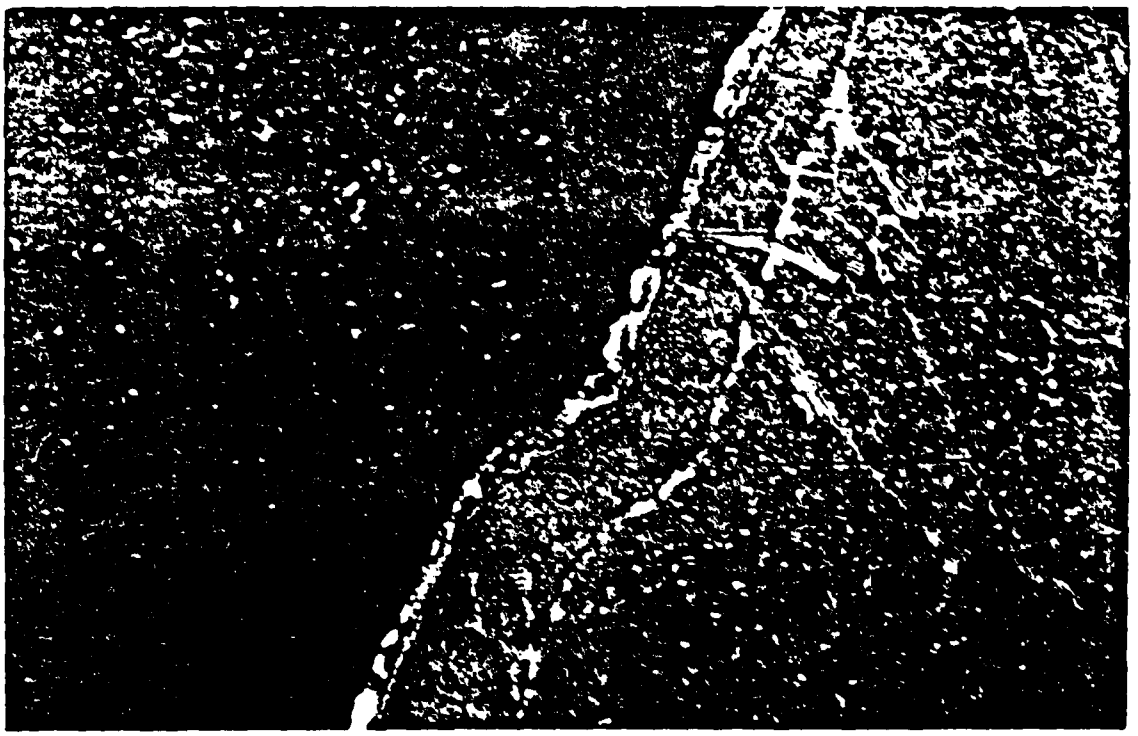

Figure 30

field technique.

While only the structural ledge component of the α_m interfacial structure could be resolved, this finding makes clear that the facets on these interfaces are of the coherent type, though almost certainly partially rather than fully coherent because of the large sizes of the α_m crystals and the substantial misfit between the two lattices. Hence, partial coherency also provides the barrier to growth during the massive transformation which leads to the formation of pronounced facets. Despite the rather unusual orientation relationships operative, facets with the crystallography observed during growth must also be present on the critical nuclei. These findings and deductions are at variance with generally accepted views of the crystallogaphy of the massive transformation, but are entirely consistent with the previously published predictions of the P.I. and his colleagues (83, 85).

2. Structure of the Lamellar Interface in a Directionally Solidified Co(Al)-CoAl Eutectic

This investigation was initially undertaken by postdoctoral research associate Amitava Guha with the support of an NSF-funded interdisciplinary grant. At the end of Dr. Guha's two year tour at Michigan Tech the study remained incomplete. Since the program also involves partially coherent fcc:bcc interfaces, Dr. Clark was asked to complete the program while waiting (vainly, as it turned out) for a commercial firm to supply a bar of Cu-38 A/O Zn alloy.

The Co(Al)-CoAl eutectic is of direct interest to the present Contract's efforts on structural barriers to growth because it includes two important variations on the previous theme: the interfaces were formed during solidification rather than during a solid-solid transformation, and one of the phases, CoAl, has a CsCl-ordered bcc structure rather than the disordered bcc structure present in the studies of the proeutectoid ferrite reaction in Fe-C-Si and the $\beta \rightarrow \alpha_m$

massive transformation in Cu-Zn.

Following the preparation of an ingot from 99.995% Co and 99.995% Al mixed in eutectic proportions, the directionally solidified eutectic was prepared by remelting the original ingot in an Al_2O_3 crucible with a graphite susceptor and induction heating under a flowing argon atmosphere. The alloy was withdrawn at the rate of 10^{-2} m/hr through a water-cooled Cu block. Approximately 5 x 10^{-2} m. of aligned eutectic structure was usually obtained from this procedure. Thin sections were then cut parallel to the growth direction with a diamond saw in order to maximize the area of lamellar interface in the foils later obtained from these specimens. A solution annealing treatment at 1150°C, performed in evacuated quartz capsules and terminated by quenching, was then imposed to eliminate precipitation within the individual phases and to stabilize as fcc the Co(Al) phase. Specimens were next ground and electrolytically polished to a thickness of 5 - 7.5 x 10^{-5} m. Discs were cut and electrolytically thinned in 30 ml. of perchloric acid dissolved in 425 ml. of absolute ethanol at ca. 25v. and 0°C. Following successive rinses in absolute ethanol, distilled water and absolute ethanol once more, the specimens were examined in a Philips EM301G microscope.

Orientation relationships were obtained accurately by means of Kikuchi line analysis, and initially in more approximate fashion by a combination of tilting and stereographic procedures. The predominant orientation relationship found was that of Kurdjumow and Sachs. Deviations of up to 3° from this relationship were sometimes observed; these deviations were of the same type observed for crystals for Cr precipitated from a dilute Cu-Cr matrix (94) and in the proeutectoid ferrite reaction (87), i.e., rotations about an axis orthogonal to both $\{111\}_{fcc}$ and $\{110\}_{bcc}$.

Habit planes of the interphase boundary were determined from the "true" directions of the misfit dislocations lying in the boundary and the "true" direction along which the interface plane intersects the foil surface. Stacking

faults within the fcc Co(Al) phase occasionally intersected the boundary; these faults are known to form on {111} planes; hence determination of their habit planes permitted an estimate of the errors accrued; these were as much as ±4°. Despite these errors, however, it could be established that the habit planes were typically irrational, lying ca. 10°-20° from $\{111\}_{Co(Al)}$ // $\{110\}_{CoAl}$. Similar results were previously obtained for the proeutectoid ferrite reaction (87) and a Cu-Cr alloy (94).

Two essentially orthogonal arrays of linear defects were usually found at the lamellar interface, as typically illustrated in Fig. 31. Within a given array, inter-defect spacings were essentially constant and usually fell in the range 4 - 6 nm. At a θ = 3° interface*, the inter-defect spacing of one of the arrays

---

*θ is the angle between the $[10\bar{1}]_{fcc}$ and $[00\bar{1}]_{bcc}$ directions (94). N-W obtains at θ = 0° and K-S is present at θ = 5 1/4°. At all θ, $\{111\}_{fcc}$ // $\{110\}_{bcc}$.

---

was markedly increased; in the example of such an interface shown in Fig. 32, this spacing became 30 nm.

The usual $\underline{g}.\underline{b} = 0$ analysis was performed on a number of interfaces and typically yielded the following results:

Set "1" $\quad a[1\bar{1}0]_{Co(Al)}$ // $a[100]_{CoAl}$

Set "2" $\quad a[01\bar{1}]_{Co(Al)}$ // $a[\bar{1}1\bar{1}]_{CoAl}$

Both Burgers vectors lie in the plane of the boundary. Since there is also only a small thickness fringe offset at these defects when viewed in weak-beam, dark-field, they may be safely termed misfit dislocations whose Burgers vectors are sessile with respect to boundary migration. For all but the a <100> Burgers vector in the CoAl phase, these vectors are double the length of their counterparts

Figure 31

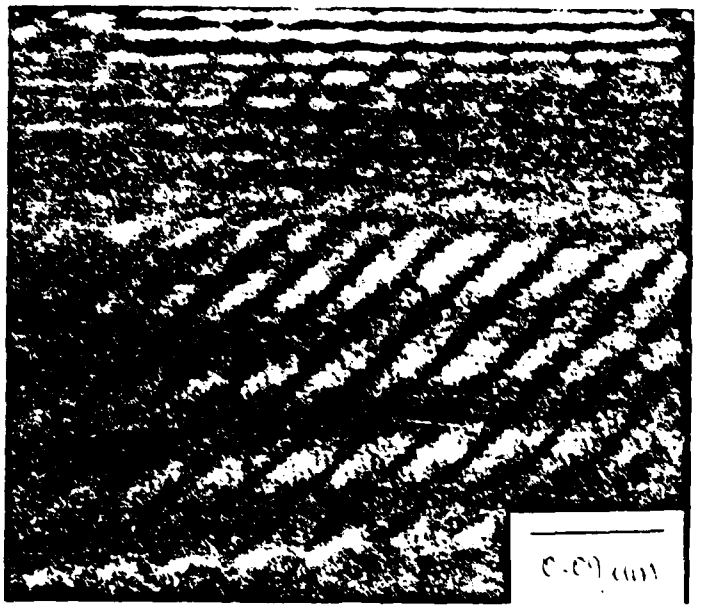

Figure 32

in the austenite and ferrite lattices in an Fe-C-Si alloy (87).

In addition to the differences in Burgers vectors, there is another, even more striking difference between the present results and those found in the proeutectoid ferrite reaction and the $\beta \rightarrow \alpha_m$ Cu-Zn transformation, namely, no structural ledges were observed at any of the interfaces examined even though both dark-field and weak-beam, dark-field were employed as well as the usual bright field technique.

The differences in Burgers vectors may be straightforwardly traced to the CsCl-type ordering of the CoAl phase. In order to avoid the creation of anti-phase boundary, translation vectors must join sites of similar type. Hence the a/2{111} Burgers vector becomes a{111}, for example. Thus the misfit dislocations can ensure preservation of the ordered structure. Doubling of the Burgers vector to accommodate the CoAl phase results in a doubling of the interdislocation spacing. For the applicable lattice parameter ratio (1.2408), the computer analysis of Rigsbee and Aaronson (88) yields either ca. 1 or ca. 2nm. at the K-S orientation relationship, with the latter being more likely because of the lower dislocation density. Doubling the latter to ca. 4 nm. yields a spacing in the range of those experimentally observed. The absence of structural ledges, on the other hand, is less readily understood. The most likely explanation appears to be that the ordered bcc lattice makes structural ledges energetically unfavorable by introducing additional "wrong" bonds. This point, and the effects of the absence of structural ledges upon lattice matching at the interphase boundary are being considered further prior to writing up these results for publication.

3. Calculation of Optimally Matching FCC:BCC Boundaries

This study is a relatively simple initial attempt to use the Bollmann (95) O-lattice technique to predict the lowest energy, and hence (in the context of nucleation theory) the most probable pair of conjugate habit planes in an fcc $\rightleftarrows$ bcc transformation as a function of the ratio of the parameter of the fcc

to that of the bcc lattice. On the Bollmann approach, two crystal lattices of specified structure and relative orientation are assumed infinite and interpenetrating. The two lattices are examined for all points which have the same internal coordinates within the respective lattices and coincide exactly at the orientation under consideration. These points form a sub-lattice, termed an "O-lattice", the size and shape of whose individual cells characterize the matching of the two crystals. For an interphase boundary the larger the volume of this O-cell the better the matching. In operational terms, the greater the area of the two-dimensional O-cell formed by the intersection of the boundary plane with the O-lattice the better the matching, since the actual matching of the crystals at the interphase boundary is the important feature. A structurally more rigorous approach, based upon this one, takes account of the fact that between any two neighboring O-points there is a discontinuity of one crystal translation vector. This discontinuity is localized at a misfit dislocation located approximately midway between the O-points. In this manner a network of misfit dislocations is constructed. Bollmann and Nissen (96) assumed that the energy of the interface varies monotonically with the spacing of the misfit dislocations. They applied these considerations to the boundary between monoclinic orthoclase and triclinic albite, and predicted the optimal orientation and boundary plane with surprising accuracy.

In these studies it was observed that each minimum energy orientation occurred when the determinant of the matrix

$$\underline{\underline{T}} = (\underline{\underline{I}} - \underline{\underline{S}}^{-1}\,\underline{\underline{R}}^{-1}) \qquad (4)$$

(where $\underline{\underline{T}}$ is the O-lattice matrix, $\underline{\underline{S}}$ the structure matrix of crystal 1 and $\underline{\underline{R}}$ the matrix expressing the relative rotation between the two crystals) changed sign. This corresponds to a situation where the O-lattice degenerates to an O-line lattice, in which the two crystals may be considered as related by a pure rotation about the O-line direction. Hence it is equally valid to search for minima in the

value of det $\underline{\underline{T}}$ for different orientations of the crystals as a function of the lattice parameter ratio. It has been shown that for any two crystals in which the three principal strains, ε_1, ε_2 and ε_3 (these are found at the Bain orientation), do not all have the same sign some rotation(s) exist for which det $\underline{\underline{T}} = 0$.

The absolute value of det $\underline{\underline{T}}$ was calculated for θ up to 10° (recall that θ is the angle between $[10\bar{1}]_{fcc}$ and $[00\bar{1}]_{bcc}$ when $(111)_{fcc}$ // $(110)_{bcc}$) for a variety of lattice parameter ratios, including those for Cu-0.33% Cr (1.253), $\beta \rightarrow \alpha_m$ Cu-Zn (1.252) and Co(Al) CoAl (1.241). Some of the computer-plotted curves are shown in Figs. 33-37. The lattice parameter ratio and the value of θ are indicated in each Figure. The curves in Figures 33 and 34 show two symmetrical minima falling near the K-S orientation relationship. Appreciably below 1.241 the minima are displaced toward the N-W relationship, coalescing to a single minimum at that relationship in the vicinity of 1.158. Note that the minima for Co(Al)-CoAl lie at $\theta = 5.4°$ and for Cu-0.33% Cr at $\theta = 5.8°$, as compared with a $\theta = 5.26°$ for the exact K-S relationship. Comparing these values with those experimentally observed shows good agreement for the Co(Al)-CoAl case, though some instances of $\theta = 3°$ boundaries were also found (as indicated in the proceeding sub-section). In the Cu-Cr case, however, a full range of orientation relationships from K-S to N-W is observed. In the latter, particularly, one might legitimately suspect that the particular lattice heterogeneity at which nucleation took place likely influenced the precise value of θ developed. In the case of $\beta \rightarrow \alpha_m$ Cu-Zn there is no agreement at all with these calculations. This should not be surprising, since as previously discussed the β grain boundaries at which nucleation took place probably exerted a potent influence upon the precise orientation relationship chosen. It would seem worthwhile, therefore, to seek the orientation relationship of α_m crystals which had demonstratably nucleated

Ratio = 1.253

$\Theta = 5.8°$

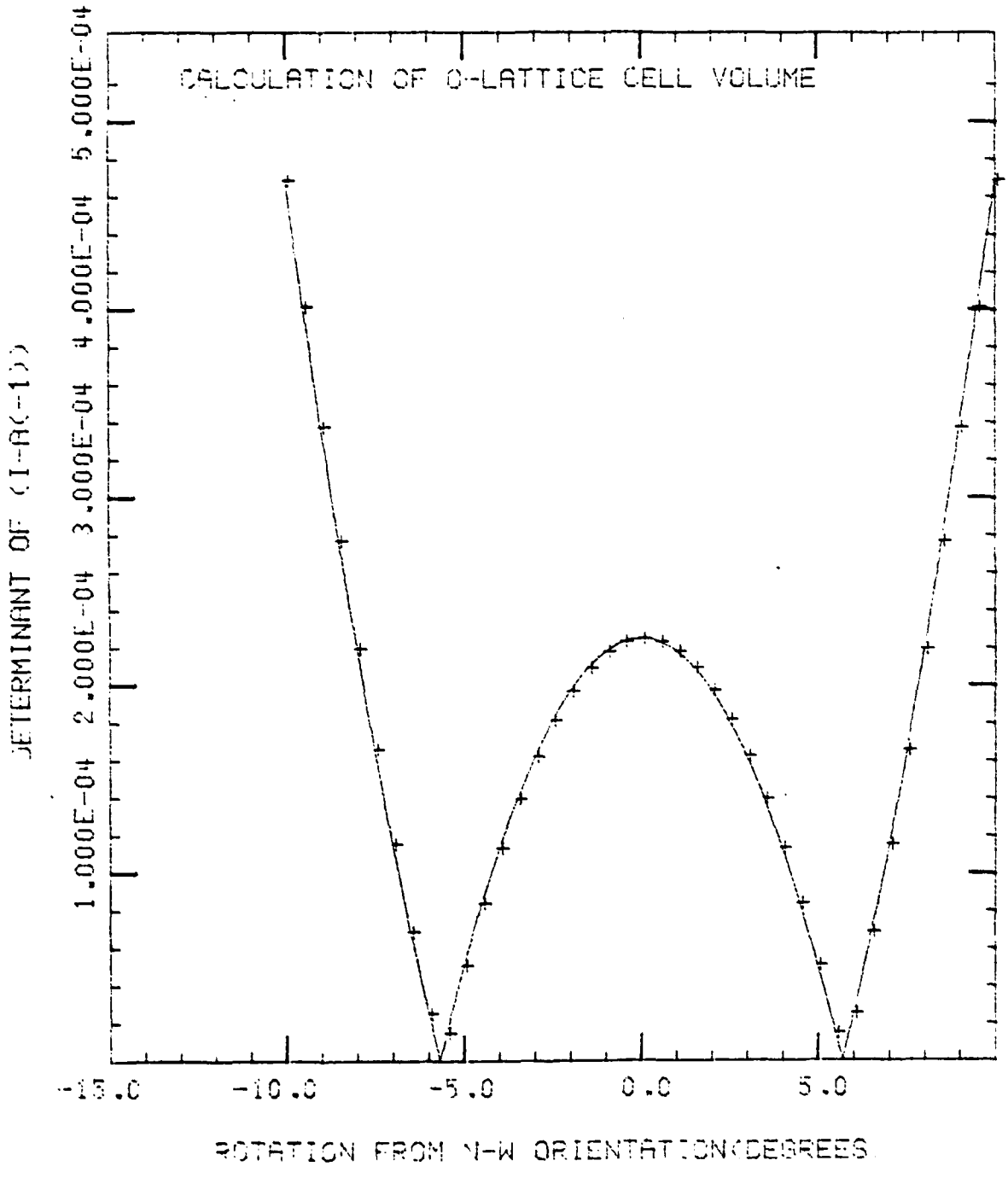

Figure 33

AD-A080 384 MICHIGAN TECHNOLOGICAL UNIV HOUGHTON DEPT OF METALLU--ETC F/G 11/6
BARRIERS TO THE MIGRATION OF INTERPHASE BOUNDARIES, PARTICULARL--ETC(U)
DEC 79 H I AARONSON, T ABE, J R BRADLEY DAAG29-77-G-0019
UNCLASSIFIED ARO-14217.1-MS NL

2 OF 2
AD A080384

END
DATE FILMED
3-80
DDC

$Ratio = 1.241$

$\theta = 5.4°$

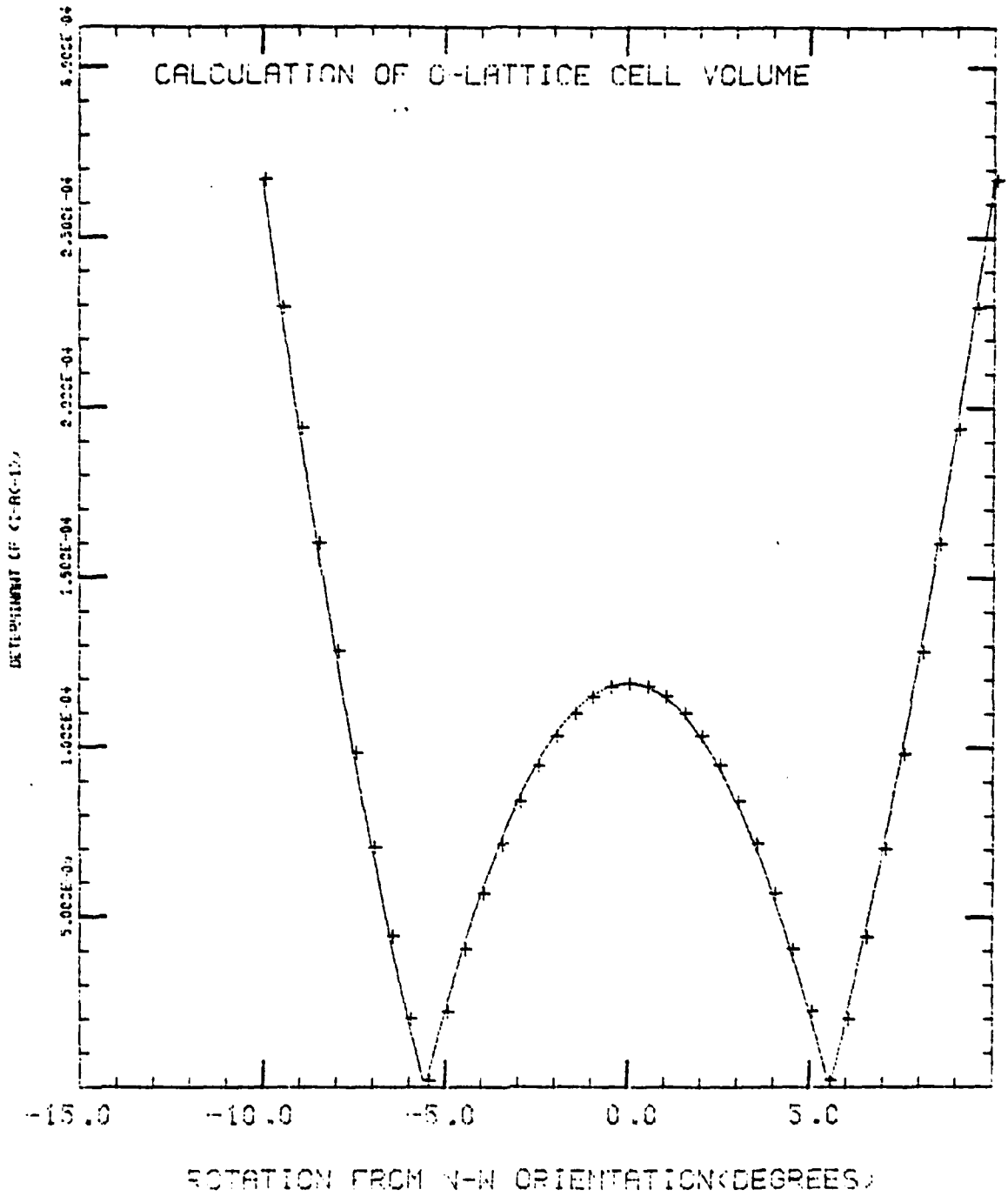

Figure 34

Ratio = 1.164
$\Theta = 2.3°$

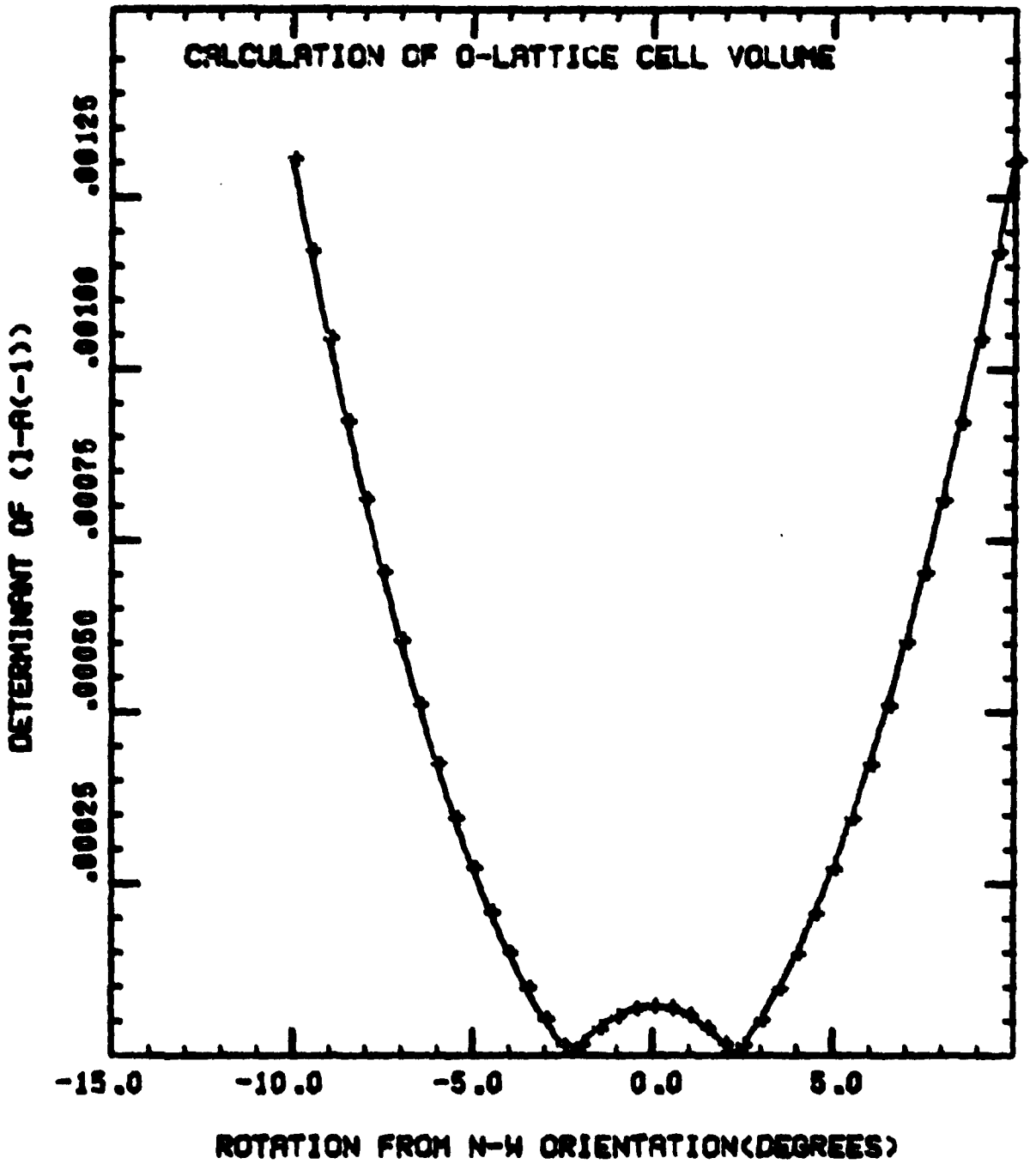

Figure 35

Ratio = 1.157
$\theta = 0°$

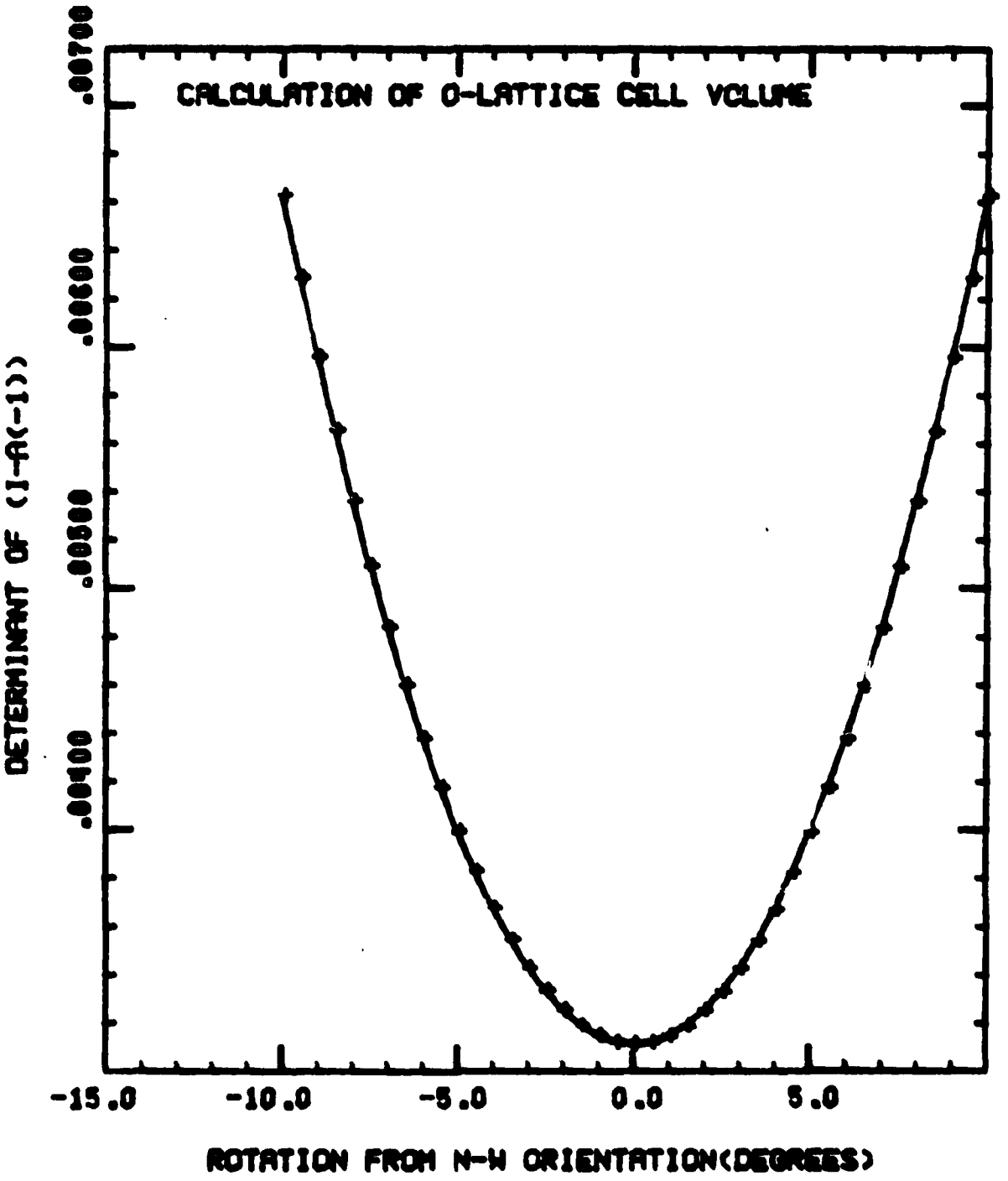

Figure 36

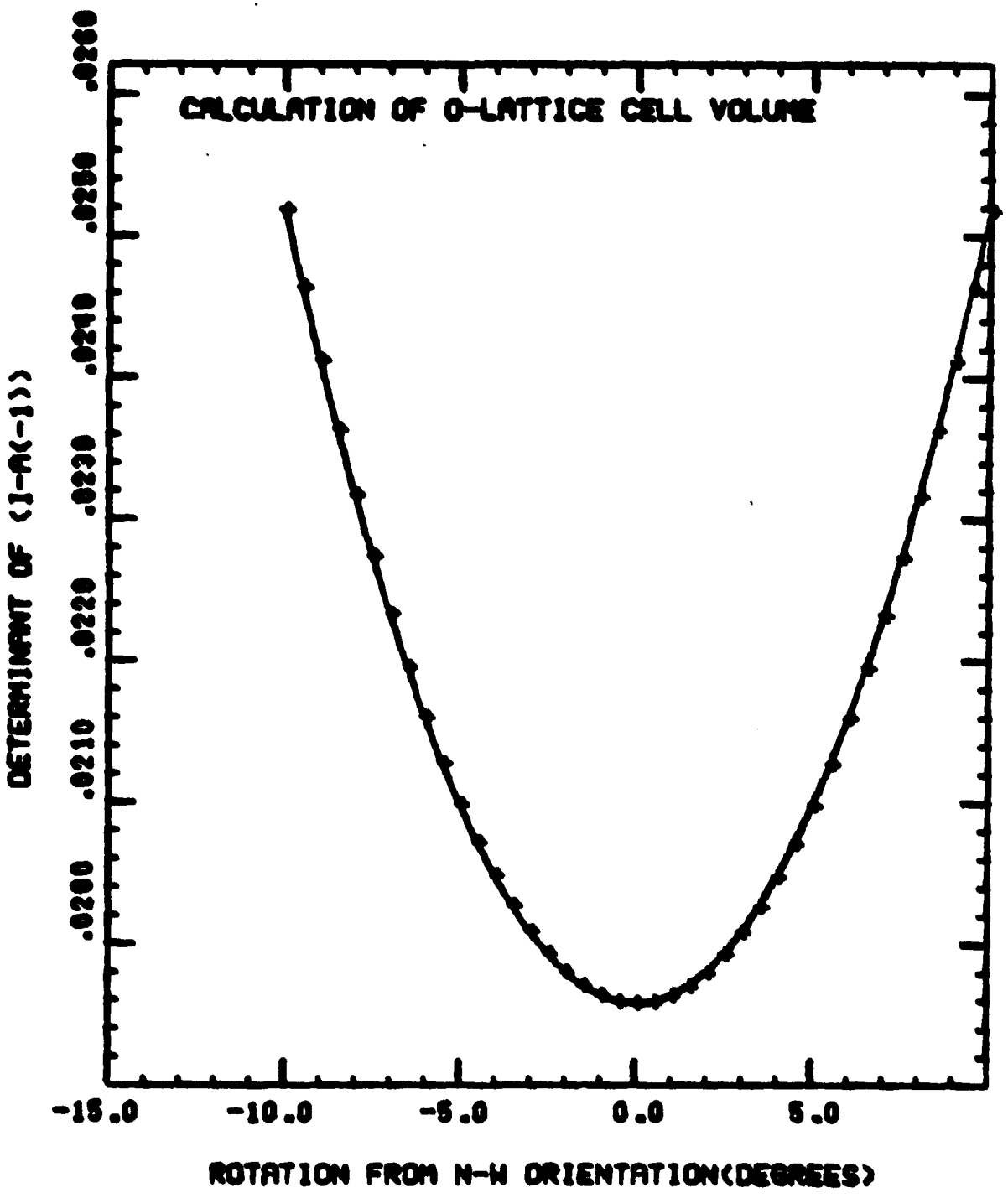
Ratio = 0.91
Θ = 0°
CALCULATION OF O-LATTICE CELL VOLUME
DETERMINANT OF (I-A(-1))
.0200
.0210
.0220
.0230
.0240
.0250
-15.0
-10.0
-5.0
0.0
5.0
ROTATION FROM N-H ORIENTATION(DEGREES)

Figure 37

in the interiors of β grains.

It should finally be noted that the present calculations apply only to cases in which $\{111\}_{fcc}$ is precisely parallel to $\{110\}_{bcc}$. Since minima are observed where low index directions in these planes are not precisely parallel, it seems not implausible to suggest that rotations apart of the $\{111\}_{fcc}$ and $\{110\}_{bcc}$ planes might also result in a lower energy orientation relationship for some lattice parameter ratios.

L. Controversies

During the term of this grant the P.I. has been involved in a number of controversies. Some are of quite recent origin, but one, that of the role, if any, of shear in the diffusional growth of precipitate plates, is now a generation old from the standpoint of the P.I.'s participation, and its origin dates back to the classic 1930 paper of Davenport and Bain (97) on the TTT-diagram and the mechanisms of austenite decomposition. Since these controversies have influenced previous research on this Contract and have exerted an even more direct effect upon the research programs proposed for the next three years, they will be briefly reviewed here.

1. The Studies of Gleiter and co-workers on the Interfacial Structure of Partially Coherent β:α Cu-Zn Boundaries

Gleiter and co-workers (98-100) have published a series of papers on TEM studies of the structure of partially coherent boundaries between equilibrium α and its β matrix. Parallel linear defects were observed in these boundaries. In the first paper, these defects were concluded to be dislocations, in the second they were described as ledges and in the third they were again termed dislocations. The P.I. and past and present postdoctorals (principally Dr. W. A. T. Clark) disputed the nomenclature which Gleiter et al used to descibe these boundaries, doubted the usefulness of the thermomechanical treatment used to secure the boundaries, criticized the TEM procedures used to characterize the boundaries

and argued the physical interpretations which Gleiter et al made of their interpretations (101). Gleiter et al (102) offered a riposte and we offered a countra-counter (103), without much net clarification. Hopefully, though, the fairly frequent references made in the literature to these Gleiter papers will continue in a more skeptical vein.

2. The Doherty Papers

Dr. R. D. Doherty of the University of Sussex has published a series of papers whose experimental aspects deal primarily with the growth kinetics of γ' Al-Ag and θ' Al-Cu plates (104-106). The principal objective of these papers was initially to disprove the view advanced by the writer and his colleagues over the past 20 years that precipitate plates thicken by a ledge mechanism when they have a crystal structure significantly different from that of the matrix phase. Some warm responses to these papers have been published, independently, by the P.I. (107-108) and by Sankaran and Laird (109, 110) in which Doherty's offerings have been disputed both en block and in detail. These responses, and lengthy, though friendly private discussions have had some effect. Doherty is currently willing to concede that plate thickening can be ledge-controlled during the early stages of thickening, and that coarsening of Al-Ag plates is also so influenced (104, 111, 112). However, Doherty is still struggling to fit continuous atomic attachment/detachment growth kinetics to the experimental measurements in an effort to utilize as much as possible the older mathematics of growth (113). He is also seeking to ascertain the growth regimes in which TEM studies ought to be made to ascertain the possible mechanisms of interface controlled growth, and thereby repeat the 1968 work of Aaronson and Laird (114) on the thickening kinetics of θ' Al-Cu plates, the 1969 paper by Laird and Aaronson (115) on the growth kinetics of γ Al-Ag plates and the more recent work of Sankaran and

Laird (116) on the growth kinetics of θ' Al-Cu and η Al-Au plates.

Perhaps one should take this type of criticism as flattery! However, a more useful good has arisen from it. The exchanges in Scripta Metllurgica on the Doherty papers have attracted the attention of Dr. John W. Cahn, who has been dialoguing with the P.I. about the precise definitions used to describe volume diffusion-controlled (VDC) and interface reaction-controlled (IRC) growth. The initial product of this dialogue was the inclusion by the P.I. of a number of categories of interphase boundary structure, not previously considered in any detail from the standpoint of growth mechanism, in a paper invited for the "Phase Transformations 1979" symposium held in April, 1979 at York University, U.K. These include interfaces bounded by crystals differing in composition but not in crystal structure or orientation, which have fully or partially coherent boundaries, the same situations in which a significant difference in long-range order obtains across the boundaries, and crystals differing slightly in structure (with full or partially coherent boundaries and with or without LRO in one of the crystals) to the point where jumps across the interphase boundary are feasible but sufficiently difficult so that their kinetics are comparable to those of long-range volume diffusion within the matrix phase. The mechanisms and kinetics of migration of each of these interfaces were considered. For none of these interfaces has an investigation been made of growth kinetics, coordinated with a parallel study of interphase boundary structure. Such a set of studies is a possibility for a future proposal, but has not been included here because more urgent projects are now planned.

These considerations have resulted, in turn, in correspondence and in three private discussion meetings, held at NBS in Gaithersburg, MD, with Dr. Cahn and with Professor J. W. Christian in an effort to construct a much broader framework for classifying and understanding diffusional growth mechanisms. The

present status of this effort, which is still continuing, is the following. Three orthogonal coordinate axes have been erected: interfacial structure, ΔF for growth and "difference in crystal structure." The first two of these axes are agreed upon; the latter is not, but what will replace it remains to be decided. In respect of coordinates along the crystal structure difference axis, we have located "same crystal structure" nearest to the origin, "marked difference in crystal structure" well away from the origin, and difference sufficient to inhibit but not prevent a jump across a fully coherent area of an interphase boundary between them; how to define this difference is the other outstanding difficulty remaining in this project. Along the interfacial structure axis, full coherency is located nearest to the origin, with sessile partial coherency, glissile partial coherency (appropriate to a shear transformation) and disordered or random close packed (rcp) structure being located successively further away. On the ΔF axis, three regimes are defined. That closest to the origin constitutes a driving force sufficiently small so that even a fully coherent boundary between two disordered solid solutions having the same crystal structure and orientation must migrate by the ledge mechanism in order to overcome the "lattice resistance to transformation" (117). The next regime allows a disordered/rcp boundary to migrate by continuous atomic attachment. The third regime provides sufficient driving force so that a glissile interphase boundary can overcome the elastic strain energy associated with its motion. Within the framework provided by this three-dimensional structure, the intersections of the lines drawn perpendicular to the above "points" on each of the axes are marked with one of three different symbols denoting volume diffusion controlled, interfacial reaction controlled or immobile. VDC is applied even when only a portion of the interphase boundary moves at rates controlled by long-range volume diffusion in the matrix phase, i.e., the riser of a ledge. IRC has been previously defined. Immobile boundaries are best exemplified by fully or

partially coherent interfaces between crystals differing markedly in structure at which no ledges are present. Once the remaining problems have been solved, surfaces will be sketched on this plot describing the bounds of the regions in which VDC, IRC or immobility predominates.

3. The Role of Shear in Precipitate Growth

Since this Contract began, three arguments have developed on this subject. These disputes are now occurring at an accelerating pace as additional researchers in the phase transformations area join those who are already urging the widest possible scope for shear mechanisms of growth. This circumstance has directly impacted the interfacial structure portion of this proposal. Two of the three projects offered are designed not only to enlarge our knowledge of interphase boundary structure per se but also to distinguish decisively between the shear and diffusional growth mechanisms in situations which the community of those interested in this controversy appears to deem important.

Clark and Wayman (118, 119) and Kinsman and Aaronson (120) have argued the meaning of planar-sided surface relief effects. The former authors consider the tent-shaped reliefs produced by θ ($CuAl_2$) rods to result from an anisotropic volume change. Kinsman and Aaronson consider that this relief is a derivative result of growth by the ledge mechanism: maintenance of partial coherency across the broad faces of a lengthening ledge permits extension of the shape change accompanying transformation; the atomic mechanism of growth, however, is the movement of atoms across the (essentially) disordered riser of the ledge. In an effort to distinguish critically between the two explanations for plane-sided, tent-shaped surface relief effects associated with θ rods, Kinsman and Aaronson examined the surface relief effects produced by grain boundary allotriomorphs of θ. Only an indistinct surface rumpling was associated with this morphology, as described by Christian (121) for an incoherent transformation. In reply, Clark and Wayman (119) argued that the allotriomorphs used by Kinsman and Aaronson were

a surface transformation effect; they found θ allotriomorphs which did appear to yield tent-shaped reliefs. They emphasized also the absence of scratch displacements. In response, Kinsman and Aaronson (120) defended the representativeness of their θ allotriomorphs and noted that some of those utilized by Clark and Wayman could well have had a habit plane parallel to the plane of the grain boundary, thereby yielding a relief effect. Also, scratch displacement is not to be expected from tents--and is in any event not an essential aspect of the point that plane-sided surface relief effects cannot be ascribed solely to a volume change.

Settling this particular argument permanently is made very difficult by the complex crystal structure of θ. However, the point made by Kinsman and Aaronson that plane-sided surface reliefs, sharing some martensitic characteristics, need not be taken as evidence of a martensitic mechanism but are indicative only of the maintenance of full or partial coherency during growth, remains a continuing issue.

Another argument with Wayman, however, should prove more useful in the development of the shear vs. diffusional growth question. Aaronson and Kinsman (122), working with Pedraza and Kittl (123), participated in measurements of the lengthening and thickening kinetics of AuCu II plates in an equiatomic Au-Cu alloy. No composition change attends this transformation but a marked change in ordering does; AuCu II is a super-superlattice. Although Smith and Bowles (124) have shown that the surface relief effects and crystallography of AuCu II plates obey the specifications of the phenomenological theory of martensite with remarkable accuracy, Kinsman and Aaronson concluded that the ordering change means that the transformation cannot be martensitic; they concluded that it is a massive transformation. (The previously noted work (90) on the massive transformation in a Ag-26 A/O Al alloy, showing reproducible orientation relationships, and the research of Clark described in section IV-K-1, demonstrating the presence of a reproducible partially coherent interfacial structure on planar facets produced during the $\beta \rightarrow \alpha_m$ CuZn massive transformation, effectively remove the non-crystallo-

graphic specification originally imposed on the massive transformation (125-126).) They deduced that the interfacial structure is fully coherent during growth (as permitted by closely spaced twins) and subsequently develops orthogonal arrays of sessile misifit dislocations. Bowles and Wayman (127) have countered with the views that: (a) the interfacial structure of AuCu II plates is one of glissile or transformation dislocations, and (b) that the ordering process takes place by atomic movements at the steps associated with the transformation dislocations.

A straightforward experiment which should distinguish between the interfacial structure portion of the two viewpoints is described in the next section as part of the research proposed for the requested renewal of this Contract. Here it should be noted that another major issue is at stake, namely, can a phase transformation which exhibits the surface relief effect and crystallography of martensite but which nonetheless involves diffusional jumps (as distinct from sub-diffusional shuffles) of substitutionally dissolved solute atoms as an intrinsic part of the transformation process still be regarded legitimately as martensitic? On the criteria advanced by Wayman (128) himself, the P.I. says that the answer to this question is no. Obviously Wayman, and to some extent Christian (129) disagrees. The P.I. is currently engaged in another dialogue with Christian in an attempt to achieve a mutually acceptable resolution of this question. Presumably Wayman ought to be brought into these discussions if agreement can be reached with Christian.

References

1. C. A. Dube, H. I. Aaronson and R. F. Mehl, Rev. de Met., 55, 201 (1958).
2. J. R. Bradley and H. I. Aaronson, Met. Trans., 8A, 317 (1977).
3. J. R. Bradley, J. M. Rigsbee and H. I. Aaronson, ibid, 8A, 323 (1977).
4. K. R. Kinsman and H. I. Aaronson, Transformation and Hardenability in Steels, p. 39, Climax Molybdenum Co., Ann Arbor, MI. (1967).
5. K. R. Kinsman and H. I. Aaronson, Met. Trans., 4, 959 (1973).
6. C. Atkinson, H. B. Aaron, K. R. Kinsman and H. I. Aaronson, ibid, 4, 783 (1973).
7. P. Boswell, K. R. Kinsman and H. I. Aaronson, unpublished research, Ford Motor Co., Dearborn, MI. (1968).
8. G. Horvay and J. W. Cahn, Acta Met., 9, 596 (1961).
9. G. R. Purdy, D. H. Weichert and J. S. Kirkaldy, Trans. TMS-AIME, 230, 1025 (1964).
10. J. S. Kirkaldy, Can. J. Phys., 36, 907 (1958).
11. D. E. Coates, Met. Trans., 3, 1203 (1972).
12. D. E. Coates, ibid, 4, 1077 (1973).
13. D. E. Coates, ibid, 4, 2312 (1973).
14. A. A. Popov and M. S. Mikhalev, Phys. Metals Metallogr., 7, 36 (1959).
15. L. S. Darken and R. M. Fisher, Decomposition of Austenite by Diffusional Processes, p. 249, Interscience, New York, NY. (1962).
16. M. Hillert, The Mechanism of Phase Transformations in Crystalline Solids, p. 231, Institute of Metals, London (1969).
17. M. Hillert, Internal Report, Swedish Inst. for Metals Research (1953).
18. A. Hultgren, Jernk. Ann., 135, 403 (1951).
19. M. Hillert, ibid, 136, 25 (1952).
20. E. Rudberg, ibid, 136, 91 (1952).
21. J. B. Gilmour, G. R. Purdy and J. S. Kirkaldy, Met. Trans., 3, 1455 (1972).
22. H. I. Aaronson, H. A. Domian and G. M. Pound, Trans. TMS-AIME, 236, 768 (1966).
23. M. Hillert and L.-I. Staffanson, Acta Chem. Scan., 24, 3618 (1970).

24. C. Atkinson, Acta Met., 16, 1019 (1968).

25. R. B. McLellan and W. W. Dunn, J. Phys. Chem. Sol., 30, 2631 (1969).

26. C. A. Dube, Ph.D. Thesis, Carnegie-Mellon University (1948).

27. C. Zener, J. App. Phys., 20, 950 (1949).

28. J. S. Kirkdaldy and G. R. Purdy, Can. J. Phys., 40, 208 (1962).

29. L. C. Brown and J. S. Kirkaldy, Trans. TMS-AIME, 230, 223 (1964).

30. J. S. Kirkaldy, B. A. Thomson and E. Baganis, Hardenability Concepts With Application to Steel, p. 82, TMS-AIME (1978).

31. M. Hillert, Acta Met., 3, 34 (1955).

32. K. Lücke and H. Stüwe, Recovery and Recrystallization of Metals, p. 131, Interscience, New York, NY. (1963).

33. M. Hillert and B. Sundman, Acta Met., 24, 731 (1976).

34. M. Guttmann, Surface Science, 53, 213 (1975).

35. D. McLean, Grain Boundaries in Metals, p. 116, Clarendon Press, Oxford, U.K. (1957).

36. J. C. Greenbank, Carbon-Solute Interactions in Solid Iron Alloys, Univ. of Sheffield (1971).

37. K. Alex and R. B. McLellan, J. Phys. Chem. Sol., 32 449 (1971).

38. A. Hultgren, Trans. ASM, 39, 915 (1947).

39. H. I. Aaronson, Trans. TMS-AIME, 224, 870 (1962).

40. H. I. Aaronson and H. A. Domian, ibid, 236, 781 (1966).

41. R. C. Sharma and G. R. Purdy, Met. Trans., 4, 2303 (1973).

42. G. R. Purdy, Acta Met., 26, 487 (1978).

43. G. R. Purdy, ibid, 26, 487 (1978).

44. R. W. K. Honeycombe, Met. Trans., 7A, 915 (1976).

45. H. I. Aaronson, M. R. Plichta, G. W. Franti and K. C. Russell, Met. Trans., 9A, 363 (1978).

46. A. T. Davenport and R. W. K. Honeycombe, 322, 191 (1971).

47. A. D. Batte and R. W. K. Honeycombe, J.I.S.I., 211, 284 (1973); Met. Sci. Jnl., 7, 160 (1973).

48. J. R. Bradley, Ph.D. Thesis, Michigan Technological Univ. (1979).

49. H. B. Aaron, Acta Met., 17, 407 (1969).

50. J. W. Cahn, Seminar at Univ. of Pittsburgh, Oct. 1979.

51. N. A. Gjostein, H. A. Domian, H. I. Aaronson and E. Eichen, Acta Met., 14, 1637 (1966).

52. J. C. Greenbank, unpublished research, Univ. of Sheffield (1971).

53. R. F. Mehemann and A. R. Troiano, Metal Progress, 70, 97 (Aug. 1956).

54. R. F. Mehemann, Phase Transformations, p. 397, American Society for Metals, Metals Park, OH. (1970).

55. C. Zener, Trans. AIME, 167, 550 (1946).

56. J. E. Hilliard and J. W. Cahn, Trans. TMS-AIME, 221, 344 (1961).

57. H. K. D. H. Bhadeshia and D. V. Edmonds, Met. Trans., 10A, 895 (1979).

58. T. Lyman and A. R. Troiano, Trans. ASM, 37, 402 (1946).

59. T. Wada, Metals Handbook, 8, 8th Ed., 409 (1973).

60. K. Mazanec and J. Cadek, Rev. Met., 212, 501 (1958).

61. P. Krahe, K. R. Kinsman and H. I. Aaronson, Acta Met., 20, 1109 (1972).

62. F. C. Hull, F. C. Colton and R. F. Mehl, Trans. AIME, 150, 185 (1942).

63. M. H. Richman, D. A. Thomas and M. Cohen, Acta Met., 7, 814 (1959).

64. K. C. Russell, Met. Trans., 2, 5 (1971).

65. R. A. Grange, private communication, U. S. Steel Research Laboratory (1970).

66. J. M. Papazian and D. M. Beshers, Met. Trans., 2, 497 (1971).

67. J. R. Bradley, G. J. Shiflet, Y. W. Lee, H. I. Aaronson and W. C. Johnson, unpublished research, 1979.

68. M. P. Seah and E. D. Hondros, Proc. Roy. Soc, A, 355, 191 (1973).

69. P. V. Ramasubramanian and D. F. Stein, Met. Trans., 4, 1735 (1973).

70. M. Hansen, Constitution of Binary Alloys, p. 1266, McGraw-Hill, New York, NY. (1958).

71. W. F. Lange III and H. I. Aaronson, Met. Trans., in press.

72. H. I. Aaronson, H. A. Domian and G. M. Pound, Trans. TMS-AIME, 236, 753 (1966).

73. L. Kaufman, S. V. Radcliffe and M. Cohen, Decomposition of Austenite by Diffusional Processes, p. 313, Interscience, New York, NY. (1962).

74. J. R. Lacher, Proc. Cambridge Phil. Soc., 33, 518 (1937).

75. R. H. Fowler and E. A. Guggenheim, Statistical Thermodynamics, p. 442, Cambridge Univ. Press, New York, NY. (1930).

76. S. Ban-ya, J. F. Elliott and J. Chipman, Met. Trans., 1, 1313 (1970).

77. W. W. Dunn and R. B. McLellan, Met. Trans., 2, 1079 (1971).

78. J. A. Lobo and G. H. Geiger, Met. Trans., 7A, 1347, 1359 (1976).

79. R. P. Smith, Jnl. Amer. Chem. Soc., 68, 1163 (1946).

80. E. F. Foo and C. H. P. Lupis, Acta Met., 21, 1409 (1973).

81. E. B. Hawbolt and T. B. Massalski, Met. Trans., 1, 2315 (1970).

82. D. Hull and R. D. Garwood, The Mechanism of Phase Transformations in Metals, p. 47, Institute of Metals, London, U.K. (1956).

83. H. I. Aaronson, C. Laird and K. R. Kinsman, Scripta Met., 2, 250 (1968).

84. J. D. Ayres and D. C. Joy, Acta Met., 20, 1371 (1972).

85. M. R. Plichta, J. M. Rigsbee, M. G. Hall, K. C. Russell and H. I. Aaronson, Scripta Met., 10, 1065 (1976).

86. D. A. Karlyn, J. W. Cahn and M. Cohen, Trans. TMS-AIME, 245 197 (1969).

87. J. M. Rigsbee and H. I. Aaronson, Acta Met., 27, 365 (1979).

88. J. M. Rigsbee and H. I. Aaronson, ibid, 27, 351 (1979).

89. L. Delaey, A. J. Perkins and T. B. Massalski, Jnl. Mat. Sci., 7, 1197 (1972).

90. M. R. Plichta and H. I. Aaronson, submitted to Acta Met.

91. M. Hillert, Decomposition of Austenite by Diffusional Processes, p. 197, Interscience, New York, NY. (1962).

92. A. D. King and T. Bell, Met. Trans., 6A, 1428 (1975).

93. D. R. Clarke and W. M. Stobbs, Met. Sci., 7, 242 (1974).

94. M. G. Hall, H. I. Aaronson and K. R. Kinsman, Surface Science, 31, 257 (1972).

95. W. Bollmann, Phys. Stat. Sol., 21A, 543 (1974).

96. H.-U. Nissen and W. Bollmann, Proc. 4th European Congress on Electron Microscopy, Rome, p. 321 (1968).

97. E. S. Davenport and E. C. Bain, Trans., AIME, 90, 117 (1930).

98. G. Baro and H. Gleiter, Acta Met., 21, 1405 (1973).

99. G. Baro and H. Gleiter, ibid, 22, 141 (1974).

100. P. Kluge-Weiss and H. Gleiter, ibid, 26, 117 (1978).

101. W. A. T. Clark, A. Guha, H. I. Aaronson and J. M. Rigsbee, Scripta Met., in press.

102. H. Gleiter and P. Pumphrey, ibid, in press.

103. W. A. T. Clark, A. Guha, H. I. Aaronson and J. M. Rigsbee, ibid, in press.

104. M. Ferrante and R. D. Doherty, ibid, 10, 1059 (1976).

105. Y. H. Chen and R. D. Doherty, ibid, 11, 725 (1977).

106. M. Ferrante and R. D. Doherty, Acta Met., 27, 1603 (1979).

107. H. I. Aaronson, Scripta Met., 11, 731 (1977).

108. H. I. Aaronson, ibid, 11, 741 (1977).

109. R. Sankaran and C. Laird, ibid, 11, 383 (1977).

110. R. Sankaran and C. Laird, ibid, 12, 877 (1978).

111. R. D. Doherty, M. Ferrante and Y. H. Chen, ibid, 11, 733 (1977).

112. R. D. Doherty, M. Ferrante and Y. H. Chen, ibid, 12, 885 (1978).

113. R. D. Doherty, Phase Transformations, 2, p. II-7, The Institution of Metallurgists/Chameleon Press, London, U.K. (1979).

114. H. I. Aaronson and C. Laird, Trans. TMS-AIME, 242, 1437 (1968).

115. C. Laird and H. I. Aaronson, Acta Met., 17, 505 (1969).

116. R. Sankaran and C. Laird, ibid, 22, 957 (1974).

117. J. W. Cahn, ibid, 8, 554 (1960).

118. H. McI. Clark and C. M. Wayman, Met. Trans., 3, 1979 (1972).

119. H. McI. Clark and C. M. Wayman, ibid, 8A, 206 (1977).

120. K. R. Kinsman and H. I. Aaronson, ibid, 7A, 896 (1976); 8A, 209 (1977).

121. J. W. Christian, Decomposition of Austenite by Diffusional Processes, p. 371, Interscience, New York, NY. (1962).

122. H. I. Aaronson and K. R. Kinsman, Acta Met., 25, 367 (1977).

123. A. J. Pedraza and J. Kittl, ibid, 24, 835 (1976).

124. R. Smith and J. S. Bowles, ibid, 8, 405 (1960).

125. T. B. Massalski, Phase Transformations, p. 433, American Society for Metals, Metals Park, OH. (1970).

126. T. B. Massalski, ibid, 6, 253 (1958).

127. J. S. Bowles and C. M. Wayman, ibid, 27, 833 (1979).

128. H. McI. Clark and C. M. Wayman, Phase Transformations, p. 59, American Society for Metals, Metals Park, OH. (1970).

129. J. W. Christian, Phase Transformations, 1, p. I-1, The Institution of Metallurgists/Chameleon Press, London, U.K. (1979).